

Studies of beta-cardiotoxin from king cobra venom on rat cardiac functions: Effect on isolated single cardiomyocyte.



A Dissertation Submitted in Partial Fulfillment of the Requirements
for the Degree of Doctor of Philosophy in Animal Physiology

Department of Veterinary Physiology

FACULTY OF VETERINARY SCIENCE

Chulalongkorn University

Academic Year 2019

Copyright of Chulalongkorn University

การศึกษามผลของสารเบต้าคาร์ทีโอทีอกซินจากพิษงูจงอางต่อการทำงานของหัวใจในหนูแรท: ผลต่อ
เซลล์กล้ามเนื้อหัวใจแบบแยกเดี่ยว



วิทยานิพนธ์นี้เป็นส่วนหนึ่งของการศึกษาตามหลักสูตรปริญญาวิทยาศาสตรดุษฎีบัณฑิต
สาขาวิชาสัตววิทยาการสัตว ภาควิชาสัตววิทยา
คณะสัตวแพทยศาสตร์ จุฬาลงกรณ์มหาวิทยาลัย
ปีการศึกษา 2562
ลิขสิทธิ์ของจุฬาลงกรณ์มหาวิทยาลัย

ธัชกร เลิศวรรณการ : การศึกษาผลของสารเบต้าคาร์ดิโอท็อกซินจากพิษงูจงอางต่อการทำงานของหัวใจในหนูแรท: ผลต่อเซลล์กล้ามเนื้อหัวใจแบบแยกเดี่ยว. (Studies of beta-cardiotoxin from king cobra venom on rat cardiac functions: Effect on isolated single cardiomyocyte.)
 อ.ที่ปรึกษาหลัก : อ. น.สพ. ดร.กิตติพงษ์ ทาจำปา

สารเบต้าคาร์ดิโอท็อกซิน (β -CTX) เป็นโปรตีนชนิดใหม่ที่ถูกสกัดได้จากพิษงูจงอางที่ถูกเสนอว่าออกฤทธิ์คล้ายยาในกลุ่มต่อต้านตัวรับชนิดเบต้า (beta-blocker) อย่างไรก็ตามข้อมูลกลไกการออกฤทธิ์ของสาร β -CTX ต่อการทำงานของเซลล์กล้ามเนื้อหัวใจนั้นยังไม่เป็นที่ทราบแน่ชัด วัตถุประสงค์ของการศึกษานี้เพื่อวิเคราะห์หาผลกระทบของ β -CTX ต่อการทำงานของเซลล์กล้ามเนื้อหัวใจและการทำงานของเส้นใยกล้ามเนื้อหัวใจในหนูแรท และสำรวจความเกี่ยวข้องของเส้นทางสัญญาณตัวรับเบต้าแอดรีเนอร์จิก (β -AR) β -CTX ถูกแยกและทำให้บริสุทธิ์ด้วยโครมาโตกราฟีสองขั้นตอนและตรวจยืนยันโดยการหาลำดับกรดอะมิโนปลายด้านเอ็น การทำงานของ β -CTX ถูกเปรียบเทียบกับโพรปราโนลอล (propranolol) ใน 3 เงื่อนไข คือในภาวะปกติ ในภาวะที่ถูกกระตุ้นด้วยไอโซโปรเทรินอล (isoproterenol) และฟอสโฟลีน (forskolin) ผลการศึกษาพบว่า β -CTX มีฤทธิ์ในการยับยั้งการหดตัวของกล้ามเนื้อหัวใจมากกว่า propranolol โดยไม่มีการเปลี่ยนแปลงของแคลเซียมในเซลล์ อย่างไรก็ตาม β -CTX ทำให้การลดลงของแคลเซียมในไซโตซอลช้าลง เป็นผลให้เกิดการคลายตัวของกล้ามเนื้อหัวใจที่แย่งลง ถึงแม้ว่า β -CTX จะมีฤทธิ์กีดการทำงานของหัวใจในภาวะที่มีทั้ง isoproterenol และ forskolin แต่อย่างไรก็ตาม การเกิดฟอสโฟริเลชันของ β -AR นั้นไม่มีการเปลี่ยนแปลง นอกจากนี้ β -CTX ยังนำไปทดสอบการทำงานของเอนไซม์เอทีพีเอส (ATPase) ในเส้นใยกล้ามเนื้อและจลนศาสตร์ของเส้นใยกล้ามเนื้อ พบว่า β -CTX นั้นสามารถกีดการทำงานของ ATPase ได้โดยไม่มีการเปลี่ยนความไวของแคลเซียมในการสร้างแรง (Ca^{2+} -sensitivity) ของเส้นใยกล้ามเนื้อ กล่าวโดยสรุป กลไกการทำงานของ β -CTX นั้นไม่ได้ออกฤทธิ์ผ่านทาง β -AR ดั้งเดิม แต่ผ่านทางการลดลงของอัตราการจับและคลายตัวของเส้นใยกล้ามเนื้อ ทำให้การทำงานของหัวใจลดลงในที่สุด

จุฬาลงกรณ์มหาวิทยาลัย
 CHULALONGKORN UNIVERSITY

สาขาวิชา สรีรวิทยาการสัตว์
 ปีการศึกษา 2562

ลายมือชื่อนิสิต
 ลายมือชื่อ อ.ที่ปรึกษาหลัก

5775505031 : MAJOR ANIMAL PHYSIOLOGY

KEYWORD: ATPase activity, Beta-cardiotoxin, cardiomyocyte function, beta-adrenergic signaling, calcium transient, rat

Tuchakorn Lertwanakarn : Studies of beta-cardiotoxin from king cobra venom on rat cardiac functions: Effect on isolated single cardiomyocyte.. Advisor: Kittipong Tachampa, D.V.M., M.Sc., Ph.D., DTBVM

Beta-cardiotoxin (β -CTX), a novel protein isolated from the King cobra (*Ophiophagus hannah*) venom has previously been proposed as a beta-blocker candidate. However, cellular mechanisms of β -CTX on cardiomyocyte is unknown. This study aimed to evaluate the impact of β -CTX on isolated rat cardiomyocyte function and the cardiac myofibrillar activity, and to explore involvement of β -adrenergic receptor (β -AR) signaling pathway. β -CTX was isolated and purified using two-step chromatographic method and confirmed by N-terminal sequencer. The function of β -CTX on cardiomyocyte was compared to propranolol in 3 conditions, basal state, with isoproterenol (ISO), and with forskolin (FSK). β -CTX exhibited more potency than propranolol to suppress the myocyte contraction without altering calcium transient. However, β -CTX prolonged the calcium decaying resulted in negative lusitropy. Although cardiac functions were blunted by β -CTX in the presence of either ISO or FSK, the phosphorylation of the downstream β -AR signaling sites were not affected. The compound was further tested on the cardiac myofibrillar ATPase activity and the kinetics. β -CTX suppressed the maximal ATPase activity without changing Ca^{2+} -sensitivity of the myofibril. In conclusion, the mechanism of β -CTX on cardiomyocyte was not mediated through classical β -AR pathway but directly suppress the actomyosin ATPase activity, depress the myofilament kinetics, and hence, reduce the cardiomyocyte functions.

Field of Study: Animal Physiology

Student's Signature

Academic Year: 2019

Advisor's Signature

ACKNOWLEDGEMENTS

I would like to gratefully thank my supervisor Dr. Kittipong Tachampa who always encourages and supports me everything. I would also like to thank Department of Physiology, Faculty of Veterinary Science, Chulalongkorn University, all committees, professors, staff, and students for all supports. I would like to thank Assoc Prof Dr Elda E Sánchez, Assist Prof Dr Montamas Suntravat, and NNTRC's personnel. I would also like to thank Prof Dr R John Solaro, Prof Dr Beata M Wolska, and Prof Dr Pieter P de Tombe, for all great laboratory experience in UIC. Thanks to Shamim AK Chowdhury, Chad M Warren, Jody L Martin, and all UIC's staff. Finally, thanks to my family and my beloved supporting friends, and Vichayanee Pumpitakkul for the best supports throughout my Ph D study.

Tuchakorn Lertwanakarn



จุฬาลงกรณ์มหาวิทยาลัย
CHULALONGKORN UNIVERSITY



จุฬาลงกรณ์มหาวิทยาลัย
CHULALONGKORN UNIVERSITY

ABBREVIATIONS

+dL/dt	Shortening velocity
-dL/dt	Re-lengthening velocity
3FTX	Three finger toxin
α -AR	Alpha-adrenergic signaling
β -AR	Beta-adrenergic receptors
β -CTX	Beta-cardiotoxin
β -AS	Beta-adrenergic signaling
μ g	Microgram
μ L	Microliter
μ M	Micromolar
μ m	Micrometer
τ	Relaxation index
τ_{Ca}	Calcium decaying index
AC	Adenylyl cyclase
ACN	Acetonitrile
ATP	Adenosine triphosphate
BB	Beta-blocker
Ca^{2+}	Calcium ion
CaT	Calcium transient
cAMP	Cyclic adenosine monophosphate
CC ₅₀	Half-maximal cytotoxic concentration
cIEx	Cation exchange
cMyBP-C	Cardiac myosin binding protein-C
cTnC	Cardiac troponin C
cTnI	Cardiac troponin I
cTnT	Cardiac troponin T
DMSO	Dimethyl sulfoxide
EC ₅₀	Half maximal effective concentration
fPLC	Fast protein liquid chromatography
FSK	Forskolin
HF	Heart failure
HPLC	High performance liquid chromatography

HRB	High relaxing buffer
IC ₅₀	Half maximal inhibitory concentration
ISO	Isoproterenol
kDa	kiloDalton
MTT	Methyl-thiazol-tetrazolium
MLC	Myosin light chain
KCV	King cobra venom
LTCC	L-type Ca ²⁺ -channel
PBS	Phosphate buffer saline
pCa	Calcium concentration (= -log [Ca])
PKA	Protein kinase A
PKC	Protein kinase C
PLC	Phospholipase C
PLN	Phospholamban
RyR	Ryanodine receptor
mg	Milligram
mL	Milliliter
mm	Millimeter
mM	Millimolar
n _H	Hill's coefficient
nM	Nanomolar
nm	Nanometer
RP-HPLC	Reverse phase HPLC
SDS-PAGE	Sodium dodecyl sodium-polyacrylamide gel electrophoresis
SERCa	Sarcoplasmic reticulum Ca ²⁺ -Pump
SPB	Sodium phosphate buffer
SRB	Standard relaxing buffer
TFA	Trifluoroacetic acid
Tm	Tropomyosin
TR ₉₀	Time-to90% re-lengthening
TX100	Triton-X 100
TBS-T	Tris-Base Saline-Tween solution

TABLE OF CONTENTS

	Page
.....	iii
ABSTRACT (THAI).....	iii
.....	iv
ABSTRACT (ENGLISH).....	iv
ACKNOWLEDGEMENTS.....	v
ABBREVIATIONS.....	vii
TABLE OF CONTENTS.....	ix
LIST OF TABLES.....	xv
LIST OF FIGURES.....	xvi
Chapter 1 Introduction.....	1
Conceptual framework.....	4
Chapter 2 Literature review.....	5
1. Cardiovascular diseases: epidemiology and importance.....	5
2. Heart failure: pathophysiology and pharmacological approaches.....	6
3. β -adrenergic signaling, Ca^{2+} homeostasis, and myofilament kinetics.....	10
4. Beta-blockers: actions and benefits.....	13
5. Venomous snakes and snakebites issues.....	14
6. Snake venom compositions and the importance of toxinology.....	16
7. King cobra venom and the discovery of β -CTX.....	19
Chapter 3 Materials and methods.....	23
1. Isolation and purification of β -CTX.....	23

1.1. Crude venom.....	23
1.2. Reverse phased HPLC (RP-HPLC).....	23
1.3. Cation exchange chromatography.....	24
1.4. Protein determination & identification.....	24
2. <i>In vitro</i> cellular viability study.....	25
2.1. Cell culture.....	25
2.2. <i>In vitro</i> MTT assay.....	26
3. Effects of β -CTX on isolated cardiomyocyte functions.....	27
3.1. Animals and animal used protocols.....	27
3.2. Isolation of adult rat ventricular myocytes.....	27
3.3. Experimental designs.....	28
3.3.1. Effects of β -CTX on isolated cardiomyocytes at the basal condition.....	28
3.3.2. Effects of β -CTX on isolated cardiomyocytes with isoproterenol stimulation.....	28
3.3.3. Effects of β -CTX on isolated cardiomyocytes with forskolin stimulation.....	29
3.4. Simultaneously measurement of myocardial contraction and calcium profiles.....	31
3.4.1. System setup and cell preparation.....	31
3.4.2. Parameters and data analysis.....	32
4. Effects of β -CTX on total phosphorylation of myofilament proteins.....	34
4.1. Myofibril preparations and experimental designs.....	34
4.2. SDS-PAGE and ProQ [®] staining.....	35

5. Western blot analysis of phosphorylated proteins involved in β -adrenergic signaling.....	36
5.1. Whole-cell lysate preparation and experimental designs.....	36
5.2. SDS-PAGE and western blot analysis.....	37
6. Detergent extracted (skinned) fiber bundles and force-pCa relationship measurement.....	39
6.1. Skinned fiber preparation	39
6.2. Measurement of force generated in different calcium concentration.....	40
7. Measurement of myofibrillar ATPase activity	41
7.1. Isolation of cardiac myofibrils	41
7.2. Measurement of ATPase activity using the malachite green assay	43
8. Statistical analysis.....	44
Chapter 4 Results	46
1. Purification and identification of β -CTX.....	46
2. <i>In vitro</i> cytotoxicity effect of β -CTX on mammalian muscle cell lines.....	49
3. Effect of β -CTX on isolated rat cardiomyocyte functions.....	51
3.1. Effect of β -CTX on ventricular myocyte functions at basal state	51
3.2. Effect of β -CTX on ISO-induced cardiomyocyte	59
3.3. Effect of β -CTX on FSK-induced cardiomyocyte.....	64
4. Effect of β -CTX on myofibrillar proteins phosphorylation	67
4.1. Alterations in total protein phosphorylation using ProQ [®] staining.....	67
4.2. Western blot analysis of specific phosphorylation sites for β -adrenergic signaling.....	71
5. Effect of β -CTX on the force-pCa relationship in the detergent extracted “skinned” fiber bundles experiment.....	72

6. Effect of β -CTX on myofibril ATPase activity	74
Chapter 5 Discussion	76
1. An alternative method to purify β -CTX from the Thai KCV.....	76
2. The cytotoxic effects of β -CTX in various mammalian muscle cell types.....	78
3. Suppression of β -CTX on cardiomyocyte contractility without contribution of intracellular calcium.....	80
4. β -CTX prolonged τ_{Ca} causing negative lusitropic effects of the ventricular myocytes	82
5. β -CTX attenuated cardiomyocyte functions in ISO-induced cells but did not affect FSK-induced cells	84
6. The action of the β -CTX was not mediated through the cAMP-PKA pathway..	88
7. β -CTX reduced actomyosin ATPase activity without changing myofibrillar dynamics.....	91
8. Other possible pathways underlying β -CTX's effect	92
Chapter 6 Conclusion	96
Appendix A.....	100
A1. Reversed-Phase HPLC	100
A2. Cation exchange chromatography	102
A3. N-terminal sequencer & identification of protein.....	103
Appendix B.....	108
B1. Cellular viability of different mammalian cell lines treated with β -CTX.....	108
B2. Cellular viability of different mammalian cell lines treated with crude king cobra venom	110
Appendix C.....	111
C1. Isolation of adult rat cardiomyocyte.....	111

C2. Spontaneous measurement of cardiac contraction and calcium profiles.....	115
C3. Hysteresis loop comparing between the propranolol and β -CTX.....	121
C4. Comparison effects between pre-treated β -CTX or propranolol on cardiomyocyte functions with the presence of isoproterenol (ISO).	122
C5. Comparison effects between pre-treated β -CTX or propranolol on cardiomyocyte functions with the presence of forskolin (FSK)	124
Appendix D	125
D1. Myofibril preparation from isolated cardiomyocytes.....	125
D2. SDS-PAGE protocols.....	127
D3. Staining protocol for phosphor-protein and total protein	129
D4. Western blot protocol.....	130
D5. Additional results from Phosphor-staining of other myofilament proteins	134
D6. Additional results from western blot analysis.....	136
Appendix E.....	137
E1. Isolation of skinned fiber bundles.....	137
E2. Measurement of the force-pCa relationship	142
Appendix F.....	145
F1. Isolation of myofibrils.....	145
F2. <i>In vitro</i> S1 actomyosin ATPase malachite green assay.....	147
Appendix G.....	151
G1. Construction and transformation of cleavable His ₆ -tag β -CTX in vector	151
G2. Large scale production and purification	155
REFERENCES.....	158
VITA.....	199



จุฬาลงกรณ์มหาวิทยาลัย
CHULALONGKORN UNIVERSITY

LIST OF TABLES

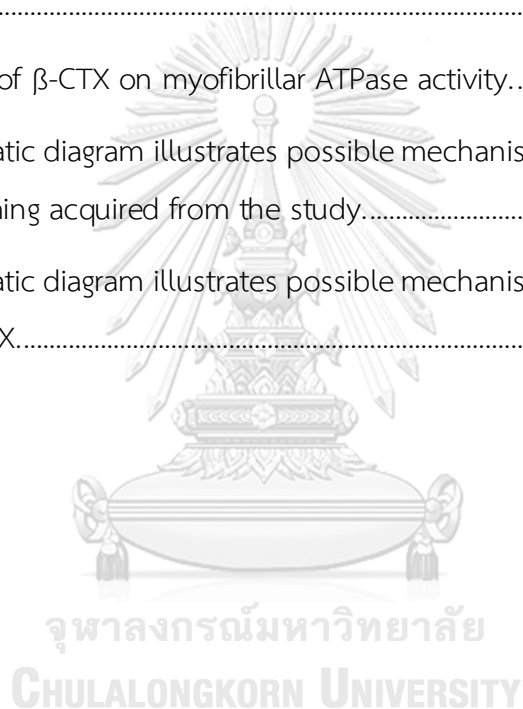
	Page
Table 1 Purification table verifying yielded of β -CTX from the crude KCV mass.....	48
Table 2. Comparison effects on cardiomyocytes between propranolol and β -CTX..	57
Table 3. Comparison effects in skinned fiber experiment between at the baseline and after receiving β -CTX. Data are represented in mean \pm S.E.M.....	73



LIST OF FIGURES

	Page
Figure 1. Schematic diagram represents the conceptual framework of the study.....	4
Figure 2. Diagram demonstrates the pathophysiology of heart failure	9
Figure 3. Schematic illustrates effects of β -adrenergic signaling on ventricular myocyte in terms of intracellular calcium and myofilament kinetics.	12
Figure 4. A three-dimensional structure of beta-cardiotoxin (β -CTX) derived from king cobra venom.....	22
Figure 5. Experimental designs determining effects of β -CTX on isolated rat cardiomyocytes in three different conditions.	30
Figure 6. Recordings and analyzing from Felix32™ software.....	33
Figure 7. Chromatographic profiles of the β -CTX purification.....	47
Figure 8. Cellular viability assay of β -CTX on different mammalian muscles cell lines.	50
Figure 9. Raw data acquisition from FeliX™32 software.....	54
Figure 10. Effects of β -CTX on isolated cardiomyocyte functions and calcium profiles.	55
Figure 11. Effects of propranolol on isolated cardiomyocyte functions and calcium profiles.....	56
Figure 12. Effects of β -CTX on functions and calcium profiles of ISO-induced cardiomyocyte.....	58
Figure 13. Effects of β -CTX on functions and calcium profiles of FSK-induced cardiomyocyte.....	63
Figure 14. Effects of β -CTX on total phosphor-proteins of cardiac myocytes at the basal state.....	65

Figure 15. Effects of β -CTX on total phosphor-proteins of ISO-induced cardiomyocytes.....	66
Figure 16. Western blot analysis of specific protein phosphorylated sites involved with β -adrenergic signaling responded to β -CTX.	69
Figure 17. Western blot analysis of specific protein phosphorylated sites involved with β -adrenergic signaling responded to β -CTX in ISO-induced cardiomyocytes.....	70
Figure 18. Force-pCa relationship of the detergent extract ("skinned") fiber bundle experiment.....	73
Figure 19. Effects of β -CTX on myofibrillar ATPase activity.....	75
Figure 20. Schematic diagram illustrates possible mechanisms of β -CTX on ventricular shortening acquired from the study.....	98
Figure 21. Schematic diagram illustrates possible mechanisms of ventricular relaxation by β -CTX.....	98



Chapter 1

Introduction

Cardiovascular diseases (CVDs) have been issued as one of the most important global health concerns (Moodie, 2016). According to WHO, CVDs accounted for the first rank cause of deaths globally involving more than 17 million deaths annually (Pons et al., 2010; G.B.D. collaborators, 2015). Heart failure (HF), a serious complication following CVDs, has also been rapidly growing with the estimation of more than 37.7 million individuals (Ziaei and Fonarow, 2016). In general, HF can be controlled by several strategies, including prescribing of pharmacological agents. These include renin-angiotensin-aldosterone (RAA) antagonists, diuretics, positive inotropic agents, and beta-blockers (BBs) (Yancy et al., 2013).

BBs are substances who block the binding of β -adrenergic agonists onto β -adrenergic receptors (Louis et al., 1994). Since the sympathetic nervous system is being overstimulated during HF condition, BBs are favorable for attenuating the overloaded of β -adrenergic signaling, the cAMP-PKA pathway (Rehsia and Dhalla, 2010). Therefore, BBs are well-documented for several prospects, such as prevention of angina pectoris, reducing systemic blood pressure and blockage of some arrhythmic pathways (Matsuda et al., 2000; Metra et al., 2001; Doughty et al., 2004; Zhang et al., 2015). To date, several BBs, such as carvedilol, metoprolol, and bisoprolol,

represented mortality benefits in HF patients with left ventricular dysfunction (Dargie, 1999; Goldstein and Hjalmarson, 1999; Poole-Wilson et al., 2003). Moreover, they were benefit for reducing chance of hospitalization in diastolic dysfunction patients (Smith et al., 2010). However, due to the limited choices of BB used in clinic to treat HF, seeking for newly BB is still required to substitute those medications.

Snake venoms, the concentrated protein cocktails, have now been interested by scientists. Despite their toxicities, bioactive components can potentially become novel pharmaceutical agents. This was firstly described by Ferreira, who discovered bradykinin-potentiating factor from the Brazilian pit viper (*Bothrops jararaca*) (Ferreira, 1965). Later, the compound was further developed into captopril, the prototype of recent angiotensin-converting enzyme inhibitors (ACEi). Until now, several snake-derived toxins have been developed for CVD benefits. Eptifibatide and Tirofiban were examples of drugs that been approved by the food and drug administration (FDA) of the United States as thrombolytic agents (Koh and Kini, 2012).

Beta-cardiotoxin (β -CTX) is a non-enzymatic protein isolated from the venom of King cobra (*Ophiophagus hannah*) (Rajagopalan et al., 2007). The previous study had proposed its β -blocker-like activity as demonstrated by its dose-dependent negative chronotropic effect and the *in vitro* binding properties on both β_1 and β_2 adrenergic receptors. Interestingly, it did not alter the contractility index in an isolated perfused heart study. These findings suggested that β -CTX

could potentially become a novel BB. However, the cellular mechanism of β -CTX on cardiomyocyte are still unknown and need to be established as a root of knowledge in developing a novel pharmacological compound. Also, the effects of β -CTX on isolated cardiomyocyte functions, its involvement of β -adrenergic signaling (β -AS), and its direct effects on myofilament kinetics had never been elucidated.

Research questions

1. What are the effects of β -CTX on isolated cardiomyocyte functions?
2. Whether the β -adrenergic signaling cascade is altered by the β -CTX action?
3. Does β -CTX have any impact on cardiac myofibril activity?

Research hypothesis

1. β -CTX may cause negative inotropic and lusitropic effects on isolated cardiomyocytes.
2. β -CTX may reduce the phosphorylation of the β -adrenergic cascade via the blockade of the β -adrenergic receptor.
3. β -CTX may reduce the activity of myofilament via the reduction of ATPase activity and suppression of myofibril Ca^{2+} -sensitivity.

Conceptual framework

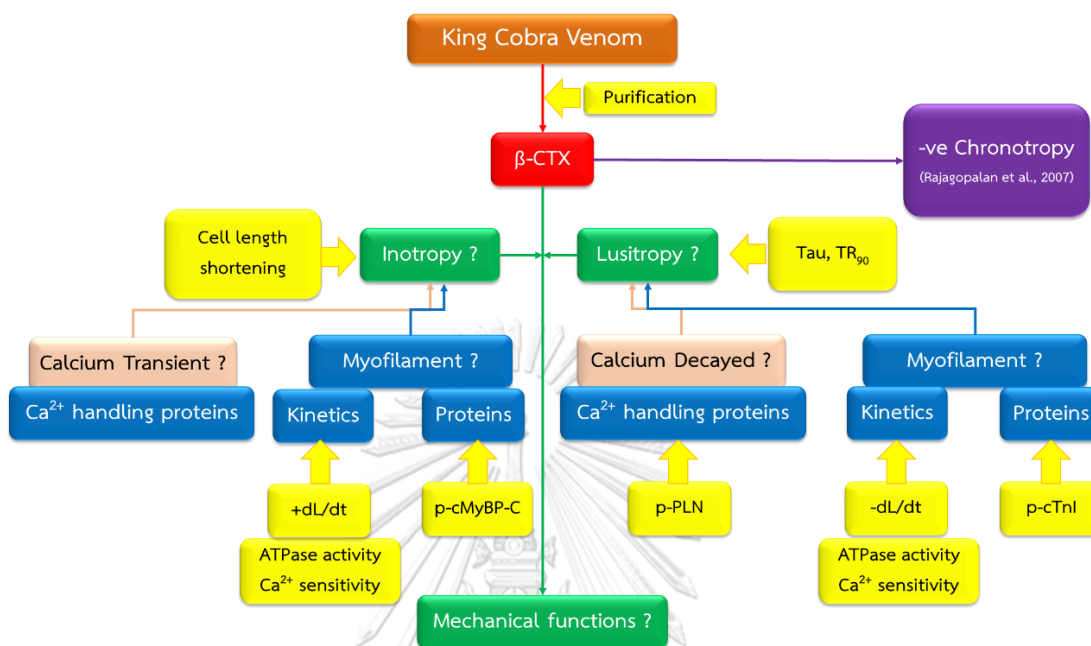


Figure 1. Schematic diagram represents the conceptual framework of the study.

Chapter 2

Literature review

1. Cardiovascular diseases: epidemiology and importance

Cardiovascular diseases (CVDs) are defined as groups of heart and vessel disorders. These are classified as cardiac abnormalities including congenital heart diseases, rheumatoid heart disease, cardiomyopathies, and cardiac arrhythmias, and vascular problems such as coronary heart diseases, cerebrovascular diseases, peripheral arterial diseases, deep vein thrombosis and pulmonary embolism (WHO, 2013). Recently, CVDs have become the most serious health issue globally. The diseases are accounted for the first rank cause of death with more than 17.3 million patients died annually (WHO, 2013). According to the Global Heart/World Heart Federation reports, among all global burden diseases, CVDs are presented in 20% and 24% of diseased men and women, respectively (Thomas et al., 2018). The problems are crucial in low-to-middle income countries where the rate of burden is ongoingly increased. As a result, too much expenditure was spent on these health issues. There are many risk factors involved in the occurrence of CVDs. Although, aging is one of the major factors as the diseases are gradually developed; however, behavioral factors including tobacco usage, less exercise, alcoholism, and unhealthy diet, accompanying with metabolic syndromes such as hypercholesterolemia,

diabetes, hypertension, and obesity are adjoining to cause CVDs (Zhao et al., 2015; Collins et al., 2017; Thomas and Lip, 2017). Therefore, in order to reduce the CVDs, these controllable factors are needed to be concerned.

2. Heart failure: pathophysiology and pharmacological approaches

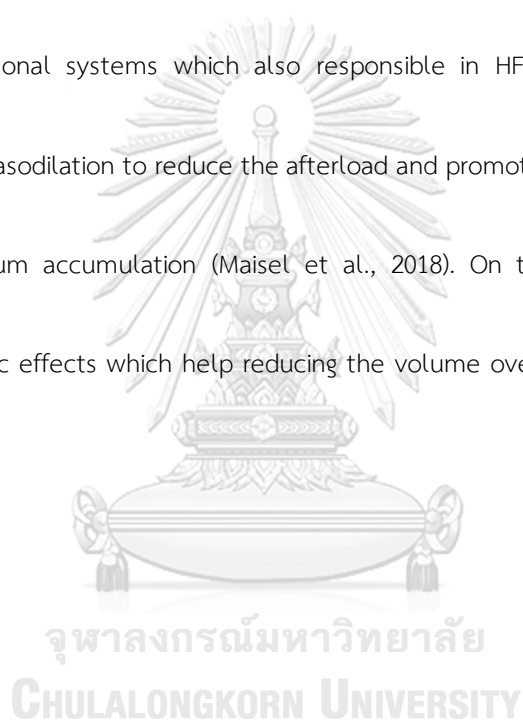
Heart failure (HF), are symptoms correlated with an inability of the heart to pump the blood to match the cellular demand (Kurmani and Squire, 2017). Apart from angina pectoris, which mostly presented in ischemic heart disease, HF is one of the most important complications occurring in CVDs patients. Recently, the HF issue has become more critical as there are more than 37.7 patients worldwide (Ziaeian and Fonarow, 2016). Besides, high expenditure on public health spending on this condition is also being reported (Savarese and Lund, 2017). Therefore, the prevention and management of heart failure are being suggested and encouraged nowadays.

Clinical syndromes associated with HF are majorly classified into two groups, right or left-sided congestive heart failure (CHF) (Tanai and Frantz, 2015). Left CHF is considered as either pressure or volume overload in pulmonary circulation resulting in pulmonary edema; and hence, causing dyspneic signs. The left ventricular dysfunction also creates low stroke volume which causes hypoperfusion to peripheral tissues. Therefore, several symptoms such as renal dysfunctions, collapse, exercise intolerance, and cardiac cachexia may occur. On the other hand,

right-sided CHF is characterized by the failure of the heart to receive the blood returning from tissues. Consequently, fluid accumulation, effusion or edema, may appear in associated with this condition. Vascular distention is a result of severe vasodilation responded by increasing of body reservoir and capacity.

In pathophysiological view, either systolic or diastolic dysfunction of the heart are the underlying cause of hypoperfusion and venous pressure symptoms (Figure 2). The mechanism begins with any CVDs that cause inadequate cardiac output. The reduction in stroke volume triggers the baroreceptor and further stimulates sympathetic nervous system. Catecholamines, such as epinephrine, norepinephrine and dopamine, are the main chemokines to ameliorate cardiac output by promoting Ca^{2+} influx to the cardiac cells resulting in positive chronotropy and inotropy. As a result, the elevation in the heart rate and contractility will increase the cardiac output to compensate the heart failure mechanism. In addition, catecholamines also directly stimulate the renin-angiotensin-aldosterone system. The hormonal pathway maintains the body pressure via the increased production of angiotensin II, causing vasoconstriction, and aldosterone, re-uptaking sodium and water, causing fluid retention. However, continuity of HF promotes the overactivity of neurohormonal systems which further worsen HF itself. The mechanisms include the overactivity of sympathetic nervous system and catecholamines, which resulted in cardiac hypertrophy, severe vascular hypertension as well as the RAAS overactivation. High amount of

angiotensin II elevates the vascular resistance and afterload whereas the aldosterone deteriorates the venous return and increases the preload of the heart. Consequently, cardiac hypertrophy, arrhythmias and fibrosis may occur. Finally, the end stage HF patients may suffer from irreversible cardiovascular remodeling as well as cardiac dysfunctions (Mazurek and Jessup, 2017). Apart from the RAAS, natriuretic peptides (NP) and antidiuretic hormone (ADH), or arginine vasopressin (AVP) are other two hormonal systems which also responsible in HF condition. The prior system majorly causes the vasodilation to reduce the afterload and promotes the natriuresis to suppress the water and sodium accumulation (Maisel et al., 2018). On the other hand, ADH majorly promotes the diuretic effects which help reducing the volume overload in HF condition (Riegger et al., 1982).



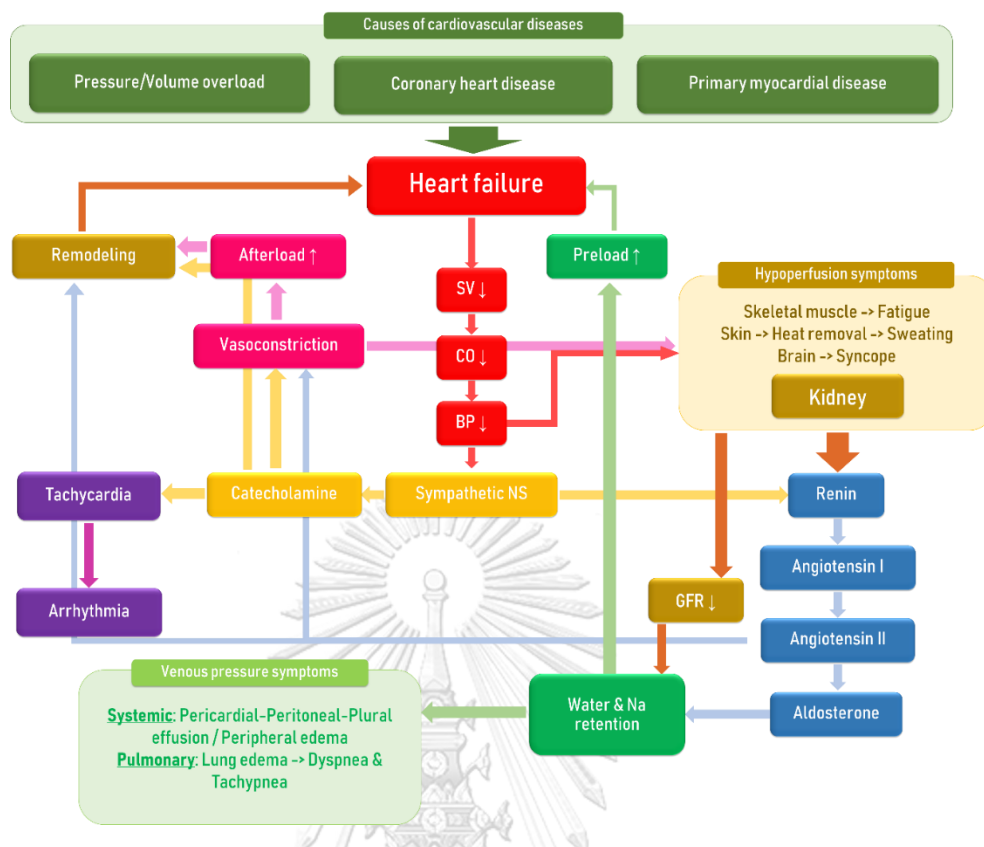


Figure 2. Diagram demonstrates the pathophysiology of heart failure

According to the guideline for the management of heart failure by the American Heart Association (AHA) and American College of Cardiology Foundation (ACCF) (Yancy et al., 2013), HF is classified into 4 clinical stages. Stage A refers to the high-risk patient without any structural heart disease or symptoms. Stage B is considered as patients with structural heart disease without showing any clinical manifestations. Stage C is used when the symptoms of heart failure are presented with promising cardiac structural changes. And finally, Stage D or end-stage HF represents the refractoriness of the disease to medications where the intervention is needed in the sufferers. To be easy for managing HF, patients are divided as an HF with either reduced (HFrEF) or preserved (HFpEF) ejection fraction. The former is considered in CVDs patients with EF less than 40% (also known as systolic HF) whereas the latter exhibited a high EF at more than 50% (also known as diastolic HF). To control heart failure, several drugs are recommended, including, angiotensin-converting enzyme inhibitors (ACEi), angiotensin receptor blockers (ARB), aldosterone antagonists, diuretics, positive inotropes, vasodilators, and β -blockers (BB) (Maron and Rocco, 2015).

3. β -adrenergic signaling, Ca^{2+} homeostasis, and myofilament kinetics

As the sympathetic nervous system is continuously being stimulated during HF conditions, the internally circulated β -agonists, including adrenaline, noradrenaline, dopamine or

dobutamine, are always being released. When they bind to the β -adrenergic receptors (β -ARs) at the ventricular myocytes (Figure 3), the G-protein subtype s, cooperated with the receptors, is activated and further promotes the activity of adenylyl cyclase (AC). The enzyme turns ATP into cAMP and increases the activity of protein kinase A (PKA). This protein is the major signaling messenger that phosphorylates other proteins in the cells; especially, Ca^{2+} -handling proteins and myofilament proteins. Phosphorylation of Ca^{2+} -handling proteins, such as L-type Ca^{2+} channel (LTCC), ryanodine receptor (RyR) and phospholamban (PLN), promote the enhancement of Ca^{2+} transients and decayed (Karczewski et al., 1987; Piacentino et al., 2003). Besides, phosphorylation of myofilament proteins, including cardiac myosin binding protein-C (cMyBP-C), cardiac troponin I (cTnI) and myosin light chain (MLC), enhance the myofilament kinetics (Wegener et al., 1989; Verduyn et al., 2007; Colson et al., 2010; Gupta and Robbins, 2014; Nixon et al., 2014). Combining both mechanisms, the ventricular myocytes increase the performance of inotropic (contraction) and lusitropic (relaxation) properties (Biesiadecki et al., 2014). Nevertheless, other factors which may alter the cardiac contractile properties are the increment of the Ca^{2+} sensitivity of myofilament proteins, cardiac troponin C (cTnC) or calmodulin (CaM), or the enhancement of actomyosin ATPase activity which promotes the cross-bridge kinetics (Cappelli et al., 1989; Olsson et al., 2004).

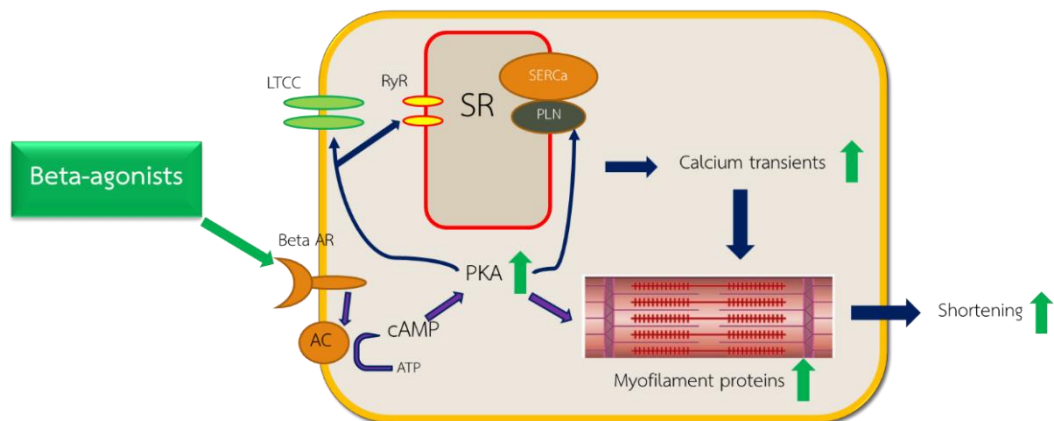


Figure 3. Schematic illustrates effects of β -adrenergic signaling on ventricular myocyte in terms of intracellular calcium and myofilament kinetics.

AR: adrenergic receptor; AC: adenylyl cyclase; ATP: adenosine triphosphate; cAMP: cyclic adenosine monophosphate; PKA: protein kinase A; LTCC: long-type Ca^{2+} channel; RyR: ryanodine receptor; PLN: phospholamban; SERCa: sarcoplasmic reticulum Ca^{2+} pump.

4. Beta-blockers: actions and benefits

As mentioned in AHA's heart failure management, BBs are recommended to use in both HFrEF and HFpEF patients (Yancy et al., 2013). This is because that β -blocking agents have vast majority effects which help to reduce the vicious cycle of heart disease progression. Firstly, they have a direct property to inhibit the binding of catecholamines on β -ARs, especially, type-1-receptor on the heart and type-2 on the vessel's smooth muscles. With this effect, the downstream signaling is also being interfered. For instance, the cAMP-PKA pathway, which promotes the phosphorylation of various proteins in the cells, is reducing its activity (Rehsia and Dhalla, 2010). The inhibition of the receptor by some BBs also counteracted the progression of cardiac remodeling. Carvedilol, one of the widely used BBs, significantly reduced the intracellular Ca^{2+} overload in heart failure condition, as well as the diastolic Ca^{2+} sparking from the sarcoplasmic reticulum (Mochizuki et al., 2007). This may be a possible underlying pathway that inhibits the progression of left ventricular hypertrophy/apoptosis in patients (Doughty et al., 2004). Apart from the heart effect, some BBs can also cause vasodilation via other mechanisms. For example, Carvedilol has a partial effect on α_1 -AR blocking accompanying with an anti-oxidative property which helps improve coronary circulation in acute myocardial infarction patients (Matsuda et al., 2000). Finally, the negative chronotropic effect, via the inhibition of the rapid depolarization and repolarization phases, could reduce the possibility of arrhythmia

occurrence. Prolongation of the refractory period by BBs can interfere the re-entrant mechanism which benefited for several arrhythmic conditions, such as atrial fibrillation and ventricular tachyarrhythmias (Gheorghiade and Lukas, 2004; Zhang et al., 2015).

Recently, several BBs have been introduced for controlling HF patients. Carvedilol (COMET trial), bisoprolol (CIBIS-II trial), and metoprolol (MERIT-HF trial) are three agents which have been proved for mortality benefits (CIBIS-II, 1999; MERIT-HF, 1999; Poole-Wilson et al., 2003). Despite improving mortality rate, other BBs are still recommended to use as an antiarrhythmic agent, including acebutolol, atenolol, esmolol, and nadolol (Al-Khatib et al., 2018). Therefore, BBs are proved to be one of the most important medications to control HF and arrhythmias. Nevertheless, current BBs still have some side-effects such as postural hypotension, dizziness, headaches, and interference on glycemic control (Louis et al., 1994). Moreover, high reports of drug intolerance may worsen HF outcomes which resulted in drug withdrawal (Waldo et al., 1996). Hence, newly β -blocking agents are still needed for substituting recently used BBs.

5. Venomous snakes and snakebites issues

Snakes are one of the most well-known venomous animals. These Squamate reptiles were distributed around the world with more than 35,001 types (Russell, 2001). Among of these, over 400 genera and more than 2,500 species can produce venom (Gutierrez et al., 2017)

Venomous snakes were categorized in the superfamily Colubroidea and were subdivided into 5 families, Viperidae, Elapidae, Hydrophiidae, Atractaspididae and Colubridae (Valenta, 2010). Their venoms were produced in the venom glands and the accessory glands which were located beside the salivary glands. The venom would flow throughout their apparatus, including the venom groove, the venom duct, and release via the orifice of the venom fang (Vonk et al., 2013). However, the venom apparatus in each family was different. Majorly, the front-fanged snakes (viperids, elapids, and hydrophiids) possess the large venom glands with the large basal lumen. They also have the specialized compressor muscles which squeezing the bolus of venom throughout the apparatus. Likewise, some rear-fanged snakes such as atractaspid species also possessed large glands and muscles. Differently, the colubrid snakes, with a primitive venomous apparatus, had an undeveloped apparatus (aglyphous) which contained small glands connected to the posterior ligament that attached with the jaws. Also, the natural habitats and behaviors of those snakes were specific. For instance, the hydrophiids, water snakes, were usually like to live near the seaside, the elapids lived in damp or tropical rainforests, the atractaspidids, burrowing asps, would like to live in the underground and the tunnels, and the viperids would prefer to live in the dry area (Valenta, 2010). Typically, the mechanism of snakebites has 4 steps, striking, mouth opening and fang elevation, venom injection, and fang retractions (Fairley, 1934).

Interestingly, half of the snakebites may cause “dry bites”, where the snakes did not release the venom.

Snakebite envenomation is currently classified in a high priority list of neglected tropical diseases (NTDs) (Williams et al., 2019). It has become a serious issue as more than 2.7 million people were bitten by the venomous snake yearly and 125,000 deaths were reported (Kasturiratne et al., 2008; Adukauskiene et al., 2011). Unfortunately, among non-lethal patients, 400,000 of them were experienced with limb amputations or permanent disabilities (Williams et al., 2019). Thailand, the tropical climate country, had also been issued at least 9,000 snakebite patients and 90 deaths per year (Kasturiratne et al., 2008). Various clinical signs were presented in patients which could be classified by their different pathological complications, for instance, local tissue necrosis or swelling, bleeding disorder and coagulopathy, cerebral arterial thrombosis, neurological signs (convulsion, paralysis, ptosis) and renal failure (WHO, 2010).

6. Snake venom compositions and the importance of toxinology

Snake venom is a cocktail of various bioactive compounds. Regarding the compositions, proteins and peptides are majorly found with vast majority effects. According to the proteomic profiles, 59 protein families were found in the snake venoms. These were classified into four dominant protein families: phospholipases A₂ (PLA₂), metalloproteases (SVMP), serine proteases

(SVSP) and three-finger toxins (3FTX); six secondary protein families: cysteine-rich secretory proteins (CRISP), L-amino acid oxidases (LAO), Kunitz peptides (KUN), C-type lectins (snaclec/CTL), disintegrins (DIS) and natriuretic peptides (NP); nine minor proteins: acetylcholinesterases, hyaluronidases, 5' nucleotidases, phosphodiesterases, phospholipase B, nerve growth factors, vascular endothelial growth factors, vespryns/ohanin, metalloproteinase inhibitors; and thirty-six rare protein families (Tasoulis and Isbister, 2017). Literally, these proteins are classified into two groups, with and without enzymatic properties. The most abundant for the former groups are PLA₂ (Kini, 2003), where the most non-enzymatic toxin found in snake venoms are 3FTXs (Utkin, 2013). Apart from these, small molecules including short-chained peptides or polyamines (Aird et al., 2016) and low molecular weight non-peptide molecule (Saha et al., 2006) are also characterized from the snake venoms.

Due to the variety of substances in snake venom, toxinology, studying in snake venom toxins, has been established by researchers for several reasons. Firstly, to understand the underlying mechanisms involved with the pathological effects in patients. Findings would allow doctors and veterinarians to be aware complications sequentially come after snake envenomation. Recently, snakebites are classified into 3 groups by their major effects on patients, neurotoxicity, hematotoxicity, and myotoxicity. Clinical features appear on snakebite patients with unknown snake types that may help the doctor suspect the snake species (Gutierrez et al.,

2017). In addition, understanding the major active ingredient would help us understand the pathophysiology occurring in snake envenomated patients. The second purpose of studying snake venom is to use an antivenin or other molecules to counteract the effect. Although antivenin is well-known to be the best option for treating snake envenomation, recent technologies have developed several molecules including engineered specific antibodies or nanoparticles regarding this purpose. Specifically blocking of the active ingredient may help inhibit the clinical manifestation in snakebite patients (Alvarenga et al., 2014; O'Brien et al., 2018). Thirdly, in the mean of knowing components in this cocktail, several ingredients were selected for use as research tools. For example, a muscarinic toxin isolated from the green mamba (*Dendroaspis angusticeps*) was characterized as a muscarinic cholinergic receptor blocker. The compound was used for studying the functional role of this receptor in both normal and pathological conditions (Servent and Fruchart-Gaillard, 2009; Servent et al., 2011). Lastly, despite their toxicity, bioactive compounds isolated from snake venoms may have therapeutic effects. Fully understanding the precise mechanism of the compounds may lead us to novel drug development or introducing new knowledge to the pharmaceutical industry (Chan et al., 2016b). The advantage has been started since captopril, the prototype of an angiotensin-converting enzyme inhibitor (ACEi), was discovered (Ferreira, 1965). Later on, several drugs originated from the venom were gradually approved by the American Food and Drug Administration (FDA), such

as eptifibatide and tirofiban, the disintegrin-derived drugs (Koh and Kini, 2012). Batroxobin, the thrombin-like serine protease enzyme, and Ximelagatran, the thrombin inhibitor derived from cobra venom, were also been approved to use clinically outside the USA for stroke or deep vein thrombosis patients (Mohamed Abd El-Aziz et al., 2019). Therefore, snake venoms are the interesting resources of natural products which perhaps comprises lots of undiscovered potential therapeutic compounds.

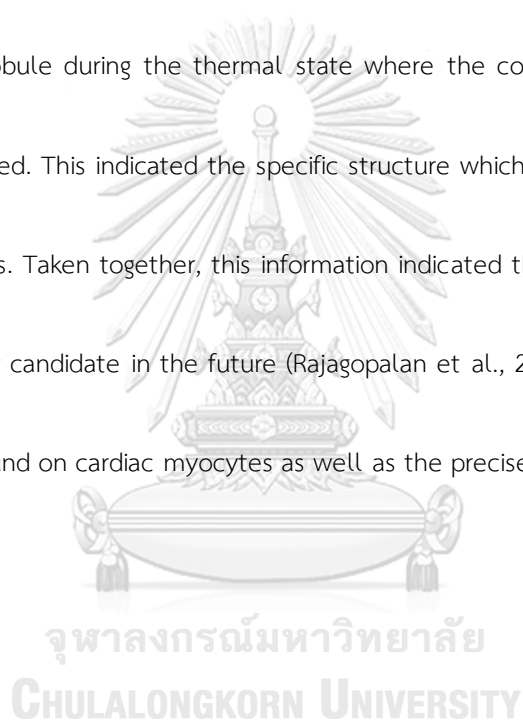
7. King cobra venom and the discovery of β -CTX

King cobra (*Ophiophagus hannah*), a member of the Elapid family, is the longest venomous snake in the world. It is majorly distributed in the South East of Asia as well as some parts of China and India (Stuart et al., 2012). The king cobra bites are deadly as the 50% lethal dosage (LD_{50}) in the mice was approximately 1.1 – 1.6 $\mu\text{g/g}$, intraperitoneally, and 0.59 $\mu\text{g/g}$, intramuscular (Tan and Hj, 1989; Danpaiboon et al., 2014). Focusing on the genomic profiles of the *O. hannah* venom, the major components found in the venom gland were 3FTXs (66.73%) where lectins were majorly encoded in accessory glands (42.70%) (Vonk et al., 2013). In the same manner, transcriptomic profiles of this snake venom, the most mRNAs transcribed belonged to the 3FTXs family (84.9%) (Tan et al., 2015). This was followed by SVMPs (3.68%), PLA_2 (2.16%), and CRISP (2.12%), respectively. Likewise, proteomic profiles of the King cobra venom

consistently represented that 3FTXs were the most abundant toxins found in Malaysian's (44.01% of crude mass) and Indonesian's (64.2% of crude mass) (Petras et al., 2015; Tan et al., 2015). All proteins included in 3FTXs were constructed with 2 β -pleated, containing five small β -strands with 4-5 disulfide bonds making 3 loops extended from the globular hydrophobic core (Roy et al., 2019). 3FTXs from the venom of King cobra were classified into 5 groups upon their structures and actions, including long-chain neurotoxin, short-chain α -neurotoxins, weak toxins, muscarinic toxin-like peptide and cardiotoxins (Petras et al., 2015). Examples of King cobra's 3FTXs were including Hannalgesin (Oh55), a long-chain neurotoxin which exhibits analgesic effect via the nitric oxide activation (Pu et al., 1995), short-chain α -neurotoxin (Oh9-1) (Chang et al., 2002), Haditoxin, the muscarinic toxin-like (Roy et al., 2010) and weak toxins DE-1 which have not been elucidated their function yet (Joubert, 1973; Joubert, 1977; Chang et al., 2006).

Beta-cardiotoxin (β -CTX), a novel member of 3FTXs had been firstly characterized in 2007 (Figure 4) (Rajagopalan et al., 2007). β -CTX or CTX-27 is the protein isolated from the King cobra venom which contains 63 amino acids, and the molecular weight is approximately 7 kDa (Rajagopalan et al., 2007). The structure consists of 5 beta-pleated strands constructing the 2 large beta-sheets. Combining the 4 pairs of disulfide bonds, the structure of β -CTX is three-finger-like with the hydrophobic globular C-terminal core (Figure 4) (Roy et al., 2019). The compound has been proposed to be a novel β -blocking agent as it could reduce the heart rate in animal

models. Moreover, the compound can also shift the binding of the synthetic β -agonist on both β_1 and β_2 adrenergic radio-labeled receptors. In addition, *ex vivo* isolated heart on the Langendorff apparatus was conducted and it showed unchanged in the left ventricular diastolic pressure. Structural change of the compound was further analyzed to clearly understanding the mechanism related to this activity (Roy et al., 2019). According to the study, β -CTX presented the α -helical molten globule during the thermal state where the conformational plasticity of the compound was altered. This indicated the specific structure which might play an important role in inhibiting the β -ARs. Taken together, this information indicated the potential of this protein to be a novel β -blocker candidate in the future (Rajagopalan et al., 2007). However, the functional study of the compound on cardiac myocytes as well as the precise mechanisms has never been investigated.



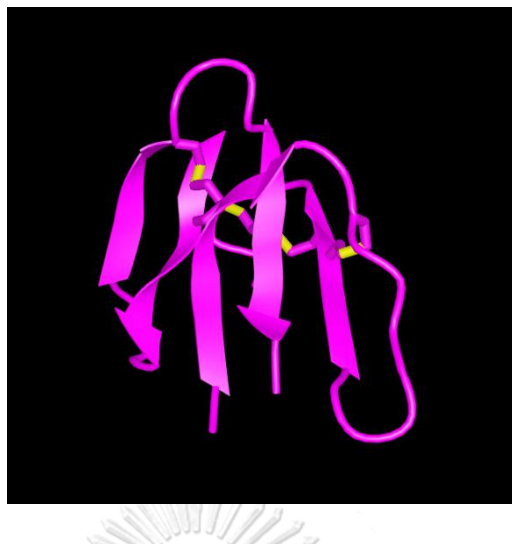


Figure 4. A three-dimensional structure of beta-cardiotoxin (β -CTX) derived from king cobra venom. The protein contains 63 amino acids with 5 β -pleated strands (pink arrows). Comparing to other elapid-derived cardiotoxins, it is proposed that the secondary three-finger-like structure is formed by 4 disulfide bonds at C3-C22, C15-C40, C44-C55 and C56-C61 (yellow bar). Of note, the C-terminus possesses the hydrophobic globular core (Rajagopalan et al., 2007).



Chapter 3

Materials and methods

1. Isolation and purification of β -CTX

1.1. Crude venom

Lyophilized crude venom of Thai King Cobra (KCV) was purchased from Queen Saovabha Memorial Institute (QSMI, Thai Red Cross society, Thailand). Two-step chromatography, reverse-phased, and anion exchange chromatography were selected to purify β -CTX.

1.2. Reverse phased HPLC (RP-HPLC)

Two-step chromatography, reverse-phased, and cation exchange techniques were selected to purify β -CTX. The RP-HPLC procedure was modified from the previously described protocol (Petras et al., 2015). The filtered crude venom (50 mg/mL) was applied to Grace[®] C18 column (Vydac 218TP[™]; 5 μ m, 300 $^{\circ}$ A, 4.6 x 250 mm; Supplemental Figure S 1D). Column was equilibrated with 0.1% v/v TFA and eluted using 80% acetonitrile (ACN) in 0.1% TFA. The solutions preparation and the gradients of the elution buffers are represented in appendix A1. The solutions were run under HPLC binary system (Waters[®] 1525) at the flow rate of 1 mL/min. Peaks were detected at 215 nm using a UV/Visible light detector (Waters[®] 2489) for 161 minutes.

Fractions were collected manually and the presence of β -CTX was determined using SDS-PAGE and N-terminal sequencer. β -CTX-containing fractions were then pooled together, lyophilized (FreeZone6; Labconco[®]), and kept for further purification.

1.3. Cation exchange chromatography

Lyophilized fractions from RP-HPLC, with the presence of β -CTX, were subsequently fractionated by a cation exchange chromatography (Waters[®] Protein Pak[™] SP 5PW, 7.5 x 75 mm; Supplemental Figure S 1E). The column was pre-equilibrated with 0.05 M sodium phosphate buffer, pH 7.4 (SPB), and eluted using 0.05 M SPB with 0.5 M of NaCl, pH 7.4. The preparation of solutions and procedures are noted in appendix A2. The presence of proteins was detected at 280 nm. Fractions were desalted using Spectra/Por[®] cellulose ester dialysis membrane (100-500 Da molecular weight cutoff). The presence of β -CTX was confirmed using SDS-PAGE and N-terminal sequencer. Purified β -CTX was lyophilized and the powder was kept at -80°C until used.

1.4. Protein determination & identification

Following the fractions collected, estimated protein concentration was determined using a UV spectrophotometer at 280 nm absorbance. Fractions were concentrated using vacuum centrifuge (Vacufuge[™]; Eppendorf) to obtain a total protein of 5 μ g. Samples were loaded into the gels and electrophoresed using a precast 4–12% Bis-Tris gel (NuPAGE[®]; Novex), at a constant

100 Volts for 95 minutes, with the reducing condition. To detect protein bands, gels were stained with SimplyBlue™ SafeStain (Life Technologies®) and background was de-stained using ultrapure water. To investigate the amino acid sequence, gels were then transferred onto 0.45 µm polyvinylidene fluoride (PVDF) membrane (Immobilon™-P; EMD Millipore®) at a constant 25 voltage for 90 minutes. Following the transferring process, selected bands were cut manually and loaded into automated Edman degradation N-Terminal sequencer (PPSQ-33B; Shimadzu®). The first 14 amino acid residues were analyzed by its commercial software (PPSQ-30 Analysis; Shimadzu®). Sequences of the acquired peptide were blasted on an online website to identify the presented bands (<https://blast.ncbi.nlm.nih.gov/Blast.cgi?PAGE=Proteins>).

2. *In vitro* cellular viability study

2.1. Cell culture

Prior to introducing β-CTX for cardiomyocyte functional tests, *in vitro* cellular viability study was conducted. Three muscle cell lines, mouse myoblast; C2C12 (ATCC®, CRL™-1772), rat smooth muscle cell; A7r5 (Sigma Aldrich®, Cat No. 86050803), and rat cardiomyoblast; H9c2 (ATCC®, CRL™-1446), were recruited in the study. All cell lines were cultured in Dulbecco's Minimum Essential Medium (DMEM; ATCC®, 30-2002) containing 10% fetal bovine serum, 50 U/mL of penicillin and 50 µg/mL of streptomycin. Cell media were changed every 2 days. Cellular

morphology was monitored daily and the cells were passaged when the complete layer of cells was observed.

2.2. *In vitro* MTT assay

The MTT (methyl-thiazol-tetrazolium) assay was conducted to test the *in vitro* cellular viability on different muscle cells. Cells in the culture flasks were harvested and loaded into each well for 1.5×10^5 cells of C2C12, 5×10^4 cells of A7r5, or 1.5×10^4 cells of H9c2. The cells were incubated in 37°C , 5% CO_2 overnight. Crude venom or β -CTX fractions were prepared in two-fold dilution in phosphate buffer saline (PBS) and filled into the wells. Culture media controls (cells in media with adding PBS instead of venom) and media blanks (no cells with media added) were also run in parallel. Each experiment was carried out in triplicate. Microscopic changes of cells were captured at 0 and 24 hours after incubation. After 24 hours, cells were then loaded with 12 μL of 0.5% MTT solution. Four hours later, media was removed and 200 μL dimethyl sulfoxide (DMSO) was re-added. Formazan color was detected using the absorbance at 570 nm.

3. Effects of β -CTX on isolated cardiomyocyte functions

3.1. Animals and animal used protocols

All animal use protocols were approved by the institutional animal care and use committee of the University of Illinois at Chicago (ACC protocol number 17-178). Male Sprague Dawley rats (3-5 weeks old, 180-250 grams) were used.

3.2. Isolation of adult rat ventricular myocytes

The ventricular myocytes isolation protocol was modified from the mouse ventricular myocyte isolation (Wolska and Solaro, 1996). Rats were anesthetized using pentobarbital sodium combining with heparin, intraperitoneally. After fully unconscious, heart and aorta were then cut and weighed. The heart was cannulated to the Langendorff apparatus and perfused with the perfusion solution (in mM; NaCl 133.5, KCl 4, NaH_2PO_4 1.2, HEPES 10, MgSO_4 1.2, dextrose 33.33 and 0.1% BSA) for 3 minutes. The perfusion was switched to the enzyme solution (perfusion solution containing CaCl_2 20 μM , 0.025% of collagenase II (Worthington[®]) and 0.003% of protease XIV (Sigma[®]) until the heart became completely digested. Ventricles were cut and in 50 μM Ca^{2+} -reintroducing solution for 10 minutes. Cells were filtrated and gravitated for 7 minutes. Consequently, cells were gradually reintroduced with 0.1, 0.2, 0.5, and 1 mM of CaCl_2 . At the final

concentration, the isolation with more than 70% of alive cells (rectangular, non-spontaneously contracting cells) was used for functional study.

3.3. Experimental designs

Aims of the study were to determine the effects of the compound on isolated cardiomyocyte in mechanical and Ca^{2+} -homeostasis aspects. Experiments were majorly separated into three protocols 1) at the basal state, 2) with the presence of isoproterenol (ISO), the β -adrenergic agonist, and 3) with the presence of forskolin (FSK), the adenylyl cyclase (AC) activator.

3.3.1. Effects of β -CTX on isolated cardiomyocytes at the basal condition

To understand the direct effect of β -CTX on isolated cardiomyocyte, cells were perfused with either compound in various concentrations. Briefly, rats were separated into 2 groups, which were β -CTX-treated and propranolol-treated. Control solution (in mM; NaCl 133.5, KCl 4, NaH_2PO_4 1.2, HEPES 100, MgSO_4 1.2, dextrose 33, CaCl_2 1.8) was used as the baseline measurement. Five concentrations were perfused to cells differently in each treatment, propranolol; 0.1, 1, 3, 10, and 30 μM , and β -CTX; 10, 30, 100, 300, and 1000 nM (Figure 5A).

3.3.2. Effects of β -CTX on isolated cardiomyocytes with isoproterenol stimulation

To clarify the β -blocking effect of β -CTX, cells were pre-incubated with the compound and perfused with the β -adrenergic stimulating drug as a dose-response curve. In this study, we

used ISO to stimulate the cells after pre-incubated with compound comparing to propranolol. In each stimulators experiment, cells were divided into 3 groups including 1) positive control-cells treated with ISO only, 2) cells pre-incubated with 0.3 μM propranolol followed by ISO (PP-ISO), and 3) cells pre-incubated with 0.3 μM of β -CTX followed by ISO (β -CTX-ISO). Concentrations of ISO used in the study were 1, 3, 10, 30, 100, 300 and 1000 nM (Figure 5B).

3.3.3. *Effects of β -CTX on isolated cardiomyocytes with forskolin stimulation*

To understand whether β -CTX can directly suppress the cAMP-PKA pathway or not, cells were treated in the condition of FSK stimulation. Similarly, cells were separated into 3 groups mimicking the previous ISO experiment in which FSK was used instead of ISO. They were including 1) the FSK-treated cells, 2) pre-incubation with 0.3 μM propranolol before FSK (PP-FSK), and 3) pre-incubation with 0.3 μM β -CTX prior to FSK (β -CTX-FSK). The concentration of FSK used in the study were 0.1, 0.3, 0.5, 1, 2, and 3 μM (Figure 5C).

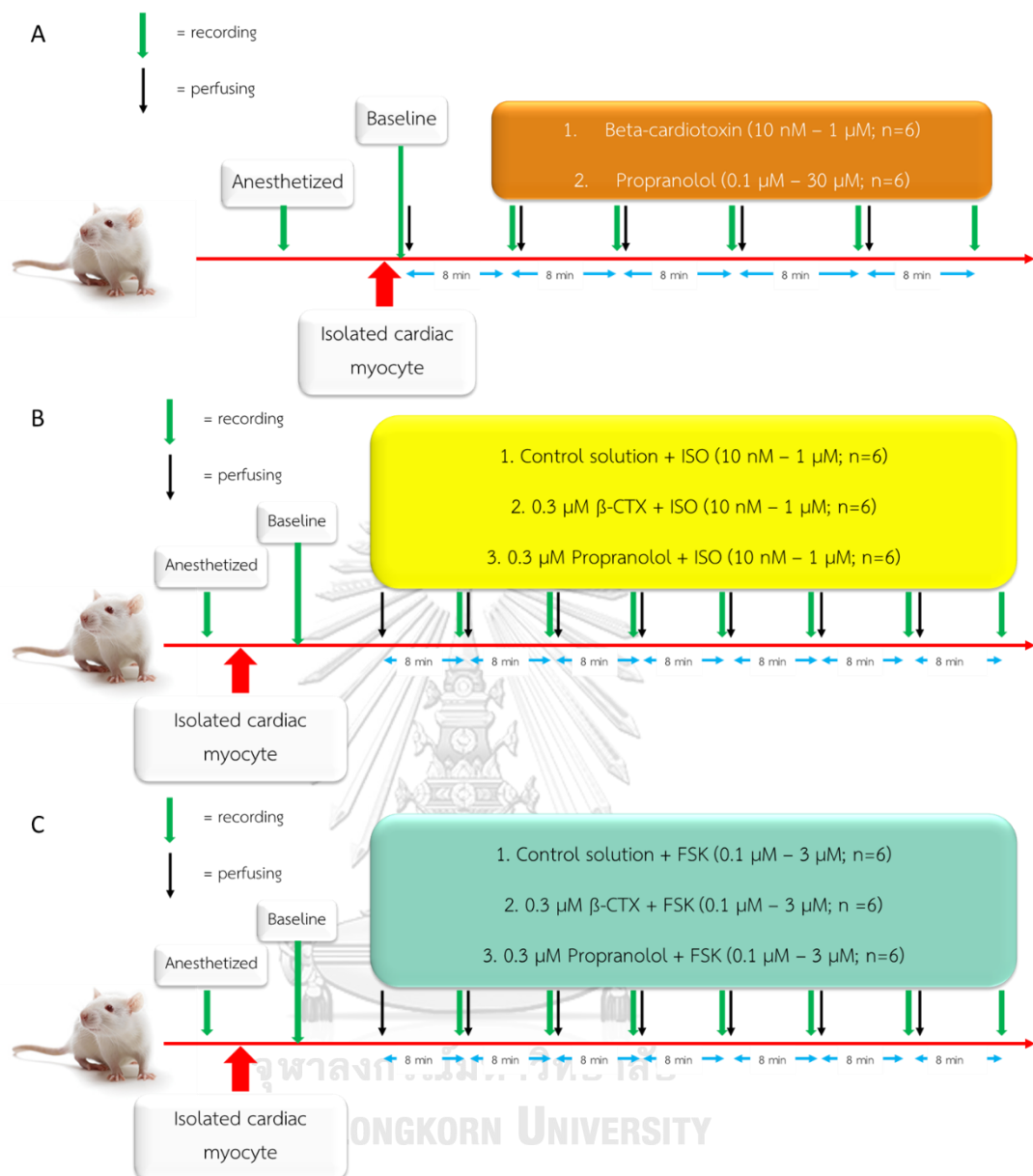


Figure 5. Experimental designs determining effects of β -CTX on isolated rat cardiomyocytes in three different conditions.

(A) At the basal state, (B) with the presence of isoproterenol, and (C) with forskolin (FSK).

3.4. Simultaneously measurement of myocardial contraction and calcium profiles

3.4.1. *System setup and cell preparation*

The simultaneous measurement of cellular mechanical function and Ca^{2+} -homeostasis was performed under Photon Technology International (PTI[®]) system. Measurement was conducted in a fluorescence-free room. Following the isolation, cells were diluted 20-fold in control solution (950 μL of control solution and 50 μL of cells solution) and 3 μL of Fura-2 AM (Invitrogen[™]), then the solution was loaded into the chamber of the inverted fluorescence microscope (Nikon[®] eclipse). We incubated the cells with Fura-2 AM for 10 minutes to allow the fluorophore to enter the cells. Then, to de-esterify, the control solution was perfused for 20-30 minutes. Non-spontaneously beating and isolated rectangular-shaped myocytes were selected for the study. The aperture was rotated to project visual on charged coupled device (CCD) camera (Hamamatsu[®]; XC-77). Cell contraction was measured and controlled by the video edge detector (Crescent electronics[®]; VED-105). Calcium profiles were acquired by excitation of Fura-2 AM at 340 and 380 nm, respectively representing Ca^{2+} -binding and Ca^{2+} -free Fura-2 AM and detected the emission at 505 nm using fluorescence lamp source (DeltaRam X[™]; PTI[®]). The signal was amplified by the photomultiplier tube (PMT; Model 814[™]). All data acquisition system (Digidata[®] 1440a) was recorded on the compatible software (FeliX32 1.42B[™], PTI[®]). Baseline data were

obtained prior to any treatments. According to the calibration, 8 minutes at a flow rate of 0.5 mL/min was used to replace the solution in chambers. Data were obtained from 8-10 contractions in each measurement. At least 3 cells (replicates) were used for one sample.

3.4.2. *Parameters and data analysis*

Digital information was transformed into numbers and automatically analyzed using Felix32 (Figure 6A) and LabChart 7™ software. Parameters acquired from the study were classified into three parts, inotropic parameters, lusitropic parameters, and calcium profiles. Contractile parameters comprised the percentage of cell length shortening and shortening velocity (+dL/dt) (Figure 6B). Cardiac lusitropy was assessed by the relaxation constant (τ ; τ), time-to-90% re-lengthening (TR_{90}) and re-lengthening velocity (-dL/dt) (Figure 6B). Finally, calcium profiles were including the amplitude of Ca^{2+} -transient (CaT) and calcium decaying time (τ_{Ca}) (Figure 6C).

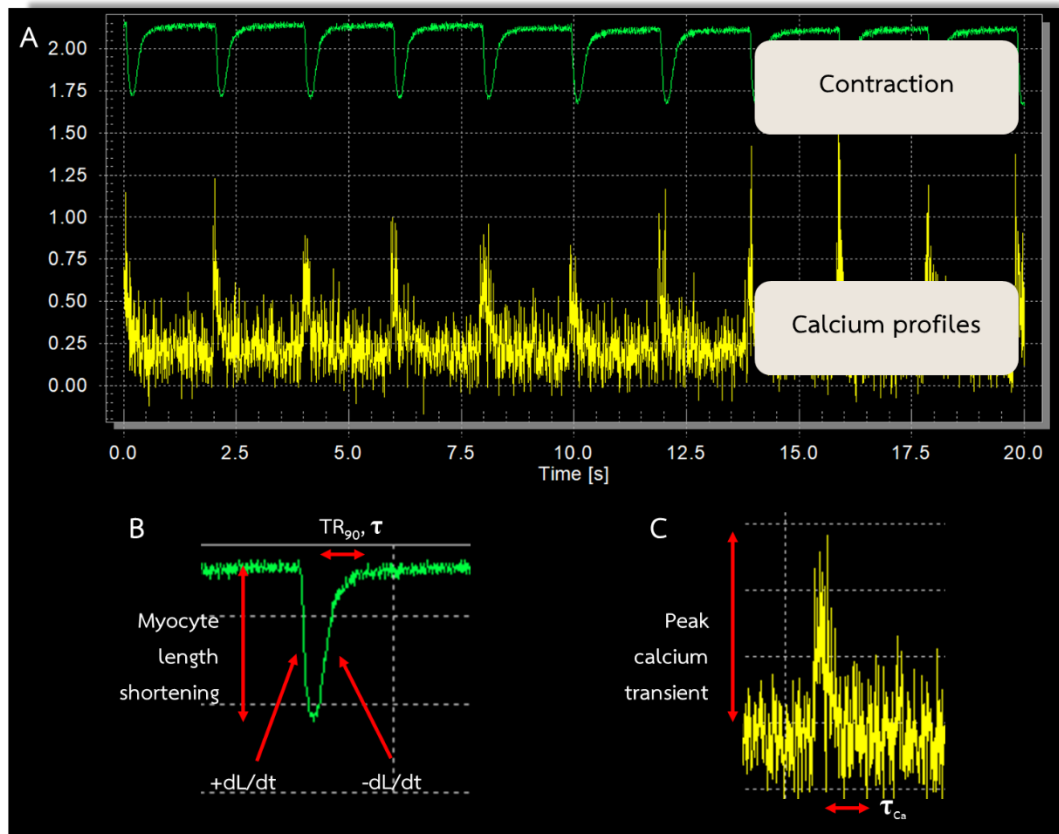


Figure 6. Recordings and analyzing from Felix32™ software.

(A) Acquisition data recorded the cell length (upper panel) and calcium profile (lower panel).

(B) As labelled, mechanical parameters obtained from the recording are myocyte length shortening, shortening velocity (+dL/dt), re-lengthening velocity (-dL/dt), time-to-90%-re-lengthening, and the relaxation index (τ).

(C) The obtained values from the calcium profiles used in this study are peak calcium transient (CaT) and the calcium decaying index (τ_{Ca}).

4. Effects of β -CTX on total phosphorylation of myofilament proteins

4.1. Myofibril preparations and experimental designs

We sought to screen the alteration in total phosphorylation of myofilament proteins.

The experiments were separated into two conditions, at the basal state and following with the ISO incubation. Following the ventricular myocyte isolation, cell solution was equally separated into 6 tubes. Cells in each tube were incubated with different treatment as followed:

- i. Control solution 8 min followed by control solution for 8 min
- ii. Control solution 8 min followed by 0.3 μ M β -CTX solution for 8 min
- iii. Control solution 8 min followed by 0.3 μ M propranolol solution 8 min
- iv. Control solution 8 min followed by 10 nM ISO solution 8 min
- v. 0.3 μ M β -CTX solution 8 min followed by 10 nM ISO solution 8 min
- vi. 0.3 μ M propranolol solution 8 min followed by 10 nM ISO solution 8 min

According to the above lists, cells in groups i. – iv. were selected for analyzing changes of total phosphorylation in myofilaments at a basal condition, whereas cells in groups i. and iv. – vi. were experimentalized as an ISO stimulating condition. Following the incubations, cells were spun at 200 \times g, 4°C for 3 minutes, and the supernatant was discarded. To obtain the isolated myofibrils, 0.5 mL of standard relaxation buffer with Triton-X (SRB-TX; in mM: KCl 75, Imidazole

10, MgCl_2 2, EGTA 2, NaN_3 1 with 1% Triton X-100) was replaced. Tissues were homogenized, vortexed, and incubated for 5 minutes. After removing the supernatant, re-weighed the tube containing myofibrils and subtracted with the previous weight. Industrial sample buffer (ISB; urea 8 M, thiourea 2 M, Tris 0.05 M, DTT 0.075 M with 3% sodium dodecyl sulfate (SDS) and 0.005% bromophenol blue, pH 6.8) was added to the solution at 1:15 ratios (1 mg of protein with 15 μL of ISB). All samples were kept in -80°C until used.

4.2. SDS-PAGE and ProQ[®] staining

Preparation of SDS-PAGE and staining protocol were written in Appendix D1 in detail. Briefly, all tubes acquired from 4.1 were slowly thawed at room temperature. Protein determination was performed using the Pierce protein assay kit (Pierce[™] 660 nm). After the protein concentration was calculated, the stock solution was made at 2 mg/mL for each treatment. A total protein of 5 μg in all samples was loaded and electrophoresed on 15% SDS-PAGE gel at a constant 200 volts for 75 minutes in SDS-tris-glycine running buffer (0.1% SDS, 0.025 M Tris-base, 0.192 M glycine).

Following the SDS-PAGE, gels were cracked and washed in ultrapure water. They were then fixed with the fixation solution (50% methanol and 10% acetic acid aqueous solution) and incubated overnight. On the day after, the fixation solution was discarded, and the gels were washed with ultrapure water thrice. To detect total protein phosphorylation, Pro-Q[®] diamond

phosphoprotein solution (Invitrogen™) was added into gels and incubated for 90 minutes. Non-specific stains were removed using the de-staining solution (Invitrogen™) for 30 minutes. The gel images were taken under a specific imager (ChemiDoc™ MP imaging system, Bio-Rad®) and the band intensity was analyzed using the commercial software (ImageLab™, Bio-Rad®). After that, the Coomassie blue stain (Biosafe™ Coomassie G-250) was added to detect the total protein loaded. Total phosphorylation was normalized upon the band intensities from ProQ® stain, representing total phosphorylation, over the one acquired from Coomassie stain, representing total protein.

5. Western blot analysis of phosphorylated proteins involved in β -adrenergic signaling

5.1. Whole-cell lysate preparation and experimental designs

To further investigate the involvement in the β -AS, changes in the phosphorylation level of PKA-related sites were observed. In this study, the whole-cell lysates of cardiac ventricle cells were used. After the cell isolation procedures, cells were grouped into 6 different treatments as same as the previous experiment. They were also classified into two major conditions, basal state, and ISO stimulation. Treatments included in the basal condition were cells receiving control solution, propranolol only, β -CTX only, and ISO only. On the other hand, ISO stimulation conditions were including cells receiving control, ISO only, preincubation with 0.3 μ M β -CTX

before ISO, and pre-incubated with 0.3 μM of propranolol prior to ISO. After treatment incubation, cells spun at 200 $\times g$ for 5 minutes at 4°C. After that, the supernatant was discarded and ISB was added at 1:15 ratios (1 mg of the whole lysate per 15 μL of ISB). Cells were thrice homogenized using Duall plastic homogenizer in a 1.5 mL microfuge tube, vortexed, and incubated for 5 minutes. All samples were kept in -80°C until used.

5.2. SDS-PAGE and western blot analysis

On the day of the experiment, all cell lysates were slowly thawed at room temperature (25°C). Similar to the ProQ[®] staining procedure, Pierce[™] 660 nm assay kit was used to determine the protein concentration of each cell lysates. After the stock of 2 mg/mL cell solutions were prepared for each treatment. A total protein of 5 μg was loaded into each well, accompanying the Dual[™] protein standard marker (BioRad[®]) and SDS-PAGE was performed using the same condition as previously mentioned (15% gel, 200 V, 75 minutes, SDS-tris-glycine running buffer). Meanwhile, the 0.22 μm PVDF membranes (Immobilon[™]) were cut and soaked with 100% methanol for 1 minute and washed out using ultrapure water. Then, membranes were equilibrated in transferring buffer (10 mM 3-Cyclohexyl-1-propylsulfonic acid; CAPS) for 30 minutes. Following the electrophoresis, gels were immediately transferred onto the prepared membranes using trans-blot[®] cell (BioRad[®]). Transferring process was conducted under 10 mM CAPS solution at a constant 20 Volts for 90 minutes.

After the transfer was done, membranes were quickly soaked with 100% methanol for 30 seconds and washed with MQ water. Then, Swift™ stain was applied to each membrane to screen the loading conditions for all lanes. After the protein bands appeared, membranes were captured under ChemiDoc™ MP imaging system (Bio-Rad®) and rapidly washed out using the de-staining kit and MQ water. Prior to antibodies (Ab) addition, membranes were then soaked in 5% non-fat dry milk in Tris Base-Saline-Tween solution (TBS-T; 50 mM Tris-Base, 200 mM NaCl, 0.1% v/v Tween-20, pH 7.5) for 1 hour to block non-specific bindings. Then, membranes were thrice washed with MQ water and the primary Ab were added into each membrane. We incubated membranes overnight at 4°C with primary Ab, in 1% BSA/TBS-T solution, of p-cMyBP-C (Ser279, Ser288, and Ser308; courtesy to Sakthivel Saddyapan), p-cTnl (Ser23/24; Cell Signaling Technology®), p-PLN (Ser16; Millipore™, and Thr17; Badrilla™). On the day after, membranes were washed with TBS-T three times with 30 minutes incubation. Following the incubation, membranes were washed with TBS-T for 30 minutes before the addition of secondary Ab (goat anti-rabbit Ab or horse anti-mouse Ab; Cell Signaling Technology®), conjugated with horseradish peroxidase. After 90 minutes of incubation, membranes were then washed with TBS-T three times, and the blots were developed by adding enhanced chemiluminescence (ECL; Clarity™, Bio-Rad®) using the ChemiDoc™ MP imager. Band densities were analyzed using ImageLab™ 6.0.1 software (Bio-Rad®). To evaluate total protein band intensities, membranes with phosphorylated

Ab were stripped using either commercial (RestoreTM PLUS, Thermo Fisher[®]) or prepared (6 M Guanidine HCl, 5 mM Tris-(2-carboxyethyl)-phosphine; TCEP, 0.3% v/v Nonidet P-40) stripping buffers membranes were washed with TBST and incubated overnight at 4°C with primary Ab of total cMyBP-C (courtesy to Rick Moss), total cTnI (Fitzgerald[®]), total PLN (BadrillaTM), and total SERCa2a (BadrillaTM). Membranes were washed thrice with TBS-T with 5 minutes of incubation. Then secondary Ab was applied and incubated for 90 minutes. Following the incubation, ECL was added and total protein blots were developed under the imaging system. Total protein band intensities were used for normalizing the phosphorylated bands. Membranes were then also added with primary Ab of β -actin (Protein techTM). The bands were developed to evaluate the loading control and all total protein were normalized with β -actin bands.

6. Detergent extracted (skinned) fiber bundles and force-pCa relationship measurement

6.1. Skinned fiber preparation

The protocol to isolate skinned fiber was previously described (Ryba et al., 2017). Briefly, male Sprague Dawley rats were all anesthetized using sodium pentobarbital at 65 mg/kg intraperitoneally. After the chest was opened, heart and aorta were removed out and soaked in the high relaxing buffer (HRB; in mM: EGTA 10, KCl 41.89, MgCl₂ 6.57, BES 100, ATP 6.22, creatine phosphate 10 and sodium azide 5; pCa 10.0). The heart was stabilized with the pin on both apex

and the base to characterize the right atria and ventricle, we removed the lateral (free) wall of the right chambers to expose the interventricular septum. The aorta was cut downward parallelly to the septum and until the papillary muscles were noticed. Muscles were cut and put into HRB containing 1% Triton X-100 (HRB-TX) to remove the cell membrane. This process was done under the stereomicroscope. We gently separated single myofibrils from each muscle; three to four fibers were acquired from each rat. All fibers were measured at 4-5 mm in length and 200-250 μm in width. Fibers were then incubated in HRB-TX for 30 minutes at room temperature.

6.2. Measurement of force generated in different calcium concentration

Twelve fibers from three rats were used in the study. After the fibers were isolated, different Ca^{2+} -concentration, which expressed as pCa, were prepared from HRB and activating buffers (in mM: EGTA 10, CaCl_2 9.98, KCl 22.16, MgCl_2 6.27, BES 100, ATP 6.29, creatine phosphate 10 and sodium azide 5; pCa 4.5). The pCa solutions preparation was written in an Appendix E2. We used 8 different pCa conditions (4.5, 5.5, 5.75, 5.85, 6.0, 6.25, 6.5, and 7.0) preparing from HRB and activating buffer. All pCa solutions were added with creatine phosphokinase enzyme (CPK) to activate the myofibril function. Each solution was separated into two conditions, with or without 1 μM of β -CTX. Fibers were mounted onto the force transducer where acetonic glue was applied to fix the fiber's length. To calibrate the fiber's sarcomere length and cross-sectional area,

refractivity of fiber at pCa 10 (HRB) and pCa 4.5 (activating buffer) were calculated before the experiment. The force generation and tension were recorded in the normal condition following by the presence of 1 μM of $\beta\text{-CTX}$ condition. Maximal tension generated, pCa₅₀ (concentration of Ca²⁺ where half-maximal tension was created), and Hill's coefficient (n_H) values were calculated for each fiber.

7. Measurement of myofibrillar ATPase activity

7.1. Isolation of cardiac myofibrils

To investigate the Ca²⁺-independent pathway controlling the myofilament kinetics, ATPase properties were tested directly with the $\beta\text{-CTX}$. Adult male Sprague Dawley rats were used for the study. To isolate cardiac myofibril, the protocol was applied from the previous publication (Layland et al., 2005). Rats were anesthetized using pentobarbital sodium at the dosage of 150-200 mg/kg. After being removed from the body, the heart was incubated into the cold standard relaxing buffer (SRB) [in mM: KCl 75, Imidazole 10, MgCl₂ 2, EGTA 2, NaN₃ 1; pH 7.2] to stop the contraction. Ventricular tissue was cut and minced into small pieces and weighed for approximately 30-50 mg. Then, one mL of SRB containing 1 mg/mL of collagenase type II (Worthington®) was added into the 2 mL Dounce homogenizer with the minced tissue to lyse the extracellular matrix for 5 minutes. Meanwhile, tissue was homogenized using the loose-fitting

pestle until the solution became homogenous. The solution was then transferred into a 1.5 mL pre-weighed microfuge tube and centrifuged at 16,000 xg in 4°C for 1 minute. After that, the supernatant was decanted, and SRB-TX was added to the pellets. The pellets were finely homogenized in ice with the tight-fitting pestle until the tissue was completely dissolved. The solution was transferred back to the microfuge tube and centrifuged at 16,000 xg in 4°C for 1 minute. The supernatant was then removed again and repeated the adding, homogenizing, and pelleting tissue in the SRB-TX twice. SRB was added to the pellet to wash out triton X-100. The solution was vortexed and spun at 5,000 xg in 4°C for 1 minute. The supernatant was removed and A-70 solution [in mM: NaCl 70, MgCl₂ 10, 3-(N-morpholino) propane sulfonic acid; MOPS 40] was replaced. The solution was mixed and centrifuged at 3,000 xg at 4°C for 5 minutes. We repeated the A-70 procedure for another wash to completely replace the solvent to A-70. Pellets were weighed and reconstituted with A-70. The protein concentration of cardiac myofibril was determined using the BioRad[®] DC assay. Briefly, each well of U-bottom 96-well plate was loaded with 5 µL of samples, 25 µL of solution A' (1 mL solution A and 20 µL solution S of the kit) and 200 µL of solution B of the same kit. Absorbance was read at 750 nm using a multichannel reader after incubated for 15 minutes at room temperature, the protein concentration was calculated in accordance with the standard bovine serum albumin (BSA) solution. Myofibril stock was incubated in 4°C and used immediately.

7.2. Measurement of ATPase activity using the malachite green assay

Myofibril stock solution was diluted with an A-70 solution to make a concentration of 0.3 mg/mL. A total of 12 μg of myofibrils was loaded into twelve microfuge tubes (40 μL was added). Different 12 conditions of calcium concentration (pCa solutions), ranging from 4.030 to 7.704 (calculated using the online website; WEBMAXC Standard website, preparing from 20 mM EGTA and 20 mM Ca^{2+} -EGTA as shown in Appendix F1), was then loaded for 10 μL in each tube. Either of 0.3 μM of β -CTX or control (A-70 solution) was added to the tube for another 10 μL , incubated for 15 minutes at 25°C. To start the reaction, 40 μL of 1.67 mM ATP was added to the reaction tubes. For every 3 minutes, 10 μL of each tube would be drawn out and added to the well containing 90 μL of 0.2 M perchloric acid (PCA) at 10°C to stop the reaction. Up to six time-point (3 minutes interval), 100 μL of malachite green solution (MG) was loaded into all wells to interact with produced inorganic phosphate (P_i) and incubated for 30 minutes at 27°C. Standard NaH_2PO_4 solutions ($\text{P}_i = 0, 0.2, 0.4, 0.6, 0.8, 1 \text{ nM}$) were also run in parallel. The amount of P_i was determined by reading at 655 nm, calculated and represented as P_i production per amount of protein per second (ng P_i /mg protein/sec). At least three plates (replicates) were used for calculating in each rat. Following the P_i production-pCa relationship was plotted, the maximal

ATPase activity, pCa_{50} (Ca^{2+} -concentration where half-maximal ATPase activity occurred), and Hill's coefficient (n_H) were calculated.

8. Statistical analysis

To assess Gaussian distribution, normality was tested using the Kolmogorov-Smirnov test with Dallal-Wilkinson-Lillie for p -value. For the *in vitro* cytotoxicity study, the non-linear curve fit was plotted from the concentration-cell viability relationship to calculate the 50% cytotoxic concentration (CC_{50}). Similarly, we assessed the effects of β -CTX on cardiomyocyte functions using the dose-response curve for each parameter. Non-linear curve fit was also plotted to calculate either half-maximal inhibitory (IC_{50}) or effective concentration (EC_{50}). At the basal condition, we compared the effect to the baseline of the cells using repeated measures ANOVA followed by Dunnett's method as a post-hoc analysis. Differently, during the stimulatory condition with either ISO or FSK experiments, two-way repeated measures ANOVA was used following by Tukey's test for multiple comparisons. We also performed the standard ANOVA in both ProQ[®] and western blot experiments. Tukey's test was also used for multiple comparisons between groups. For the force-pCa relationship, the sigmoidal concentration-response curve fit was applied. A paired t-test was used to compare the obtained parameters, maximal tension generated, half-maximal pCa_{50} , and n_H . For the ATPase experiment, on the other hand, an

unpaired t-test was conducted to compare the effect of maximal ATPase activity, pCa_{50} , and n_H between myofibrils receiving control and β -CTX. All data were represented as mean \pm S.E.M. Statistical significance was considered at a p -value of less than 0.05. All statistical analysis was performed under commercial software.



Chapter 4

Results

1. Purification and identification of β -CTX

In the first purification step, RP-HPLC, chromatographic profiles (Figure 7A) demonstrated different 48 peaks from the crude KCV. After the protein bands were identified from SDS-PAGE (Figure 7B) and N-terminal sequencing (Table S1), β -CTX was detected in fractions 15th and 16th. The retention time was around 54-59 minutes where the gradient of solution B was approximately 34-36%. Both β -CTX-containing fractions were subsequently subjected to the second step purification, cIEx chromatography. Chromatogram (Figure 7C) represented the 4 subfractions where both 3rd and 4th contained pure compound with around 7.5 kDa as estimated by SDS-PAGE (Figure 7D). They were further confirmed as purified β -CTX from N-terminal sequencing (Supplemental Table S1). However, both subfraction 3rd and 4th were named differently as β -CTX-1 and -2, respectively. According to the table of purification, the amount of protein recovered from the crude venom mass was totally around 0.53% w/w (Table 3).

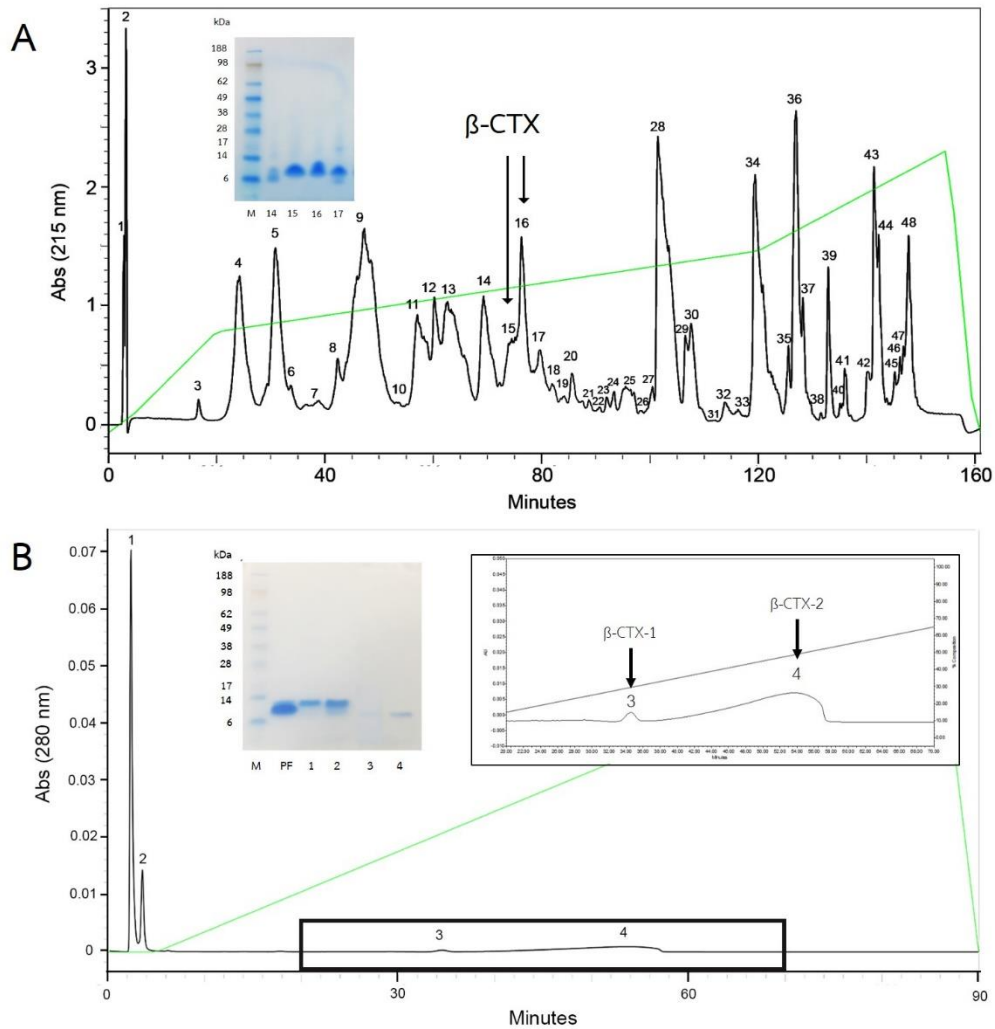


Figure 7. Chromatographic profiles of the β -CTX purification.

(A). Reverse phase chromatographic profile represents fractions containing β -CTX (arrows), identified by SDS-PAGE (inset) and automated N-terminal sequencer. (B) Cation exchange chromatogram of the pooled fractions (PF) 15-16th from the reverse phase HPLC. (Inset) β -CTX-1 and -2 was identified in both subfraction 3 and 4, respectively (arrows). All fractions were determined the protein constituents by the running SDS-PAGE (inset) and N-terminal sequencer. M = protein marker (SeeBlueTM Plus2, Thermo Fisher[®])

Table 1 Purification table verifying yielded of β -CTX from the crude KCV mass

Purification step	Volume (mL)	Protein concentration (mg/mL) ^a	Total protein (mg) ^b	Recovery of protein (%) ^c
Crude KCV	4	100	200	100
C18-HPLC	4.71	2	9.42	4.71
cIEx				
β -CTX 1	0.14	1.2	0.17	0.08
β -CTX 2	0.36	2.5	0.9	0.45
Total			1.07	0.53

^a Protein concentration was obtained using spectrophotometer at 280 nm.

^b Total protein was calculated by multiplying (total volume; mL) x (protein concentration; mg/mL).

^c Recovery of protein was defined as the total protein recovered from each purification step.



2. *In vitro* cytotoxicity effect of β -CTX on mammalian muscle cell lines

Prior to the functional studies on cardiomyocytes, cytotoxicity of β -CTX on skeletal (C2C12), smooth (A7r5), and cardiac (H9c2) cell lines, was initially conducted. Microscopic pictures (Figure 8A) illustrated that 0.2 mg/mL of β -CTX (28.57 μ M) induced cytotoxicity to A7r5 cells as indicated by the morphological changes and cell deaths (Figure 8; top middle; arrows). However, non-lethal effects were observed to both C2C12 and H9c2 cells up to the concentration of 0.8 mg/mL (114.09 μ M) (Figure 8A; top left and right). According to the MTT assay, the cellular viability of different muscle cells ($n = 3$) was plotted upon the β -CTX concentration as shown in Figure 8B. Results demonstrated that β -CTX reduced the cellular viability in A7r5 cells, only, with the cytotoxic concentration (CC_{50}) of at approximately 0.07 ± 0.01 mg/mL (9.41 ± 1.14 μ M) (Figure 8B). On the other hand, β -CTX did not affect cellular viability in C2C12 and H9c2 up to 0.8 mg/mL. In contrast to the crude venom, KCV significantly reduced cell viability in both C2C12 and A7r5 as shown in the appendix (Supplemental Figure S2A). The calculated CC_{50} of KCV on the skeletal myoblast and smooth muscle were 0.07 ± 0.02 mg/mL and 0.02 ± 0.01 mg/mL, respectively (Supplemental Figure S2B).

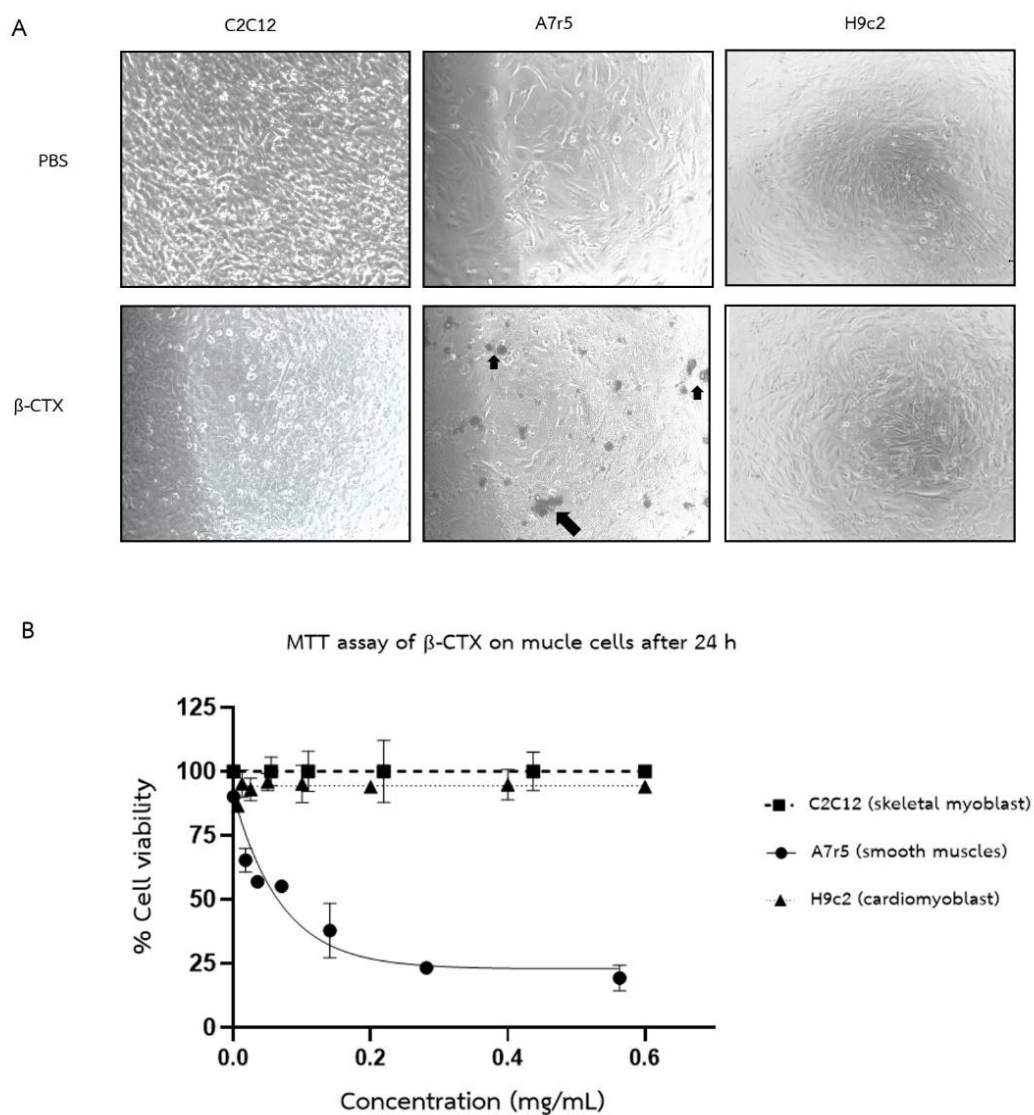


Figure 8. Cellular viability assay of β -CTX on different mammalian muscles cell lines.

(A) Representative microscopic pictures of C2C12, A7r5 and H9c2 muscle cell lines treated with either PBS (top) or β -CTX (bottom). Concentration of β -CTX on C2C12 and H9c2 was 0.8 mg/ml, and on A7r5 was 0.2 mg/mL, respectively. Morphological changes as well as dead cells (arrows) were observed in only A7r5 cells treated with β -CTX. (B) Percentage of cell viability as function of toxin concentration ($n = 3$; three replicates for each n). Data are presented as mean \pm S.E.M.

3. Effect of β -CTX on isolated rat cardiomyocyte functions

3.1. Effect of β -CTX on ventricular myocyte functions at basal state

The effects of β -CTX on isolated cardiomyocytes functions were tested and shown in Figures 9 and 10. We represented the raw plot of cardiomyocyte contraction before and after receiving β -CTX in Figure 10A. The percentage changes of cell length shortening (Figure 10B) and the rate of length change by time (+dL/dt; Figure 10C), were demonstrated as an inotropic assessment. Significant suppression of both cell length shortening and +dL/dt was observed, indicating the dose-dependently negative inotropic property of β -CTX ($p < 0.05$). The non-linear curve-fit was applied on both parameters, revealing the IC_{50} of 95.97 ± 50.10 nM and 10.23 ± 1.52 nM, respectively. The diastolic function of the cells was also measured as presented in Figure 10D-10F. The relaxing index (τ) was prolonged after receiving the highest concentration of β -CTX ($p < 0.05$; Figure 10D). The calculated EC_{50} from the non-linear curve fit was about 29.47 ± 12.74 nM. However, there were no changes in the time-to-90% re-lengthening (TR_{90}) after treated cells with β -CTX (Figure 10E). The re-lengthening velocity (-dL/dt) of the cardiac myocyte was also suppressed significantly ($p < 0.05$) by β -CTX with an approximate IC_{50} of 22.91 ± 17.53 nM. Figure 10G displayed the representative plot of calcium profiles at the baseline (BL) and after β -CTX. Interestingly, the amplitude of Ca^{2+} transient (CaT) and Ca^{2+} -decaying time (τ_{Ca}), of the cells were

responded differently as shown in Figure 10H and 10I. The alteration in the peak CaT was not affected by β -CTX (Figure 8H). Contrarily, β -CTX at 1 μ M could significantly prolong τ_{Ca} (Figure 10I). The latter was responded in a dose-dependent manner with the EC_{50} of approximately 55.83 \pm 13.67 nM.

On the other hand, the propranolol, a standard β -blocker was also tested with the cardiac myocyte function to compare the effect with β -CTX. Here, we demonstrated the effects of propranolol on the isolated cardiomyocyte function in Figure 11. Figure 11A showed a representative recording of cell shortening at the baseline (BL) and after receiving 1 μ M of propranolol. Figures 11B and 11C displayed the percentage of change from baseline of myocyte length shortening and $+dL/dt$. The negative inotropic responded by propranolol were observed in a dose-dependent manner, as indicated by the IC_{50} of both cell length shortening and $+dL/dt$ values of $7.86 \pm 1.05 \mu$ M and $6.62 \pm 1.13 \mu$ M, respectively. Propranolol also inhibited cardiac lusitropy as presented in Figure 11D–11F. The non-linear curve-fit revealed that propranolol could reduce $-dL/dt$ of the cells dose-dependently with the IC_{50} of approximately $5.16 \pm 1.13 \mu$ M (Figure 11D). In addition, the TR_{90} (Figure 11E) and τ index (Figure 11F) were also prolonged in a concentration-dependent, with the calculated EC_{50} of $7.10 \pm 0.82 \mu$ M and $9.40 \pm 0.50 \mu$ M, respectively. The recordings of the CaT were sequentially plotted, comparing cell responses

before and after receiving propranolol (Figure 11G). The declination of the amplitude of the CaT (Figure 11H) and the prolongation of τ_{Ca} (Figure 11I) was exhibited in a dose-dependent manner. The calculated IC_{50} on CaT and EC_{50} on τ_{Ca} was approximately $12.93 \pm 10.57 \mu\text{M}$ and $12.51 \pm 1.56 \mu\text{M}$, respectively.

The comparison effects represented by the calculated EC_{50}/IC_{50} between β -CTX and the standard BB were shown in Table 2. The effective concentration of β -CTX was significantly lower than the propranolol-treated group in all parameters (myocyte shortening; $p = 0.0004$, $+dL/dt$; $p = 0.0016$, $-dL/dt$; $p < 0.0066$, τ ; $p < 0.0001$, and τ_{Ca} ; $p = 0.0002$). Due to the limited effects in the TR_{90} and peak CaT from β -CTX-treated cells, the comparison could not be compared in these parameters. The hysteresis loop was also plotted upon the relationship between the normalized cell length and the normalized CaT during a contraction cycle (Supplemental Figure S5). Results showed that compared to the baseline, $1 \mu\text{M}$ of β -CTX increased the area of the loop (Figure S5A); whereas, $30 \mu\text{M}$ of propranolol reduced (Figure S5B).

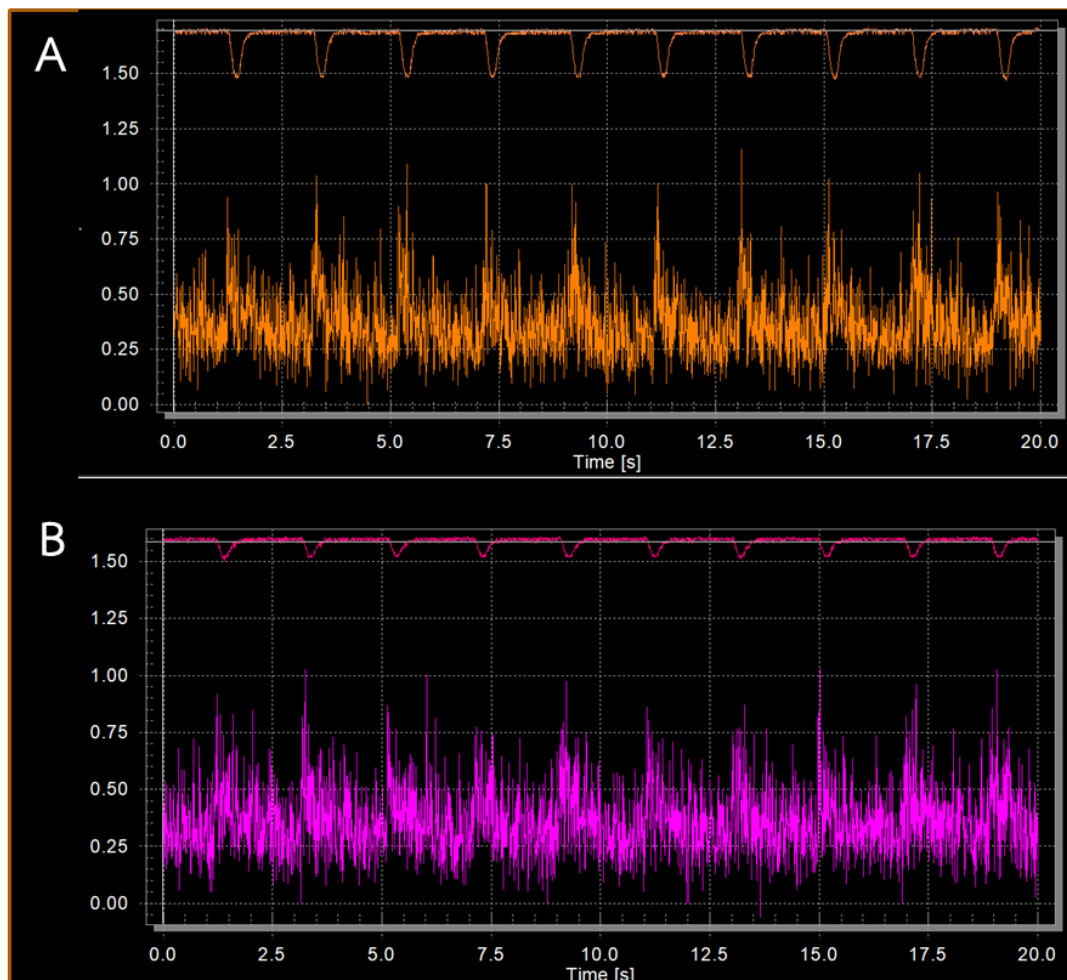


Figure 9. Raw data acquisition from FelixTM32 software.

Comparison of cardiac contraction and calcium profile are performed between the ventricular myocyte at the (A) baseline and (B) after receiving 0.3 μM of β-CTX. Noted the significantly reduction in the myocyte shortening (upper panel of each graph) without changing in the

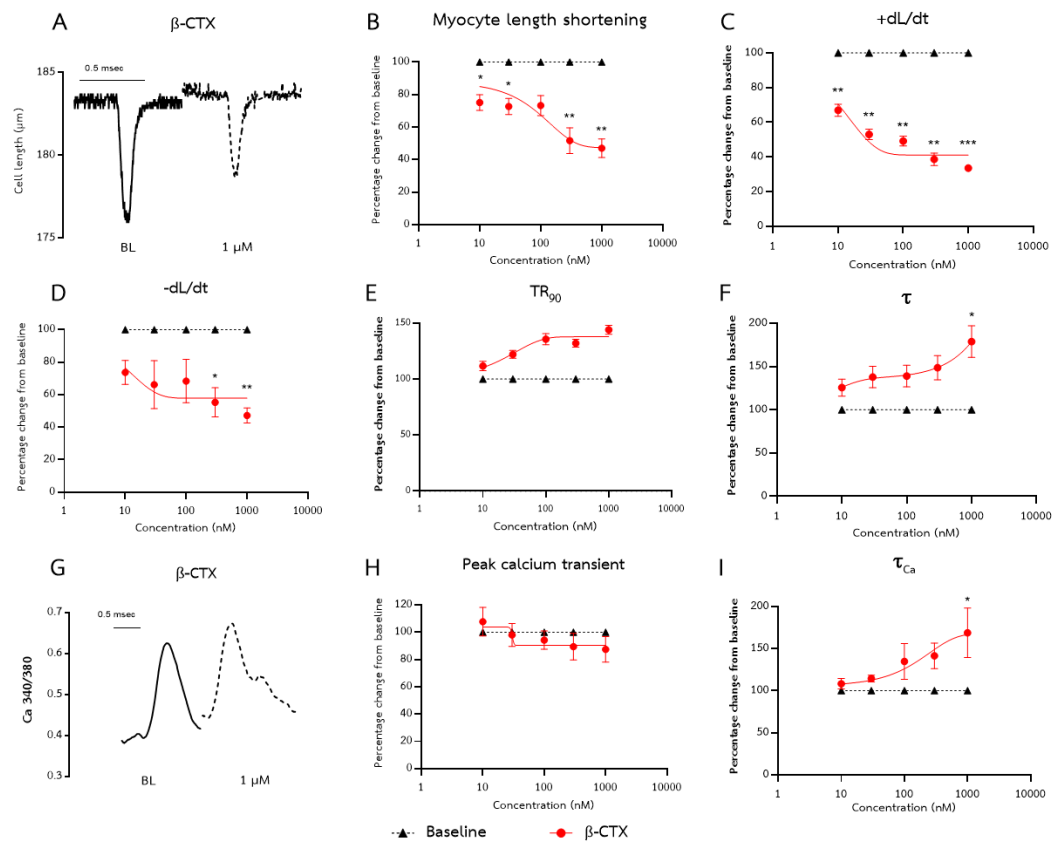


Figure 10. Effects of β -CTX on isolated cardiomyocyte functions and calcium profiles.

Raw plots of cell length (A) comparing between the baseline and after receiving 1 μM of β -CTX. The non-linear dose-response curves present changes in inotropic parameters; cell length shortening (B) and +dL/dt (C), lusitropic parameters; -dL/dt (D), TR_{90} (E) and τ (F). Spontaneous measurement of Ca^{2+} profiles is also plotted (G), along with the percentage changes in peak CaT (H) and τ_{Ca} (I) comparing to the baseline. Data are represented in mean \pm S.E.M. and analyzed using repeated measured ANOVA following the Dunnett's method. * $p < 0.05$, ** $p < 0.01$ vs baseline, *** $p <$

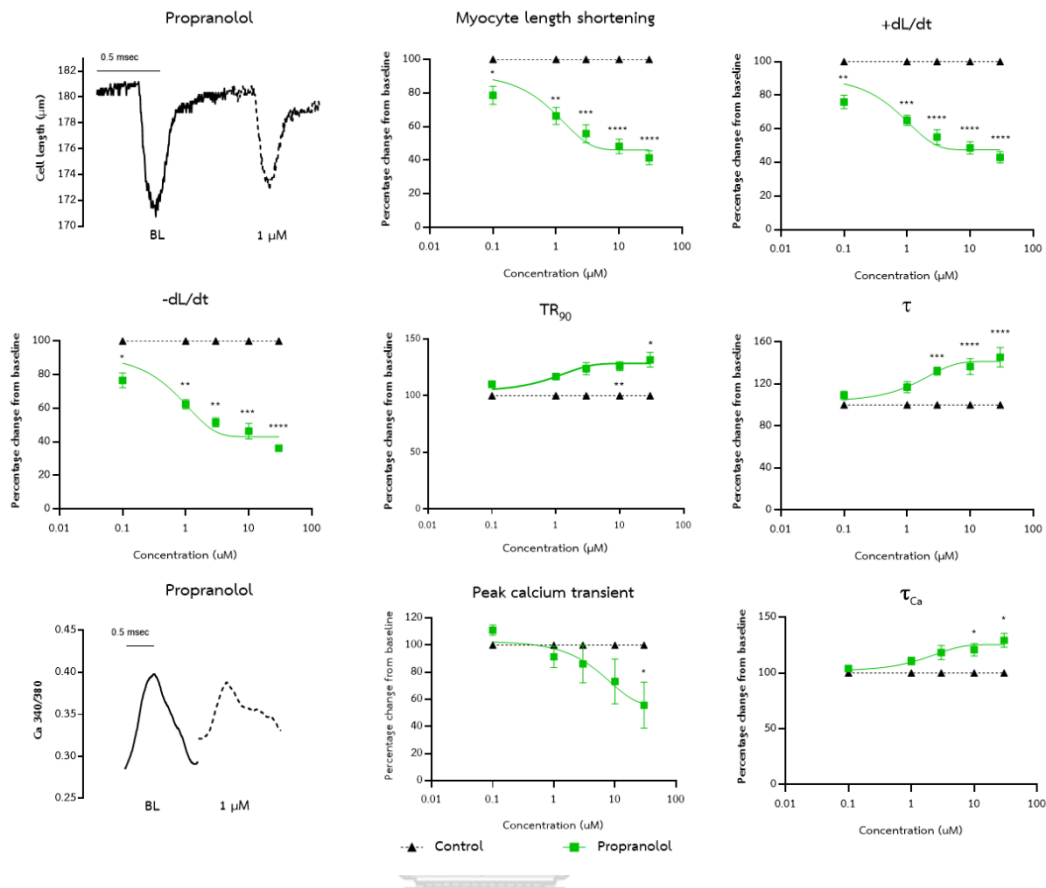


Figure 11. Effects of propranolol on isolated cardiomyocyte functions and calcium profiles.

Raw plots of cell length (A) comparing between the baseline and after receiving 1 μM of propranolol. The non-linear dose-response curves present changes in inotropic parameters; cell length shortening (B) and +dL/dt (C), lusitropic parameters; -dL/dt (D), TR_{90} (E) and τ (F). Spontaneous measurement of Ca^{2+} profiles is also plotted (G), along with the percentage changes in peak CaT (G) and τ_{Ca} (H) comparing to the baseline. Data are represented in mean \pm S.E.M. and analyzed using repeated measured ANOVA following the Dunnett's method. * $p < 0.05$, ** $p < 0.01$, *** $p < 0.001$, **** $p < 0.0001$ vs baseline.

Table 2. Comparison effects on cardiomyocytes between propranolol and β -CTX.

EC_{50}/IC_{50}	Propranolol (nM)	β -CTX (nM)	<i>p</i> -value
Myocyte length shortening	7,860 \pm 1,050	95.97 \pm 50.1	0.0004
+dL/dt	6,620 \pm 1,130	10.23 \pm 1.52	0.0016
-dL/dt	5,160 \pm 1,130	22.91 \pm 17.53	0.0066
TR ₉₀	7,100 \pm 820	50.05 \pm 9.25	< 0.0001
τ	9,400 \pm 500	29.47 \pm 12.74	< 0.0001
Peak CaT	12,930 \pm 10,570	-	-
τ_{Ca}	12,510 \pm 1560	55.83 \pm 13.67	0.0002

EC₅₀: Half maximal effective concentration; IC₅₀: Half minimal inhibitory concentration; +dL/dt: shortening velocity; -dL/dt: re-lengthening velocity; TR₉₀: time-to-90% re-lengthening; τ : tau index; CaT: calcium transient; τ_{Ca} : calcium decaying index. Data are resented as mean \pm S.E.M. Calculated EC₅₀ or IC₅₀ are extrapolated from non-linear dose-response curve. The comparison was performed using unpaired t-test.



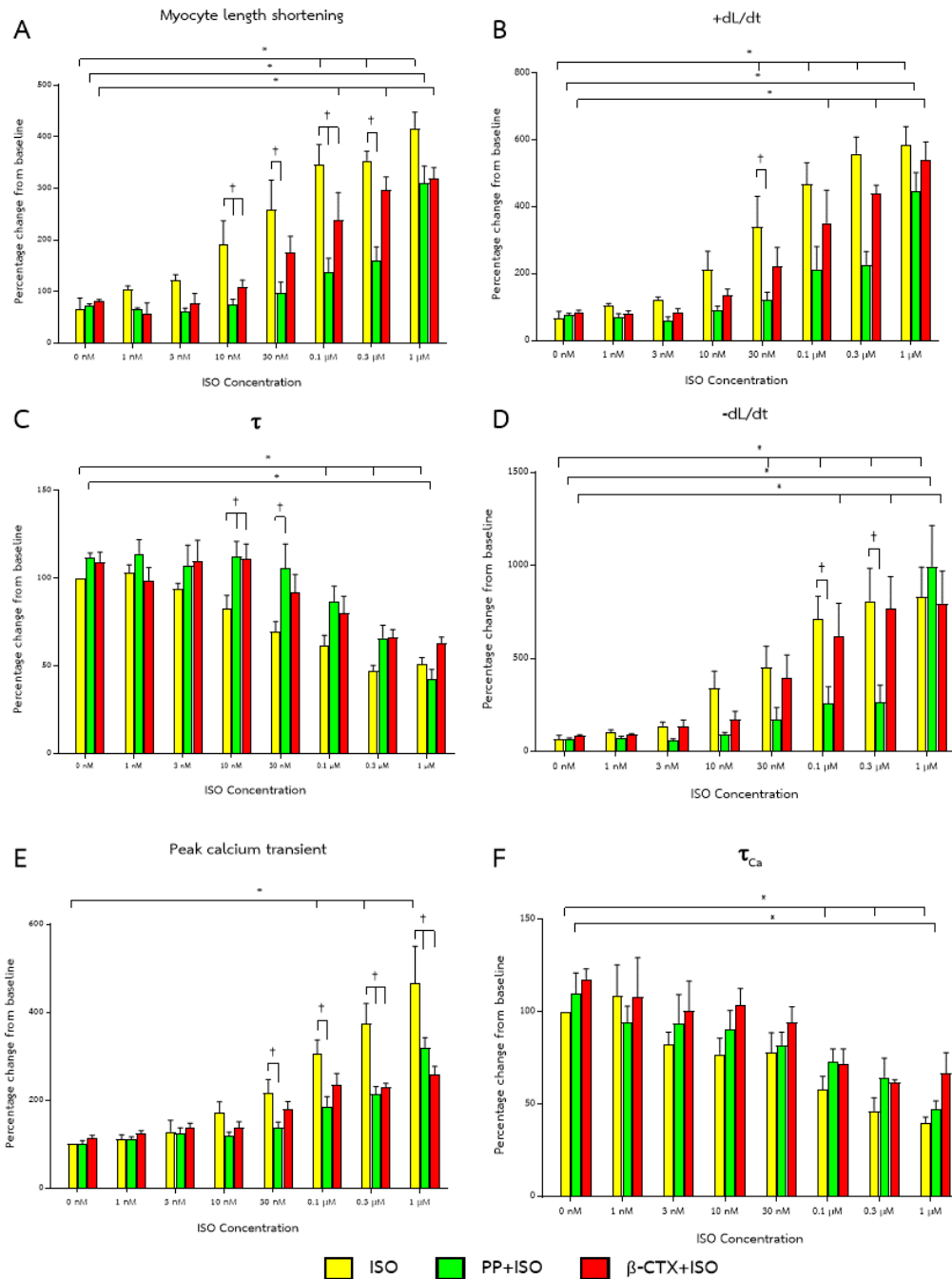


Figure 12. Effects of β-CTX on functions and calcium profiles of ISO-induced cardiomyocyte.

Cells ($n = 6$) were treated with isoproterenol (ISO), propranolol and ISO (PP+ISO) and β-CTX+ISO. Bar graphs represent percentage changes from baseline of (A) cell length shortening, (B) +dL/dt, (C) τ , (D) -dL/dt, (E) Cat and (F) τ_{Ca} . Data are represented as mean \pm S.E.M. Two-way repeated measured ANOVA was used to analyze the data, following by the Tukey's as a post-hoc analysis. * $p < 0.05$ vs baseline, † $p < 0.05$ vs ISO-induced group.

3.2. Effect of β -CTX on ISO-induced cardiomyocyte

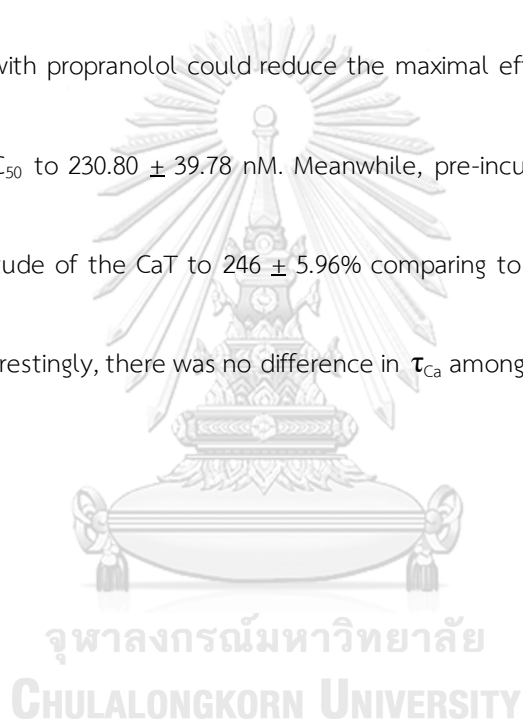
The comparison data between the effects of β -CTX and propranolol, in the presence of ISO, was illustrated in Figure 12. Figures 12A and 12B illustrated the inotropic responses, myocyte length shortening, and +dL/dt, respectively. Similarly, ISO robustly activated both parameters in a dose-dependent manner. Focusing on myocyte shortening (Figure 12A), the effect of ISO started to significantly increase from baseline at around 10 nM. In the presence of propranolol, the effects of ISO were attenuated from 10 nM to 300 nM. The Addition of 0.3 μ M of β -CTX showed suppression in ISO effect at 100 nM. However, using 1 μ M of ISO overcame the attenuation effect of both propranolol and β -CTX. On +dL/dt parameter (Figure 12B), the ISO stimulatory effect was shown from 30 nM. The pre-treatment with propranolol showed attenuation of the ISO effect at 30 nM. On the other hand, the addition of β -CTX did not show any alleviation of this parameter. Figure 10C and 10D represented the lusitropic effect of cardiomyocytes that responded to treatments. The relaxation index (τ ; Figure 12C) was significantly reduced by ISO in a dose-dependent manner. Interestingly, the presence of either propranolol or β -CTX significantly lengthened the index when compared to the ISO-treated group at 10 nM. The re-lengthening velocity (Figure 12D) was also affected by the ISO. It began to significantly raise from the baseline at 30 nM. Pre-incubation with propranolol reduced the ISO effects at 100 nM and 300 nM. On the contrary, β -CTX could not reduce the ISO impact in both lusitropic parameters. The calcium

profiles, CaT and τ_{Ca} , responded to treatments were demonstrated in Figure 12E and 12F, respectively. Perfusing with ISO gradually elevated CaT, as well as prolonged τ_{Ca} , in a dose-dependent manner. In both propranolol and β -CTX pre-treated groups, the elevated CaT by ISO was reduced from 30 nM to 1 μ M (Figure 12E). However, no response was observed in τ_{Ca} while combined treatment with either propranolol or β -CTX with ISO comparing to the control ISO-treated cells (Figure 12F).

The graphical illustration of the dose-response curve in all parameters was reported in Appendix C (Supplemental Figure S6 and Table S2). Figure S6A and S6B demonstrated the percentage changes from baseline of inotropic parameters, cell length shortening, and +dL/dt, respectively. Promisingly, cells treated with ISO robustly improved both parameters in a dose-dependent manner with the estimated EC_{50} of 19.93 ± 3.88 nM and 84.28 ± 15.58 nM, respectively. In addition, the effects of ISO on the cell length shortening and +dL/dt were maximized to $370.10 \pm 28.06\%$ and $792.50 \pm 36.84\%$, respectively (Table S2). The pre-incubation of the cells with 0.3 μ M of propranolol before ISO could shift the dose-response curve to the right in both cell length shortening and +dL/dt (Figure S6A and S6B). The estimated EC_{50} from the non-linear curve fit are 451.40 ± 108.77 nM and 884.90 ± 275.89 nM for myocyte length change and +dL/dt, respectively which were significantly higher than cells treated with ISO alone ($p < 0.01$; Table S2). However, the maximal effects of the cells were attenuated while using a higher

concentration of ISO. In contrast, cells pre-treated with 0.3 μM of $\beta\text{-CTX}$ represents a different shifting pattern. The calculated EC_{50} of cell length shortening and $+\text{dL}/\text{dt}$ was not significantly altered from the ISO-treated group but the maximal effects of both contractile parameters were disrupted from the ISO-treated group (Table S2). For the lusitropy aspects, the percentage change from baseline of τ index and $-\text{dL}/\text{dt}$ parameters were illustrated in Figure S6C and S6D. Likewise, ISO-treated cells markedly elevated the $-\text{dL}/\text{dt}$ and reduce the relaxing index, in a concentration-dependent manner. The calculated EC_{50} of $-\text{dL}/\text{dt}$ and IC_{50} of τ from the non-linear dose-response curve fit were approximately $57.01 \text{ nM} \pm 10.94$ and $17.80 \pm 3.11 \text{ nM}$, respectively. The effect of ISO on $-\text{dL}/\text{dt}$ of cardiomyocytes was maximized to $862.60 \pm 40.5\%$ where the τ index was decreased down to $54.63 \pm 1.65\%$ (Table S2). Cells pre-treated with propranolol prior to ISO exhibits the attenuation effects by increasing EC_{50} of τ and $-\text{dL}/\text{dt}$ to $173.50 \pm 37.62 \text{ nM}$ and $638.30 \pm 137.2 \text{ nM}$, respectively ($p < 0.05$; Table S2). However, cells in this group did not change either minimal or maximal effects of τ and $-\text{dL}/\text{dt}$, comparing to the ISO-treated group. Cells pre-treated with 0.3 μM of $\beta\text{-CTX}$ were responded in contrary to the propranolol group. Figure S6C demonstrated the dose-dependent attenuation effect by $\beta\text{-CTX}$ on the maximal $-\text{dL}/\text{dt}$ ($445.40 \pm 20.68\%$) comparing to the ISO-treated group ($p < 0.05$). Moreover, the compound also prolonged τ for $63.90 \pm 3.78\%$ from the baseline which was significantly more than cells treated with ISO only ($p < 0.05$; Figure S6D). Nevertheless, there were no changes in the EC_{50} ($32.50 \pm 6.08 \text{ nM}$)

comparing to the control-ISO group (Table S2). In Ca^{2+} homeostasis, the cells perfused with ISO showed a marked elevation of the peak CaT in a dose-dependent manner (Figure S6E). The effect of ISO was maximized to $434.10 \pm 14.73\%$ with calculated EC_{50} of 74.59 ± 12.76 nM (Table S2). The standard β -agonist also dose-dependently shortened the τ_{Ca} (Figure S6F) where the minimized effect is $44.21 \pm 7.72\%$ from the resting and the IC_{50} is 44.81 ± 9.99 nM (Table S2). The cells pre-incubated with propranolol could reduce the maximal effect of ISO to $324.90 \pm 11.70\%$ and increased the EC_{50} to 230.80 ± 39.78 nM. Meanwhile, pre-incubating cells with β -CTX could attenuate the amplitude of the CaT to $246 \pm 5.96\%$ comparing to the baseline with the EC_{50} of 32.05 ± 6.08 nM. Interestingly, there was no difference in τ_{Ca} among groups.



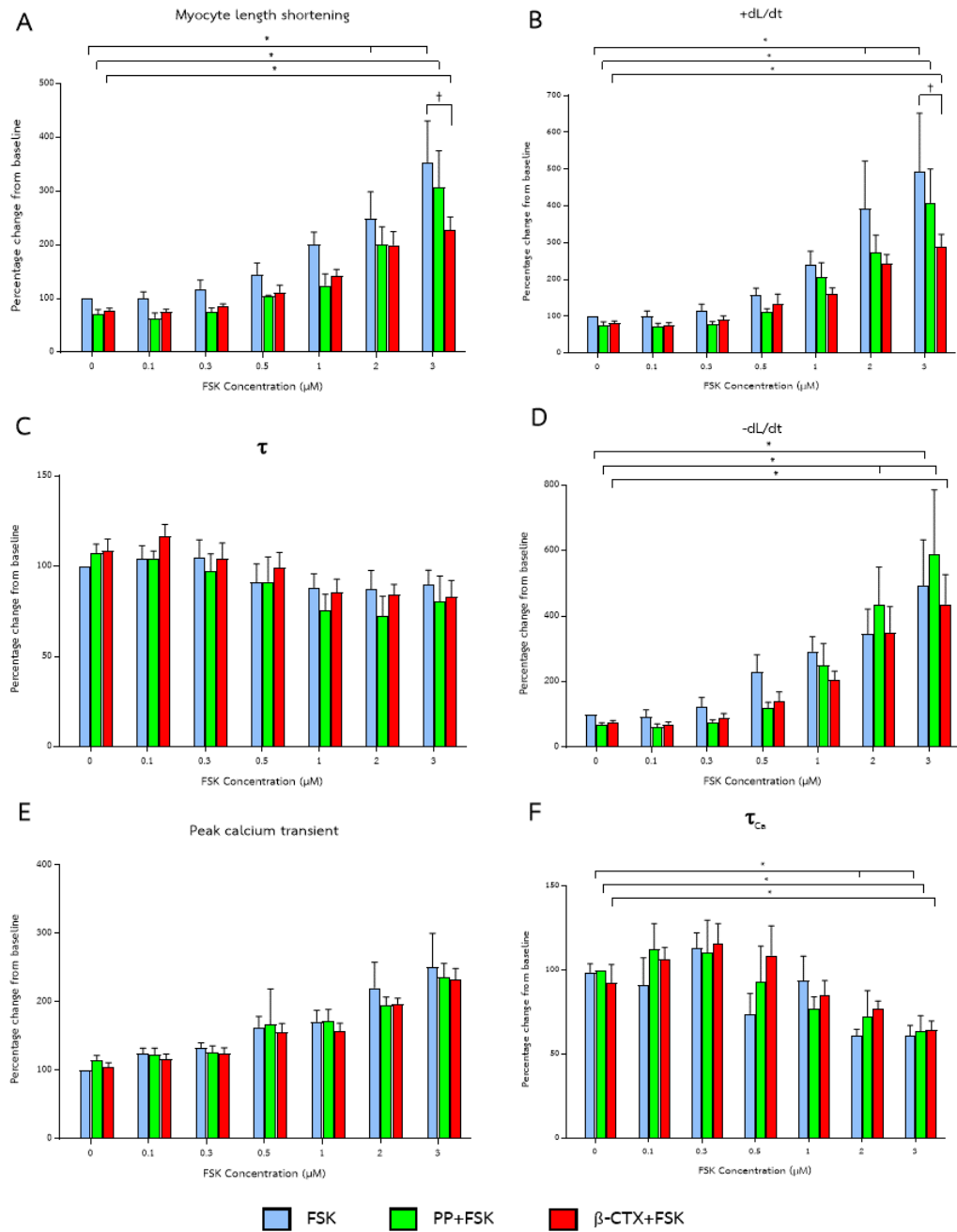


Figure 13. Effects of β -CTX on functions and calcium profiles of FSK-induced cardiomyocyte.

Cells ($n = 6$) were treated with forskolin (FSK), propranolol and ISO (PP+FSK) and β -CTX+FSK. Bar graphs represent percentage changes from baseline of (A) cell length shortening, (B) $+dL/dt$, (C) τ , (D) $-dL/dt$, (E) τ_{Ca} and (F) τ_{Ca} . Data are represented as mean \pm S.E.M. Two-way repeated measured ANOVA was used to analyze the data, following by the Tukey's as a post-hoc analysis.

* $p < 0.05$ vs baseline, † $p < 0.05$ vs FSK-induced group.

3.3. Effect of β -CTX on FSK-induced cardiomyocyte

The comparative effects of β -CTX to propranolol in the presence of FSK were illustrated in Figure 13. Figure 13A and Figure 13B represented the inotropic parameters, myocyte length shortening, and $+dL/dt$. Promisingly, the incremental dose of FSK dose-dependently promoted both parameters. While using 3 μ M of FSK, the presence of β -CTX reduced the stimulatory response of FSK in which did not show in propranolol pre-treated group. Figure 13C and 13D represents the comparison in relaxation index and $-dL/dt$ between groups. Although there was no difference between groups and concentration in the τ index (Figure 13C), using 2 and 3 μ M of FSK still significantly increased the rate of relaxation of cardiomyocytes (Figure 13D). Pre-incubation with either propranolol or β -CTX did not affect the activity of FSK at any concentrations. The calcium homeostasis alteration was compared in Figure 13E and 13F as CaT and τ_{Ca} , respectively. Despite showing a dose-dependent manner elevation of the CaT values, the significant elevation could not be noticed in any concentration used in the study (Figure 13E). Whereas, the higher dosage of FSK showed the significance of depression in the τ_{Ca} value. There was no impact of neither propranolol nor β -CTX on calcium profiles in the presence of FSK. We also represent the dose-response curve in Appendix C (Supplemental Figure S7). Since none of the parameters had reached the plateau effects, the calculation, by extrapolating from the non-linear curve, of maximal/minimal effects as well as EC_{50}/IC_{50} , could not be conducted.

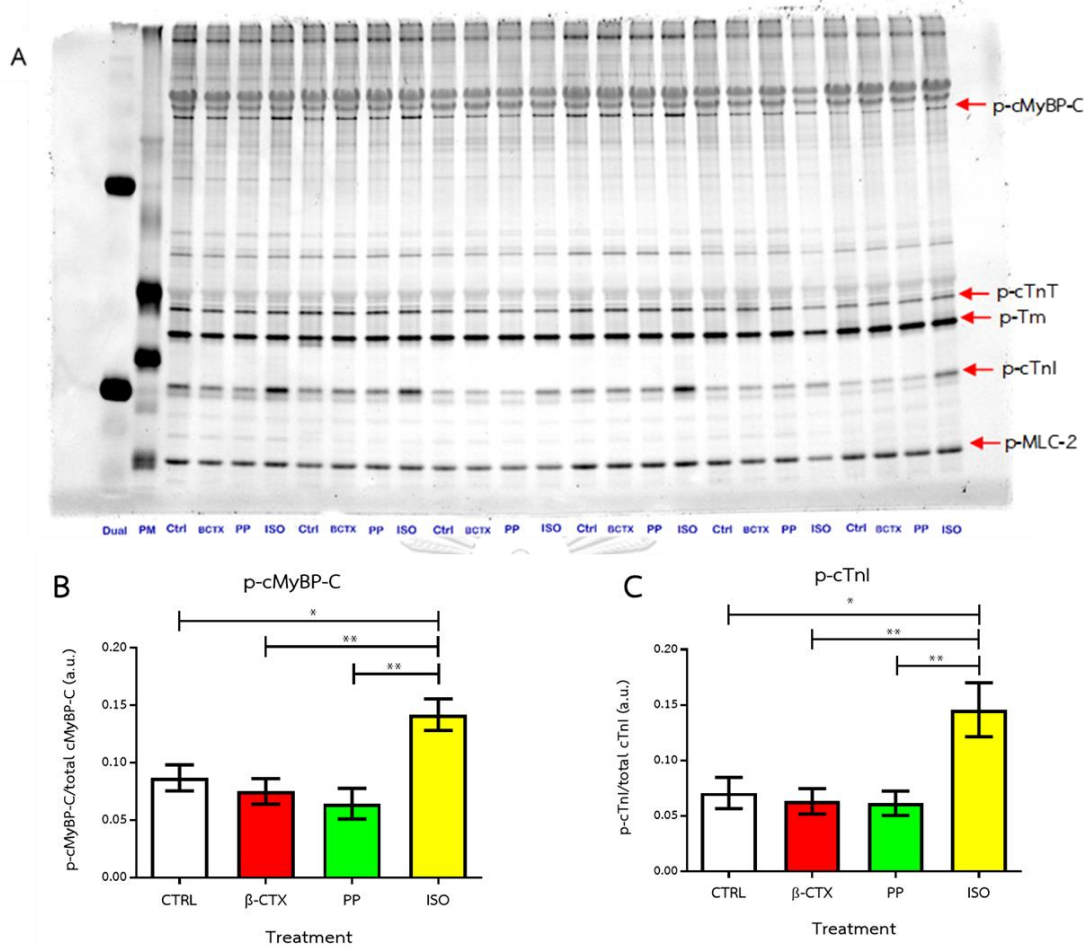


Figure 14. Effects of β -CTX on total phosphor-proteins of cardiac myocytes at the basal state.

(A) ProQ[®] staining of myofibrils ($n = 6$) in the basal condition comparing between different treatments; control (CTRL), β -CTX, propranolol (PP) and isoproterenol (ISO). Lane 1: Bio-Rad[®] precision plus protein[™] standard marker, Lane 2: PeppermintStick[™] phosphoprotein molecular weight standard. cMyBP-C: cardiac myosin binding protein-C, cTnT: cardiac troponin T, Tm: tropomyosin, cTnI: cardiac troponin I, MLC-2: myosin light chain-2. The total protein phosphorylation from (B) p-cMyBP-C and (C) p-cTnI is also represented. Data are shown in mean \pm S.E.M. and analyzed using one-way ANOVA following by Tukey's method as a post-hoc analysis.

* $p < 0.05$, ** $p < 0.01$.

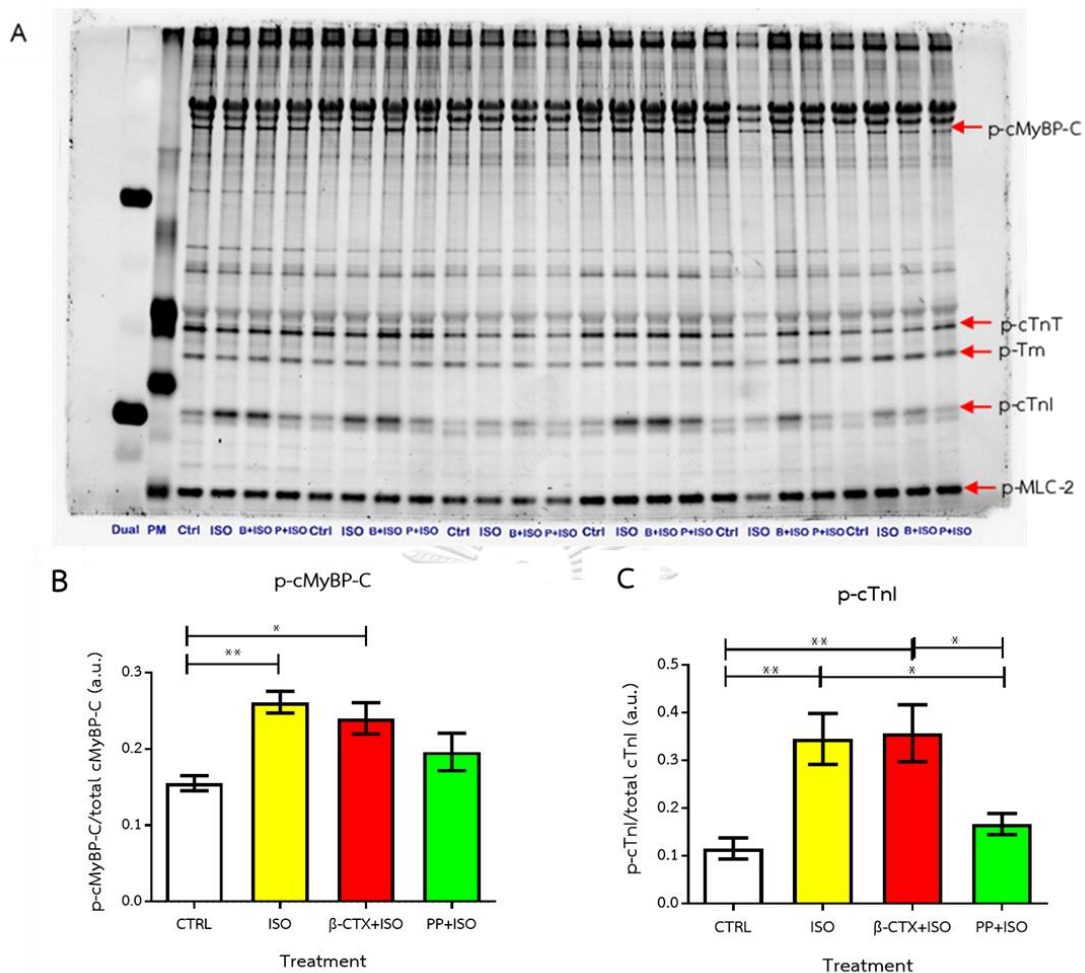


Figure 15. Effects of β -CTX on total phosphor-proteins of ISO-induced cardiomyocytes.

(A) ProQ[®] staining of myofibrils ($n = 6$) in the presence of ISO condition comparing between different treatments; control (CTRL), β -CTX (BCTX), propranolol (PP) and isoproterenol (ISO). (A) Gel was stained with ProQ diamond[™] for phosphorylation. Lane 1: Bio-Rad[®] precision plus protein[™] standard marker, Lane 2: PeppermintStick[™] phosphoprotein standard. cMyBP-C: cardiac myosin binding protein-C, cTnT: cardiac troponin T, Tm: tropomyosin, cTnI: cardiac troponin I, MLC-2: myosin light chain-2. The total protein phosphorylation from (B) p-cMyBP-C and (C) p-cTnI is also represented. Data are shown in mean \pm S.E.M. and analyzed using one-way ANOVA following by Tukey's method as a post-hoc analysis. * $p < 0.05$, ** $p < 0.01$

4. Effect of β -CTX on myofibrillar proteins phosphorylation

4.1. Alterations in total protein phosphorylation using ProQ[®] staining

The total phosphorylation of myofilament proteins was screened before the specific site phosphorylation determination to evaluate the possible involved proteins which might be affected by β -CTX. Figure 14 depicted the ProQ[®] phosphor-staining on cardiomyocytes incubated with β -CTX at the basal state comparing to the control, propranolol, and ISO. Promisingly, cells treated with ISO showed a significant elevation of cardiac myosin binding protein-C (cMyBP-C) and cardiac troponin I (cTnI) band intensities compared to the control group (Figure 14B and 14C). Interestingly, neither propranolol nor β -CTX could alter any of the protein phosphorylated bands (Figure 14). To further investigate the involvement of the β -AS inhibition, cardiomyocytes were tested with β -CTX in the condition of ISO presentation. Figure 15 showed the ProQ[®] staining of cardiomyocytes treated with β -CTX with the presence of ISO, comparing to the negative control, ISO only and propranolol pre-treated groups (Figure 15A). Incubation with ISO could promote the phosphorylation of cMyBP-C and cTnI from the negative control ($p < 0.01$) as previously indicated. Pre-incubation of propranolol attenuated the phosphorylation level of cTnI stimulated by ISO (Figure 15C); however, this effect did not occur in cMyBP-C (Figure 15B). On the other hand, cells pre-treated with β -CTX before ISO did not show any reduction of protein

phosphorylation when compared to the ISO-treated group (Figure 15). Analysis of other myofilament proteins total phosphorylation by ProQ staining was shown in Figure S8 and S9. We found that the band intensities of desmin (Figure S8A and S9A), cardiac troponin T (cTnT; Figure S8B and S9B), tropomyosin (Tm; Figure S8C and S9C), and myosin light chain-2 (MLC-2; Figure S8D and S9D) were at the similar level comparing among groups.



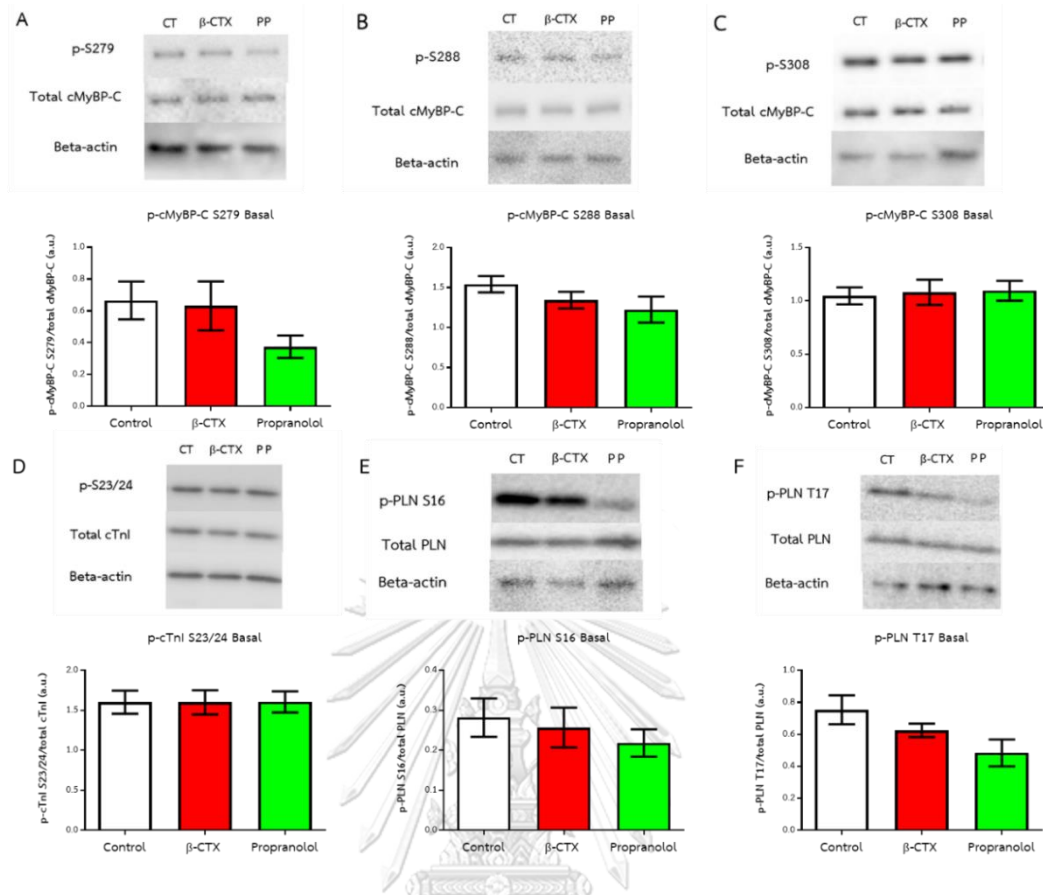


Figure 16. Western blot analysis of specific protein phosphorylated sites involved with β -adrenergic signaling responded to β -CTX.

Cells ($n = 6$) were treated with control (CT), β -CTX or propranolol (PP). Phosphorylation level normalized to the total protein expression of (A) Ser279, (B) Ser288 and (C) Ser308 of cMyBP-C; (D) Ser23/24 of cTnI, (E) Ser16 and (F) Thr17 of PLN. Data are presented in mean \pm S.E.M. and analyzed using one-way ANOVA following by Tukey's method as a post-hoc analysis.

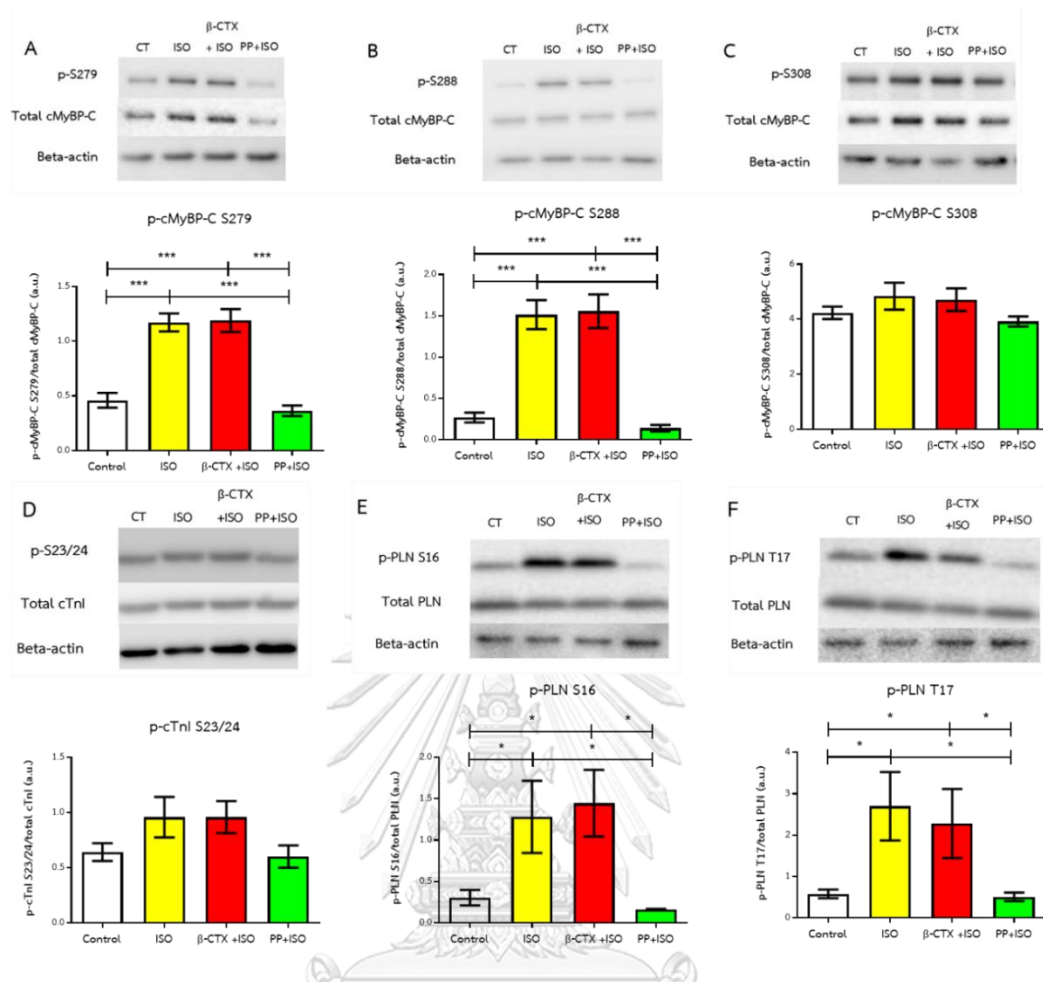


Figure 17. Western blot analysis of specific protein phosphorylated sites involved with β -adrenergic signaling responded to β -CTX in ISO-induced cardiomyocytes.

Cells ($n = 6$) were treated with β -CTX+ISO comparing to control (CT), ISO only, and propranolol with ISO (PP+ISO). Phosphorylation level normalized to the total protein expression of (A) Ser279, (B) Ser288 and (C) Ser308 of cMyBP-C; (D) Ser23/24 of cTnI, (E) Ser16 and (F) Thr17 of PLN. Data are presented in mean \pm S.E.M. and analyzed using one-way ANOVA following by Tukey's method as a post-hoc analysis. * $p < 0.05$, *** $p < 0.001$.

4.2. Western blot analysis of specific phosphorylation sites for β -adrenergic signaling

To further elucidate the mechanism of β -CTX on β -AS, the specific phosphorylation sites of proteins responded to protein kinase A (PKA), such as cMyBP-C at Ser279, Ser288, and Ser308; cTnl at Ser23/24; and phospholamban (PLN) at Ser16 and Thr17, were evaluated. Figure 16 displayed the western blot analysis of myofilament proteins with the incubation of β -CTX at the basal state. Results demonstrated that propranolol mildly reduced the phosphorylation levels at Ser279 of cMyBP-C (vs control, $p = 0.0683$; Figure 16A) and Thr17 of PLN (vs control, $p = 0.0572$; Figure 16F) comparing to the control group. On the contrary, β -CTX did not exhibit any alterations in phosphorylation of PKA-related sites of these proteins (Figure 16A-16F).

Figure 17 demonstrated the western blot analysis of proteins after incubating in the presence of ISO conditions. Figure 17A-17C illustrated the alterations of cMyBP-C phosphorylation at Ser279, Ser288, and Ser308 sites, respectively. With the presence of ISO, the cells robustly elevated the phosphorylation at two sites, Ser279 and Ser288 comparing to the control ($p < 0.05$; Figure 17A and 17B). Pre-incubation of propranolol attenuated the stimulatory effect of ISO at both Ser279 and Ser288 sites. In contrast, β -CTX-treated before ISO did not exhibit any changes in protein phosphorylation comparing to the ISO-treated group (Figure 17A and 17B). Meanwhile, there were no differences in the Ser308 phosphorylation level among groups (Figure 17).

Interestingly, the unchanged effect was also found in the phosphorylation sites Ser23/24 of cTnI (Figure 17D), indicated by a similar level of the band intensities among groups. The comparison of phosphorylation levels of PLN is shown in Figure 17E and 17F. Likewise, Ser16 and Thr17 were similarly responded to ISO where the phosphorylation levels are higher than the control group (Figure 17E and 17F). However, the activated bands were attenuated by propranolol, but no effects induced by β -CTX (Figure 17E and 17F).

5. Effect of β -CTX on the force-pCa relationship in the detergent extracted “skinned” fiber bundles experiment

To investigate the direct effect of β -CTX on Ca^{2+} sensitivity the force generated and Ca^{2+} concentration (pCa) relationship curve was plotted in Figure 18A. The analysis of the myofilament dynamics demonstrated that β -CTX did not affect the Ca^{2+} sensitivity of the skinned fiber as indicated by the superimposed curve comparing before and after receiving the compound (Figure 18A). Maximal tension generated, pCa_{50} , and Hill's coefficient (n_H) were calculated from the sigmoidal dose-response curve comparing before and after receiving β -CTX (Table 3). Finding revealed an unremarkable difference in all parameters.

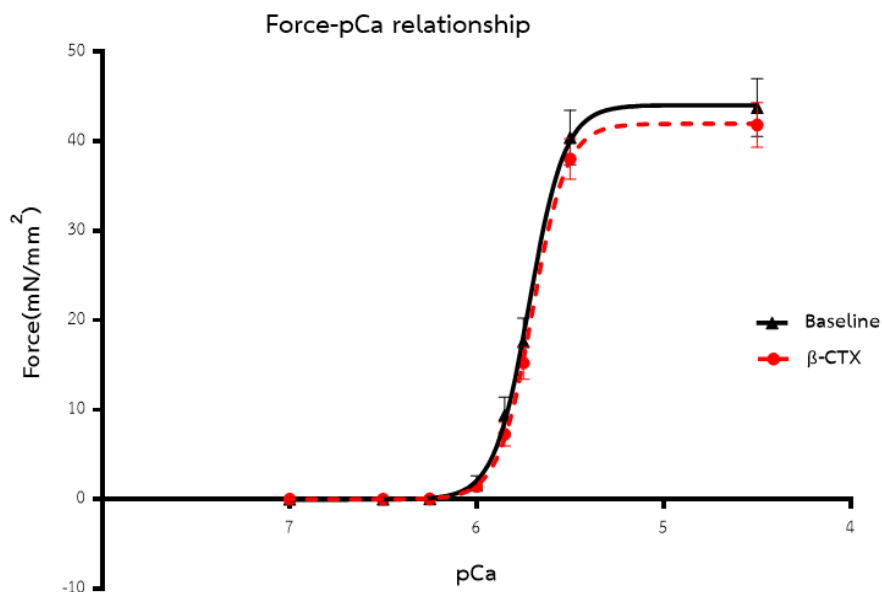


Figure 18. Force-pCa relationship of the detergent extract ("skinned") fiber bundle experiment. Data were compared before and after receiving β -CTX ($n = 9$). Data are shown in mean \pm S.E.M. and analyzed using student paired t-test.

Table 3. Comparison effects in skinned fiber experiment between at the baseline and after receiving β -CTX. Data are represented in mean \pm S.E.M.

	Baseline	β -CTX	p-value
Maximal force	44.04 \pm 1.81	41.96 \pm 1.34	> 0.05
pCa ₅₀	5.72 \pm 0.02	5.70 \pm 0.02	> 0.05
Hill's slope (n_H)	4.60 \pm 0.85	4.78 \pm 0.66	> 0.05

6. Effect of β -CTX on myofibril ATPase activity

We also speculated the effect of the β -CTX on the myofilament kinetics by performing the malachite green assay on myofibrillar proteins. The ATPase activity was assessed by the inorganic phosphate (P_i) produced during time points. The relationship between the ATPase activity and the pCa is depicted in Figure 19. The sigmoidal curve of the relationship demonstrated the right-shifted of the curve in the myofibrils receiving β -CTX ($p < 0.05$; Figure 19A). At the highest pCa (pCa = 4.03), β -CTX significantly reduced the maximal ATPase activity (0.97 P/sec) comparing to control (0.92 P/sec; Figure 19B). The calculated pCa₅₀, in accordance with the non-linear sigmoidal curve, was also depressed by 1 μ M of β -CTX (pCa₅₀ = 5.57; $p < 0.05$) compared to control myofibers (pCa₅₀ = 5.69; Figure 19C). However, there was no change in the n_H coefficient between the two groups (Figure 19D).

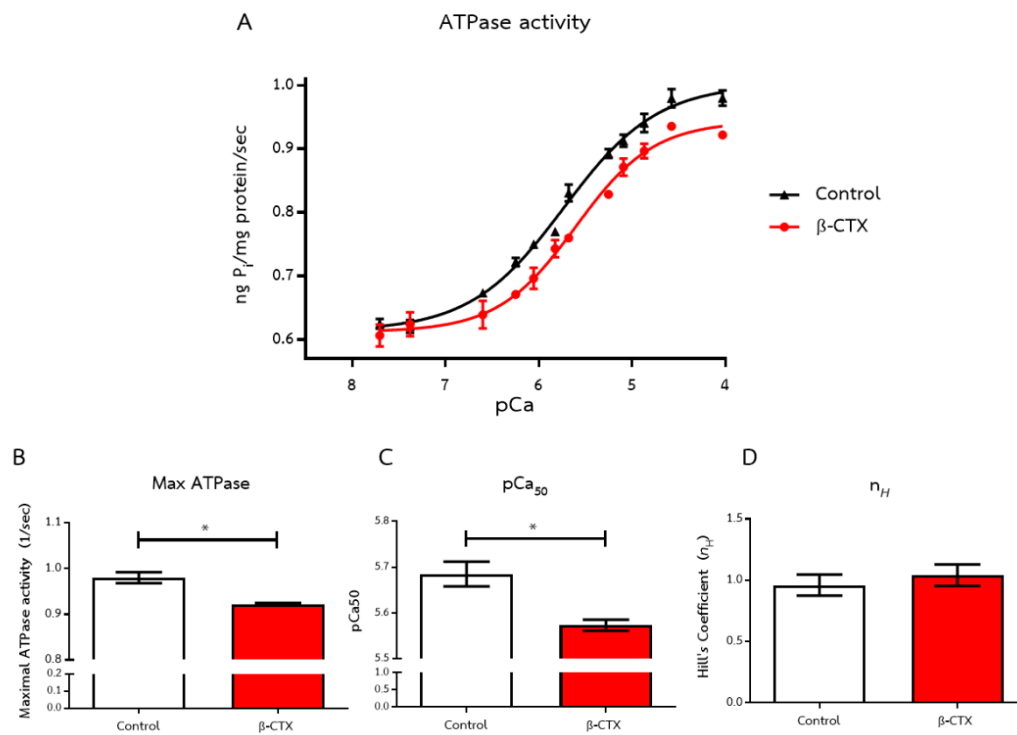


Figure 19. Effects of β -CTX on myofibrillar ATPase activity.

(A) Calcium-response curve of ATPase activity comparing between control ($n = 6$) and β -CTX ($n = 5$). Bar graphs illustrate the comparison effects in (B) maximal ATPase activity, (B) pCa₅₀ and (C) n_H . Data are shown in mean \pm S.E.M. and analyzed using unpaired t-test. * $p < 0.05$.

Chapter 5

Discussion

1. An alternative method to purify β -CTX from the Thai KCV.

Beta-CTX was firstly isolated and purified by the sequential use of size exclusion following by the RP-HPLC was conducted under the FPLC system (Rajagopalan et al., 2007). Due to the cost and availability of the system, we modified the method and switch to use RP-HPLC as the first step instead. Regarding this modification, the purification procedure was adapted from the proteomic study of the Indonesian's King Cobra venom (Petras et al., 2015). The chromatographic profiles from our study revealed a similar pattern to the original method. Moreover, the retention time of the fractions containing β -CTX was found at 58-64 minutes which were similar to the previous study (Petras et al., 2015). However, according to the SDS-PAGE and N-terminal sequencing, mixtures of other 3FTXs such as long-chain neurotoxin (LNTX; accession number P01387.1) and weak toxin (DE-1; accession number P01412.2) were included in the β -CTX-containing fractions (15th and 16th). Comparing between theoretical isoelectric focused point (pI) among these molecules, β -CTX possessed the highest pI (8.85), following by LNTX (8.05) and DE-1 (4.72). Therefore, we chose the cation exchange chromatography (cEx) under phosphate buffer, pH 7.4, condition. After the purification steps, the pure β -CTX was characterized by SDS-

PAGE and the automated Edman's degradation technique. In terms of cost-effectiveness, the method used in our study may provide benefit(s) when comparing to the previous FPLC method.

Although β -CTX had been previously described from the venom of Thai king cobra (Danpaiboon et al., 2014), this was the first report to isolate and purify β -CTX from the Thai snake. The percentage yielded of the compound from the Thai KCV (0.5% w/w mass) in this study was similar to the Malaysian KCV (Tan et al., 2015). However, the amount of β -CTX presented in the KCV is varied in other regions, including Indonesian (0.7% w/w), Hainan (0.8% w/w) and Guangxi (2 % w/w) (Chang et al., 2013; Tan et al., 2015). Apart from the difference in the geographical distribution of the snakes, the variations in the venoms are also contributed by other factors, including the age, season and the nutrition (Chippaux et al., 1991). Despite that the 3FTXs are the most abundant protein family presented in the KCV, β -CTX is a minor ingredient (accounted for 8.7% of all 3FTXs) (Petras et al., 2015). According to the gene bank database, additional 5 genes are encoding the precursors of other cardiotoxins (CTX 9, 14, 15, 21 and 23) from the King cobra venom glands (accession number ABB83631, ABB83632, ABB83633, ABB83634, and ABB635) (Rajagopalan et al., 2007). These proteins are different in few amino acid residues (2-5 sites), including T13K, K21R, V23I, E52V, and L54V from the β -CTX. Although have not been characterized yet, the two different subfractions from our study may be produced by

one of these encoding genes. Since the very high homology between the two isoforms (Arg to Gly at the 1st residue), they were believed to have similar functions (Rajagopalan et al., 2007).

2. The cytotoxic effects of β -CTX in various mammalian muscle cell types.

In the previous study, *in vivo* cytotoxicity of the β -CTX was conducted in mice where the neurological symptoms (labored breathing, loss of locomotion, and unconsciousness) and lethal dosage were reported at 100 mg/kg, intraperitoneally (Rajagopalan et al., 2007). In our current study, the *in vitro* cytotoxicity in muscle cells was basically performed prior to the study of cardiovascular physiological responses. Interestingly, β -CTX exhibited cytotoxicity in rat smooth muscle with none lethal effects in neither skeletal nor cardiac myoblasts up to 0.8 mg/mL. Until now, there were no reports explaining cytotoxicity mechanisms caused by this novel compound. However, other related cobra-derived CTXs show cytotoxic effects in other cell types such as neuronal, endothelial, cardiac and skeletal muscles, and cancerous cell lines (Lin Shiau et al., 1976; Ou et al., 1997; Wang et al., 2005; Tsai et al., 2006). It is well-published that the cytotoxic by elapid-derived CTXs is mediated through the perturbation of either cellular or sarcolemma membranes which further disrupts membrane stability and cytosolic Ca^{2+} -homeostasis (Wang et al., 1997; Chen et al., 2007). Concerning on the structuring-functional properties of the CTXs, membrane lytic regions are notably correlated to the presence of the specific cationic residues,

such as Lys12, Lys18, and Lys35, and the cytotoxic regions are including the aromatic residues, Tyr/Trp11 and/or Tyr/Trp22 (Kumar et al., 1997). However, Roy and colleagues have previously proved that β -CTX may not exert this property due to the loss of positively charged and the cytotoxic regions comparing to other CTXs (Roy et al., 2019). Interestingly, a recent study had shown that CTXVIII4 acquired from Taiwanese Cobra venom (*Naja mossambica*), could translocate through the cell membrane and disrupt the outer mitochondrial membrane of the cortical neurons (Zhang et al., 2019). Combining the evidence from far-UV spectroscopy that the β -CTX also contains the hydrophobic region at the C-terminal (Rajagopalan et al., 2007). We postulated that this mechanism may underlie the β -CTX's cytolytic property. Nevertheless, the cytotoxicity of the β -CTX needs further investigation. We also speculated that the absence of striated muscle cytotoxicity might be that the concentration of β -CTX used in the experiment was not reached or the lack of targeted receptors in the myoblast cells.

In addition, our study revealed the robust toxicity of the KCV on both muscle cell lines. Geographic variations influence the protein compositions, including CTXs, and therefore alter the toxicity of KCV from different regions (Chang et al., 2013; Tan et al., 2019). The effects were correlated to previous *in vivo* cytotoxicity study in mice where the LD₅₀ of the Thai crude KCV were 1.1 μ g/g and 0.59 μ g/g via intraperitoneal and intramuscular routes, respectively

(Danpaiboon et al., 2014). Nevertheless, the cellular cytotoxicity caused by the crude KCV was majorly discussed by the activity of the L-amino acid oxidases (LAAOs) (Li Lee et al., 2014).

3. Suppression of β -CTX on cardiomyocyte contractility without contribution of intracellular calcium

This was the first study to evaluate the effects of β -CTX on *ex vivo* isolated cardiomyocytes. In the current study, we found that the β -CTX drastically reduced both the extent and the rate of the changes in the myocyte shortening. Contrarily, the blunting of cardiac inotropic was not found in the previous *ex vivo* isolated perfused heart experiment (Rajagopalan et al., 2007). Since the concentration of β -CTX used in the recent (up to 1 μ M) and previous (5 μ M) studies were different, we postulated that the *ex vivo* perfusion may not deliver enough concentration to the cells as ours did on isolated cardiomyocyte directly. Some other snake venom toxins also display negative inotropic property via various mechanisms. For example, calciseptine, a 3FTX protein isolated from the black mamba (*Dendroaspis polylepis polylepis*) venom, dose-dependently inhibits rat atrial myocyte contractility and causes smooth muscle relaxation through a specific blockage of L-type Ca^{2+} channels (LTCC) (de Weille et al., 1991). *Dendroaspis* natriuretic peptide (DNP) also reduces Ca^{2+} influx via LTCC, resulting in reduced ventricular contraction (Park et al., 2012). Angusticeps-type toxins, peptides isolated from *Dendroaspis angusticeps*, also show a negative inotropic and chronotropic impact via the

inhibition of cholinergic receptors (Lee et al., 1985). Although the depression in contractility observed from our findings was correlated to the Taiwan cobra (*Naja oxiana*) derived CTX (Averin et al., 2019); in contrast, other studies revealed that other elapids-derived CTX proteins demonstrated positive inotropic effects on the cardiomyocytes (Harvey et al., 1982; Wang et al., 1997). Apart from the toxins, there are other drugs or chemicals which contribute the negative inotropic property are including the Ca^{2+} channel blockers (e.g. verapamil or diltiazem), Na^+ channel blockers (such as quinidine, flecainide or mexiletine), BBs (including propranolol, carvedilol or landiolol) and myosin II ATPase inhibitors (notably, blebbistatin, N-benzyl-*p*-toluene sulphonamide; BTS, or 2,3 butanedione monoxime; BDM) (Mochizuki et al., 2007; Butler et al., 2015; Chung et al., 2015; Kobayashi et al., 2015; Watanabe et al., 2017; Gao et al., 2018).

Interestingly, our results demonstrated that the amplitude of the CaT during the contraction was not altered upon the reduction in myocyte shortening, indicating the Ca^{2+} -independent negative inotropic effect. It is well known that intracellular Ca^{2+} plays an important role in driving myofilament dynamics as well as the ventricular contractility (ter Keurs et al., 1988). The increase of cytosolic Ca^{2+} is occurred by the influx of extracellular Ca^{2+} through LTCC and released the cation from the sarcoplasmic reticulum (SR) via the ryanodine receptor (RyR) (Shin et al., 2008). Therefore, we inferred that the effects of β -CTX on ventricular myocyte functions may not mediate through this mechanism. Other Ca^{2+} -independent inotropic pathways

are including the activation of nitric oxide (Cawley et al., 2011), the reduction in Ca^{2+} -sensitivity of myofilament fibers or ATPase activity (Butler et al., 2015), or through the prolonged action potential duration which further deteriorates contractile properties (Housmans et al., 1995).

4. β -CTX prolonged τ_{Ca} causing negative lusitropic effects of the ventricular myocytes

Lusitropic parameters acquired from our studies demonstrated that β -CTX suppressed the rate of cell relaxation (indicated by prolongation of TR_{90} and τ index) and the rate of re-lengthening (reduction in $-\text{dL}/\text{dt}$). This information indicated the blunting in ventricular relaxation and impaired diastolic function of the cardiomyocyte induced by β -CTX. This was supported by the evidence from our study that β -CTX prolonged the decay of CaT (τ_{Ca}). We proposed the following pathway may responsible for diminishing ventricular relaxation. In general, the removal of cytosolic Ca^{2+} is under controlled by the re-uptaking of Ca^{2+} into SR directly via sarcoplasmic reticular Ca^{2+} ATPase pump (SERCa), indirectly regulated by the phosphorylation of phospholamban protein (PLN), as well as the effluxes of Ca^{2+} ion via sarcolemma Ca^{2+} ATPase pump and $\text{Na}^+/\text{Ca}^{2+}$ counter transporter (Shin et al., 2008). There are several mechanisms that contributed the negative lusitropic effect. For example, potassium channel blockers (notably, 4-aminopyridine, amiodarone or nifekalant) which prolong the action potential duration by slowing down the K^+ efflux, and, hence, impair the relaxation (Kocic et al., 1999; Salgado et al., 2007; Ishizaka et al., 2019). Inhibition of SR Ca-handling proteins by using thapsigargin (Bassani and

Bassani, 2003), ryanodine or dantrolene sodium (Pucelik, 2007) also exerts negative lusitropy by altering Ca^{2+} re-uptaking into the SR. α_1 adrenergic, (phenylephrine), angiotensin II and endothelin agonists (sarafotoxin; SRTX) share a similar positive inotropic and negative lusitropic effects on the ventricular myocytes via the activation of G_q -coupled proteins and phospholipase C (PLC) activity (Vila-Petroff et al., 1996; Salas et al., 2001; Konrad et al., 2005). According to this pathway, the protein kinase C (PKC) is being activated and the Ca^{2+} efflux is reduced by disruption of the $\text{Na}^+/\text{Ca}^{2+}$ exchanger (Salas et al., 2001). Interestingly, atenolol is the only β -adrenergic antagonist to cause negative lusitropy due to partially binding property to the α_1 AR (Vila-Petroff et al., 1996). Of note, several toxins had been previously demonstrated the negative cardiac lusitropy effect. For example, SRTX-i3 (Mourier et al., 2012) and SRTX-m (Mahjoub et al., 2015), were shown to reduce ventricular relaxation parameters in both *in vivo* hemodynamic and echocardiographic studies, indicating impaired diastolic dysfunction of the heart. Although the molecular mechanisms underlying the action of these compounds have never been investigated, these SRTXs structures are endothelin-like and the action may mediate through the PKC activity as aforementioned. Therefore, we speculated that the mechanisms controlled the reduction in τ_{Ca} and ventricular lusitropy may be mediated by β -CTX through either direct inhibition of the Ca^{2+} -handling proteins, Ca^{2+} -pumps and PLN, or the cross-talking signaling via the inhibition of GPCR cooperated with PLC and PKC activity.

5. β -CTX attenuated cardiomyocyte functions in ISO-induced cells but did not affect FSK-induced cells

In this study, ISO or FSK was introduced to the cardiomyocytes to stimulate the β -AS or activate the AC. Promisingly, findings showed that both β -agonist and the AC activator promoted the inotropic and lusitropic responses in isolated cardiomyocytes. During both conditions, the positive inotropy was associated with the elevation of the amplitude of the CaT; whereas, the τ_{Ca} was not altered regardless of the negative lusitropy. It is well known that the β -ARs are coupled with the G-proteins. After the receptor is bound to the β -agonist, G-protein subunit α_s would further stimulate the AC function, turning ATP into cAMP, and switch on the cAMP-PKA pathway (de Lucia et al., 2018). As an active enzyme, PKA consequently phosphorylates other Ca^{2+} -handling proteins (such as LTCC, RyR, and PLN), to promote the elevation of intracellular Ca^{2+} (Shin et al., 2008), and myofilament proteins (notably, cMyBP-C and cTnI), to accelerate myofibrillar dynamics (Colson et al., 2008; Rao et al., 2014).

Focusing on the ISO-stimulating condition, findings revealed that β -CTX attenuated the stimulatory effect of ISO in most parameters. The deterioration effects of the myocyte functions, inotropy, and lusitropy by β -CTX were similar to those found in the basal condition, without ISO. However, the blunting effect of peak CaT was found only in the ISO-stimulating condition. We postulated that the ISO-induction would help increase the sensitivity of detecting β -blocking

effects in both amplitudes of shortening and the CaT as previously described (Watanabe et al., 2017). Hence, the effect of β -CTX on intracellular Ca^{2+} movement in ISO-treated cells needs further investigation. Besides, unchanged of the EC_{50} was also observed in β -CTX+ISO comparing to the ISO-treated cells, indicating the non-competitive binding property. Comparing to the propranolol, as a competitive β -blocking agent, we found that the compound alleviated the cardiomyocyte functions in a different pattern from the β -CTX-treated group. At the basal state, the toxin showed a higher potency to abolish cardiac myocyte shortening as expressed by the lower IC_{50} than propranolol. Since the results from *in vitro* studies were contrary to the recent *ex vivo* experiments, the hidden actions of the β -CTX are needed to be elucidated. Moreover, the blunting effects of cardiomyocyte functions caused by propranolol in this study were associated with the interruption of the Ca^{2+} -homeostasis which was not presented in the β -CTX-treated cells. The evidence supported the possibility that the action β -CTX is unlikely to be the BBs. In the ISO-treated cells, pre-incubation with the propranolol before ISO significantly caused higher EC_{50} (or IC_{50}) with similar plateau effects as the positive control. Literally, it is known that propranolol has the potential to block the binding of ISO to the β -AR as represented by the shifting concentration-effect curve to the right (Hermsmeyer et al., 1982). Generally, β -blockers reduce the activity of adenylyl cyclase, the cAMP-PKA pathway, and hence, the Ca^{2+} -homeostasis (Strang et al., 1994). Since the peak CaT was not affected by the compound, we speculated that

β -CTX may directly act on other non-classical β -adrenergic pathways. Increasing the dosage of the β -agonist could overcome the binding capacity of propranolol and, hence, maximize the cardiomyocyte responses. Since the β -CTX reacted differently from propranolol, results strongly supported our observation that this toxin may non-competitively bind to the β -ARs. Focusing on the structural-activity relationship of adrenergic ligands, β -agonists such as epinephrine and norepinephrine usually contain the catechol group (aromatic ring with two hydroxyl groups) and the amine group. The former reacts to the Ser215 and Ser212 residues in the helix V whereas the latter binds ionically to the Asp113/Asn312 of the helix III of the receptor (Strader et al., 1988; Finch et al., 2006; Katritch et al., 2009; Chan et al., 2016a). Indeed, ISO is previously reported that the hydrogen bonds are formed in Ser203, Ser204, and Ser207 of TM5, Asn216 of TM6, Tyr308 of TM7 (Vanni et al., 2011). Although there are common regions to bind both β -ARs, the specific sites to selectively bind the β -1 AR are composed of three amino acids, Leu110, Thr117 and Val120 of the transmembrane 2, where the β -2 selectivity site is located at Tyr308 of TM7 of the receptor (Isogaya et al., 1999). On the other hand, BBs, similarly, possess a binding pattern that competitively shifts the bond formation between the agonists (Chan et al., 2016a). Although the structural conformation of β -CTX is known; however, the exact binding residues of the compound on the adrenergic receptors are not fully understood yet. It is believed that the three-finger toxin formation, associated with some specific residues, is responsible for this binding as proved by

that the synthesized single strand peptide of β -CTX does not interact with either β -1 or -2 ARs (Rajagopalan et al., 2007).

In the FSK-induced cells, findings demonstrated that the pre-incubation of β -CTX prior to FSK inhibited the inotropic functions of the ventricular myocytes comparing to the control cells; whereas other parameters were unchanged. We inferred that the toxin partially had a direct effect on AC activity. However, the mechanism of action through this compound needs further investigation. It is generally known that β -AR is one of the most important G-protein coupled receptors (GPCRs) which cooperated with the AC activity, and cAMP-PKA pathway (Hohl and Li, 1991). Apart from the β -ARs, other GPCRs involved with the AC activity in the cardiomyocytes are including the muscarinic receptor and adenosine receptors (A1, A2A, A2B, A3) (Harvey, 2012; Vecchio et al., 2017). Although propranolol is a known β -blocking agent which reduces the AC activity (Witte et al., 1998); however, the effects that occurred in this study were not clearly observed. Unlike other BBs (nebivolol, carvedilol, bucindolol, and metoprolol), attenuation of the force of contraction, induced by FSK, was detected after these compounds were perfusing to ventricular myocytes (Brixius et al., 2001). We speculated that the concentration of propranolol used in the study was not reached. Moreover, the recent findings were inconsistent with the previous study that the administration of FSK, after the cardiogenic shock of propranolol overdose, could reverse the vital signs in dogs (Whitehurst et al., 1999). Therefore, findings

suggested that even though β -CTX possesses a non-competitive inhibitory property on the β -ARs, it does not mediate through the classical- β -adrenergic pathway.

6. The action of the β -CTX was not mediated through the cAMP-PKA pathway

To further determine the effect of β -CTX on the adrenergic signaling pathway we employed the protein modification by phosphorylation study. Hence, two experiments, ProQ[®] phosphor-staining and western blot for specific sites were performed to prove whether the action of β -CTX mediated via the classical β -AS. This is the first study to reveal the effect of the snake toxin on the β -adrenergic pathways. On the myofilament phosphor-staining experiment, ISO-treated cells augmented phosphorylation levels in cMyBP-C and cTnI comparing to control; whereas, neither β -CTX nor propranolol did not have any impact. However, the ISO-stimulating conditions allowed the propranolol to exhibit its effect by alleviating the intensity of the phosphorylation bands. Meanwhile, pre-treated cells with β -CTX prior to ISO was ineffective. In associated with the western blot experiment of the specific phosphorylation sites studies, similar results were noticed in the basal state. However, in the ISO-treated cells, modestly activation of the cAMP-PKA was observed by promoting the phosphorylation of cMyBP-C at Ser279 and Ser288, cTnI, and PLN at Ser16 and Thr17. As expected, pre-incubation with propranolol before the ISO markedly showed attenuation effects comparing to the ISO-treated cells. In contrast, cells incubating with β -CTX did not show any inhibitory effects. Therefore, we concluded that the

blunting of ventricular functions by the β -CTX in the previous functional study was not mediated through the cAMP-PKA signaling, literally through non-classical β -AS.

In general, the classical cAMP-PKA pathway induced by β -agonists would be maximized through the activation of p-cMyBP-C and p-cTnI (Gresham and Stelzer, 2016). Apart from the formation of the thick filament, phosphorylation of cMyBP-C also regulates ventricular myocyte systolic and diastolic functions via myofibrillar kinetics (Flashman et al., 2004; Tong et al., 2008; Rosas et al., 2015). Theoretically, there are 17 phosphorylation sites of cMyBP-C; however, well-published sites responsive for PKA in mice (rats) are Ser273 (Ser279), Ser282 (Ser288), Ser302 (Ser308), and Ser307 (Ser313) (Gautel et al., 1995; Jia et al., 2010). In the current study, only Ser279 and Ser288 were augmented in ISO-stimulating condition whereas Ser308 was not affected which was similar to the previous report where Ser308 is responded to PKA in S313A mutated-rats (Ponnam et al., 2019). Although phosphorylation at Ser282 was also reported to be the modulator of other Ser273 and Ser302 phosphorylation in mice (Sadayappan et al., 2011), we speculated that the mechanism was species-dependent and did not occur in the rats. On the other hand, the effect of ISO on the phosphorylation of cTnI is surprisingly controversial where the PKA could not increase phosphorylation at the Ser23/24 site, although the total phosphor-staining is being activated. It has been known so far that cTnI is a substrate for PKA (Pratje and Heilmeyer, 1972; Stull et al., 1972) where the S23/24 is the only site of cTnI which is responded

to PKA (Solaro and van der Velden, 2010). This discrepancy needs further elucidation. For the Ca^{2+} -handling protein phosphorylation, PLN is one of the most important structures regulating the Ca^{2+} -re-uptaking into SR, via SERCa ATPase pump. The alteration of Ser16 and Thr17 phosphorylation in ISO-treated cells observed from the study supports the previously known knowledge that these dual sites are responsible for the β -agonist and cAMP-PKA pathway (Chu and Kranias, 2002). In our study, the pre-incubation of propranolol exhibited the β -blockade activity by attenuating all responsive phosphorylation sites activated by ISO. The reduction in PKA-phosphorylated sites is also found in other BBs, such as landiolol, metoprolol, and carvedilol, where the p-Ser2808 of ryanodine receptor (RyR), as well as Ser-16 and Thr-17 of p-PLN, are reduced (Mochizuki et al., 2007; Zhang et al., 2012; Kobayashi et al., 2015). Contrarily, β -CTX affected none of these phosphorylation residues, indicating non-involvement of the cAMP-PKA pathway. Apart from PLN, other Ca^{2+} -handling proteins responded to PKA are including Ser1700 and Thr1704 of the voltage-gated Ca^{2+} -channel (VGCC) subtype 1.2 (CaV1.2), p-Ser2809 of Ryanodine receptor subtype 2 (RyR2) and Ser465 of the small-conductance Ca^{2+} -activated channel K^+ channel (SK) (Witcher et al., 1991; Brunet et al., 2015; Lei et al., 2018; Hamilton et al., 2019). Although we did not study the involvement of β -CTX on of these sites; however, our findings suggested that β -CTX was unlikely exerted classical β -blocking activity as previously described by Rajagopalan and colleagues (Rajagopalan et al., 2007)

7. β -CTX reduced actomyosin ATPase activity without changing myofibrillar dynamics

Although the attenuation effects of β -CTX on ISO-treated cells could be explained by that the maximal CaT could not reach, the underlying mechanism causing negative inotropic and lusitropic responses in the basal condition, without ISO or FSK stimulation, were still need further investigation. Here, we demonstrated that β -CTX inhibited the ATPase activity resulting in an alteration in the myofilament kinetics. The myofibril enzyme activity is well-known in its role in the cross-bridge cycling rate as well as the velocity of the fibers (Seagren et al., 1971; Cappelli et al., 1989). Thus, we speculated that the blunting of the ventricular myocyte functions by β -CTX may mediate through this mechanism. However, it was interesting that although the Ca^{2+} sensitivity of the myofiber enzyme activity was disrupted, still, the Ca^{2+} sensitivity to generate the force by the fibers remained constant. Previous research had shown that the alteration in ATPase activity is not correlated with the P_0 tension in the isometric condition (Bottinelli et al., 1994). Although Ca^{2+} is one of the most important factors activating the contractile process, other myofilament proteins may involve in the mechanism, including the troponin complex and cMyBP-C (Tong et al., 2004; Geeves and Ranatunga, 2012; Martin-Garrido et al., 2018). Also, the unchanged of the pCa-force relationship in isometric fiber study is a different story of *ex vivo* isotonic functional studies. Literally, each BB affects both experiments differently, resulting in a different outcome. For example, long-term carvedilol administration reduced the Ca^{2+} -dependent

ATPase consumption but did not change the myofibrillar Ca^{2+} -sensitivity; whereas, metoprolol did not alter ATPase activity but increased the myofibrillar Ca^{2+} -sensitivity via the upregulation of cTnI (Brixius et al., 2007). However, the acute effects of carvedilol, metoprolol, and nebivolol, was ineffective to change the Ca^{2+} -sensitivity of the myofibers (Bundkirchen et al., 2001). Taking together, we, therefore, concluded that a reduction in ATPase activity may involve the inhibition of ventricular myocyte shortening; however, other mechanisms interfering myofilament proteins may be another target for this protein.

8. Other possible pathways underlying β -CTX's effect

Based on our findings, we proposed that β -CTX may not classify as a classical beta-blocker agent. Rather, it may act via multiple target proteins besides the classical cAMP-PKA pathway. In general, the 3FTXs family is very well-known for its multi-target actions (Kini and Doley, 2010). For example, ρ -Da1a, from green mamba (*Dendroaspis angusticeps*), shows a binding affinity to both α_1 and α_2 adrenergic receptors (Maiga et al., 2012). Muscarinic toxins from Elapidae were also reported to impact cardiac function via activation of type 2 or 3 muscarinic receptors (Ponicke et al., 2003). Clearly, further studies possibly involving these aforementioned cellular mechanisms are needed to fully elucidate the molecular mechanisms of action underlying the cardiac impact of king cobra snake derived β -CTX. Here, we listed three possible

mechanisms that related to our results, the direct inhibition to other Ca^{2+} handling proteins, the nitric oxide pathways, and the other G_q -protein coupled receptors (GPCRs) which coupled the phospholipase C activity.

According to the results, alteration in Ca^{2+} homeostasis was exhibited during the ISO-stimulating condition. Therefore, β -CTX might directly mitigate the level of Ca^{2+} via either the Ca^{2+} influx via VGCC or Ca^{2+} released from SR via RyR. As previously described, Ca^{2+} is a secondary messenger regulating the myofibrillar contraction; therefore, it may directly explain the findings in the functional studies. However, the blockade of the VGCC or the RyR2 activity is still needed to be investigated. Calciseptine, FS-2, C10S2C2, and S4C8, are examples of toxins belonging to 3FTX-family which possess LTCC antagonist activity (de Weille et al., 1991; Watanabe et al., 1995). It has already been published that the hanging residues (Met45-Trp46-cis-Pro47-Tyr48) between two prolines (Pro42 and Pro49) at the third loop of these compounds are competitively bound to the LTCC (Schleifer, 1997; Kini et al., 1998). Despite that β -CTX (63 amino acids) is similar in the structure and the size to these compounds (60 amino acids); however, it does not contain the specific inhibition sites as in those compounds. Hence, structural-functional studies of β -CTX are needed.

Notably, the second possible pathway that may involve the β -CTX activity is the nitric oxide (NO) pathway. NO is known as a free radical gas that modulates cellular functions throughout the body. There are three different species of the nitric oxide synthase (NOS) in the cell, including neuronal (nNOS), endothelial (eNOS) and inducible (iNOS) forms. The former two types, nNOS and eNOS, are called constitutive enzymes (cNOS) which normally regulate the intracellular physiological signaling; whereas, iNOS is induced during the inflammatory stage (Bredt, 2003). Interestingly, in the normal condition, the two cNOS activity are opposing each other, eNOS blocks the Ca^{2+} influx via VGCC, while nNOS induces Ca^{2+} released from RyR (Bredt, 2003). Apart from the Ca^{2+} mobilization, NO classical pathway is mediated through the activation of soluble guanylyl cyclase (sGC) that turn GTP into cyclic cGMP and further activates protein kinase G (Meier et al., 2017). However, this downstream signaling is not directly modulated by NO itself in the cardiomyocytes but occurred in cardiac fibroblasts (Menges et al., 2019). The Dendroaspis natriuretic peptide (DNP) is an example of the snake toxins which accelerate the GC-cGMP-PKG activity and, hence, inhibits the LTCC (Zhang et al., 2010). Notexin, the myotoxic phospholipase acquired from the tiger snake (*Notechis scutatus scutatus*), causes skeletal muscle injury via the increased production of free radical NOs that induces the apoptotic process (Liu et al., 2015). Thus, we speculated that the cross-talking between the cGMP-PKG pathway or alteration in Ca^{2+} -homeostasis by NO may be possibly induced by β -CTX.

The last mechanism which may be possibly altered by β -CTX is the blockade of GPCR co-operated with PLC activity. There were reports revising the crosstalk between β -adrenergic signaling with the angiotensin II receptor (Barki-Harrington et al., 2003), and endothelin receptors (Araki et al., 2000). Besides, there was evidence of a cAMP-independent pathway induced by β_2 -AR (Galaz-Montoya et al., 2017). Generally, PLC is an enzyme which turns phosphatidylinositol 4,5 bisphosphate (PIP_2) into diacylglycerol (DAG) and inositol triphosphate (IP_3). The former would further induce the protein kinase C (PKC) activity and the latter binds to its receptor (IP_3R) at the SR causing the release of Ca^{2+} (Tobin, 1997). PKC has its action as PKA, phosphorylation of intracellular proteins. These proteins are involving in the Ca^{2+} -mobilization, LTCC (Ser1928) and PLN (Ser16, Thr17), and the myofilament kinetics cMyBP-C (Ser273, Ser302) and cTnI (Ser23/24, Ser43/45, Thr144) (Edes and Kranias, 1990; Hartmann and Schrader, 1992; Lu et al., 2010; Bardswell et al., 2012; Raifman et al., 2017). Since β -CTX showed non-specific inhibition on β -ARs (Rajagopalan et al., 2007), the protein may non-specifically block other GPCRs, resulted in the depression of CaT and myofilament dynamics. Therefore, the action of β -CTX on this mechanism needs further investigation.

Chapter 6

Conclusion

Taken together, our acquired information introduces novel knowledge in the toxinological field and physiological aspects of Ca^{2+} -homeostasis and myofilament kinetics in cardiomyocytes. Firstly, we were able to isolate and purify the compound based on alternative technique, sequential used of reverse phase following by cation exchange chromatography. The purified protein induced cytotoxicity in the rat smooth muscle cell lines, on the contrary, it did not show any lethal effect on the striated myoblasts. We were also able to explain the effect as well as the possible mechanism(s) of β -CTX performed on isolated ventricular myocyte functions. At the basal state, Ca^{2+} -independent negative inotropic effect was detected. The effect was explained by that β -CTX could directly alter myofibril ATPase activity and further reduce myofilament kinetics (Figure 20). On the other hand, β -CTX prolonged the Ca^{2+} -decayed resulting in reduced ventricular relaxation (Figure 21). In contrast, during the ISO-stimulating condition, the Ca^{2+} -dependent effect by β -CTX was clearly observed, and hence, exhibiting a negative inotropic as well as lusitropic properties. Further studies on Ca^{2+} homeostasis are needed to elucidate the Ca^{2+} -dependent pathway. Although the non-competitive β -antagonistic effect was suspected, β -CTX did not have any impact via classical β -AS as observed from our experiment. In addition, the

Ca²⁺-sensitivity of the myofibers was not altered by the compound. Thus, phosphorylation on other myofilament proteins was expected to be the underlying mechanism. Since the precise mechanisms of β -CTX are, yet, unknown; therefore, further studies on the aforementioned possible mechanisms as well as the elucidation on Ca²⁺ homeostatic pathways are required.

Our study provides a shred of novel evidence in which the protein derived from elapids possessed ATPase inhibitory property. Discovery in this Ca²⁺-independent mechanism of β -CTX may provide insight into drug development for some specific myocardial diseases caused by the oversensitivity of the ATPase activity (e.g. Hypertrophic cardiomyopathy). Besides, this protein can potentially be a substrate for developing a novel β -blocking agent which reduces heart rate as well as the cardiac stiffness. Moreover, in the heart failure condition, where the ATP consumption is high, reducing ATPase activity while getting similar maximal tension may preserve the bioenergetics in the failing cardiomyocytes.

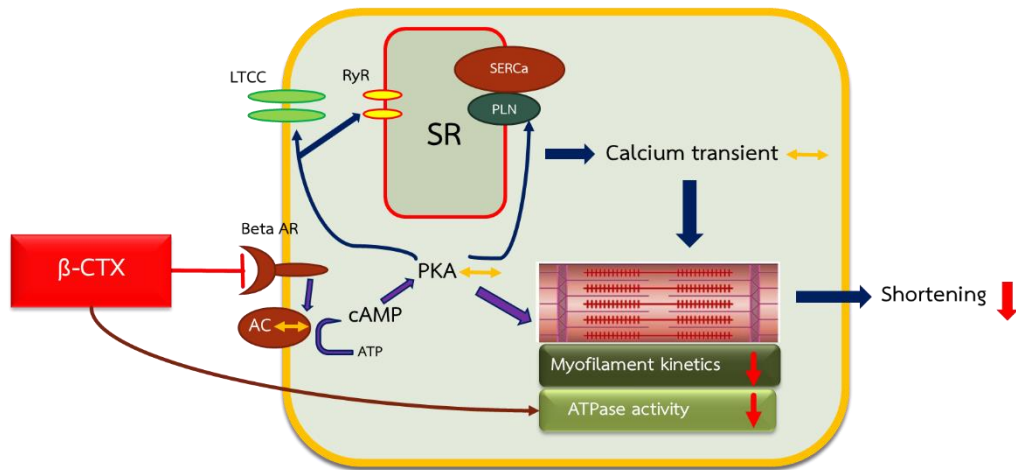


Figure 20. Schematic diagram illustrates possible mechanisms of β -CTX on ventricular shortening acquired from the study.

The non-competitive inhibition on β -AR may occur without mediating through the classical cAMP-PKA pathway. The compound also directly disrupts myofibril ATPase activity which resulting in the reduced myofilament kinetics and myocyte shortening.

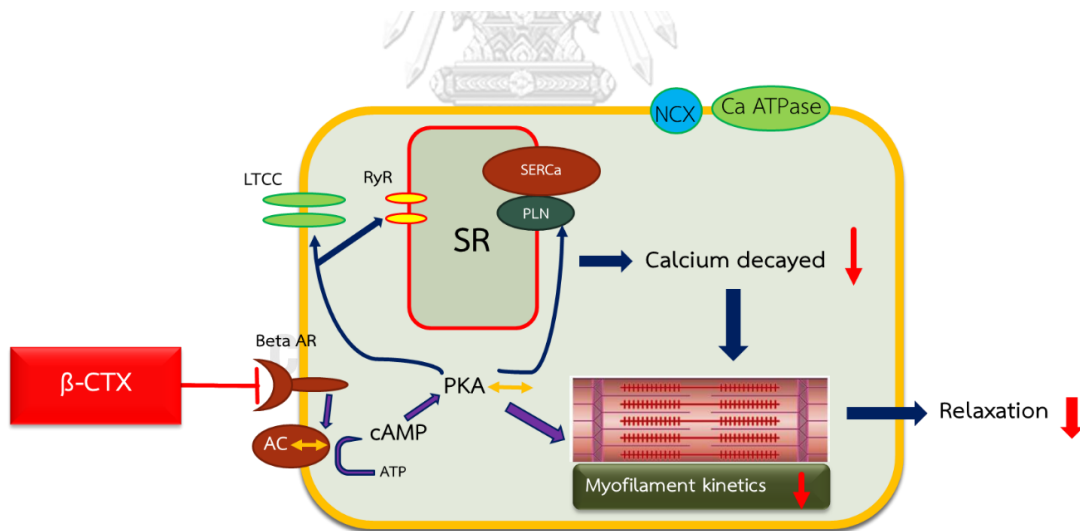


Figure 21. Schematic diagram illustrates possible mechanisms of ventricular relaxation by β -CTX. The prolongation in calcium decayed is speculated to be the underlying mechanism which reduces myofilament kinetics and lusitropic property of the cardiac myocyte. However, it is, yet, still unknown how does the β -CTX reduce the capability to lowering intracellular calcium.



จุฬาลงกรณ์มหาวิทยาลัย
CHULALONGKORN UNIVERSITY

Appendices

Appendix A

Purification & identification of β -CTX from king cobra venom

A1. Reversed-Phase HPLC

1.1. Materials and solutions

1. HPLC system
 - Binary pump (Waters[®] 1525)
 - UV/Vis detector (Waters[®] 2489)
2. Filtered 0.45 μ m GHP membrane (Acrodisc[®], Life Science)
3. Jupiter C18 column
 - Grace[®] Vydac 218TP[™] (5 μ m, 4.6 mm. i.d. x 250 mm)
4. Crude venom
 - Thai king cobra venom; (*Ophiophagus hannah*)
5. Solution A: 0.1% trifluoroacetic acid (TFA)
 - 4 L of MQ water + 4 mL of 100% TFA
6. Solution B: 80% Acetonitrile (ACN) in 0.1% TFA
 - 3.2 L of 100% ACN + 800 mL of 0.1% TFA

1.2. Procedures

1. Column setup
 - a. Install the column. Make sure the flow is going from lower to upper.
 - b. Run the column and check for leakages.
2. Venom preparation
 - a. Reconstitute the crude venom by Solution A to make a concentration of 50 mg/mL (50 mg of lyophilized crude venom in 1 mL). Vortex until the solution becomes fully dissolved.
 - b. Filter the solution with a 0.45 μ m GHP membrane. Put into the new tube.
 - c. Measure the concentration of the crude venom using OD 280 nm. Assume that the extinction coefficient of the crude venom is 1 /M•cm.
 - d. Reconstituted venom could be kept in 4°C and use within 1 week.

3. Method setup

- a. According to Petra's protocol (Petras et al., 2015), we used 160 minutes running at 1 mL/min flow rate and the gradient as following:

Time (minute)	Solution A	Solution B
5	100-95%	0-5%
20	95-60%	5-40%
120	60-30%	40-70%
155	30-100%	70-0%
161	100%	0%

- b. For blank setup, shorten the time used for each step as follow;

Time (minute)	Solution A	Solution B
2	100-95%	0-5%
10	95-60%	5-40%
35	60-30%	40-70%
45	30-100%	70-0%
51	100%	0%

4. Running procedure

- a. At the beginning of the day, clean the column by running the blank procedure until the chromatogram becomes stable.
- b. Once the column and sample are ready, wash the injecting syringe with 100% methanol 1X and MQ H₂O 3X. Take 200 μ L of venom solution and load it into the channel.
- c. Go to the control panel, click on the running button, when the pop-up window is shown, turn the knob at the injection site clockwise, load the venom into the machine and turn the knob back to the same position, then, let the HPLC automatically run.
- d. Start collecting the fractions by concentrating on the OD₂₁₅. When the number is starting to go higher, the peak is coming, manually collect the solution into the tube and change the tube when the peak return to baseline or the next peak is coming.

A2. Cation exchange chromatography

2.1. Materials & Solutions

1. HPLC system
 - Binary pump (Waters® 1525)
 - UV/Vis detector (Waters® 2489)
2. Filtered 0.45 µm GHP membrane (Acrodisc®, Life Science)
3. Cation exchange column
 - Waters® Protein Pak™-SP 5 PW (7.5 mm i.d. x 75 mm)
4. Lyophilized fractions
5. Solution A': 0.05 M Sodium phosphate buffer; pH 7.4
 - Na₂HPO₄ (Base): 8.63 g
 - NaH₂PO₄ (Acid): 6.14 g
6. Solution B': 0.05 M Sodium phosphate buffer with 0.5 M NaCl; pH 7.4
 - Na₂HPO₄ (Base): 8.63 g
 - NaH₂PO₄ (Acid): 6.14 g
 - NaCl: 58.5 g

2.2. Procedures

1. Column setup
 - a. Install the column. Make sure the flow is going from lower to upper.
 - b. Run the column and check for any leakages.
2. Solution preparation
 - a. Reconstitute the lyophilized solution obtained from RP-HPLC to make a concentration around 10-15 mg/mL (calculated from OD at 280 nm; assuming the extinction coefficient is approximately 1/M•cm).
 - b. Reconstituted venom could be kept in 4°C and use within 1 week.
3. Method setup
 - a. We used 90 minutes running at 1 mL/min flow rate and the gradient as follow:

Time (minute)	Solution A'	Solution B'
5	100%	0%
75	100-30%	0-70%
80	30%	70%
85	30-0%	70-100%
90	0-100%	100-0%

4. Running procedure

- a. Start cleaning the column by running the blank procedure.
- b. Once the column and sample are ready, wash the injecting syringe with 100% methanol 1X and H₂O 3X. Draw 200 µL of venom solution and put it into the loading channel.
- c. Go to the control panel, click on the running button. When the pop-up window is shown, turn the knob at the injection site clockwise, load the venom into the machine and turn the knob back to the same position, then, let the HPLC automatically run.
- d. Collect the peak by concentrating on the OD₂₈₀. When the number is starting to go higher, the peak is coming, manually collect the solution into the tube and change the tube when the peak returns to baseline or the next peak are coming.

A3. N-terminal sequencer & identification of protein

3.1. Materials and Solutions

1. N-terminal sequencer (PPSQ™-33B, Shimadzu®) and software (PPSQ-30 analysis)
2. N-terminal solutions [37% Acetonitrile (MeCN), 1-Chlorobutane (BuCl), Ethyl acetate (AcOEt), Trifluoroacetic acid (TFA), 5% Phenyl Isothiocyanate n-heptane solution (PITC), 25% TFA]
3. Amino acid standard
4. PVDF membrane with protein bands

3.2. Procedure

1. Check the gas tank pressure (should be around 0.2 – 0.3 psi) and waste bottle (should have around 100 mL of the fluid left).
2. Refilled all reagents to sufficiently provide for the long sequencing runs.
3. Turn on the UV lamp and oven and change the flow rate to 1 mL/min. Wait for the machine to set up the system. Set the baseline to zero until it is stable.
4. Meanwhile, prepare the standard of amino acids by adding 85.5 µL of 37% acetonitrile (MeCN) and 4.5 µL of the amino acid standard.
5. Run the PTH-AA set up to standardize the machine.
6. Manually calibrate the peaks gathered from the software as specific amino acids.
7. Check the flow rate back to 1 mL/min. Re-stabilize the baseline.

8. Prepare the samples. Cut single protein bands from the transferred membrane (up to three samples per run). Wash membranes with 500 μ L MQ H₂O 3X.
9. Take off all reactors and clean with 100% methanol. Put new samples onto the reactor.
10. Dry the sample.
11. Put on the coverage membrane to the reactor lid to protect from leaking. Snap the lid and put the reactor back in the right position. Closed the reactor tightly and check for the leakage before starting the run.
12. Start the automated N-terminal analysis. It will take 1 hour for 1 residue analyzing.
13. Read the file by checking the outstanding peak in each residue running. Identify the protein on <https://blast.ncbi.nlm.nih.gov/Blast.cgi?PAGE=Proteins>.





Figure S 1. (A) Reconstituted crude king cobra venom with approximately concentration of 50 mg/mL. (B) Loading knob of the HPLC machine. (C) binary HPLC system (Waters® 1525) and the UV/Vis light detector (Waters® 2489). (D) C18 column for RP-HPLC (Grace® Vydac 218TP™). (E) SP 5W column for the cation exchange chromatography (Waters® Protein Pak™).

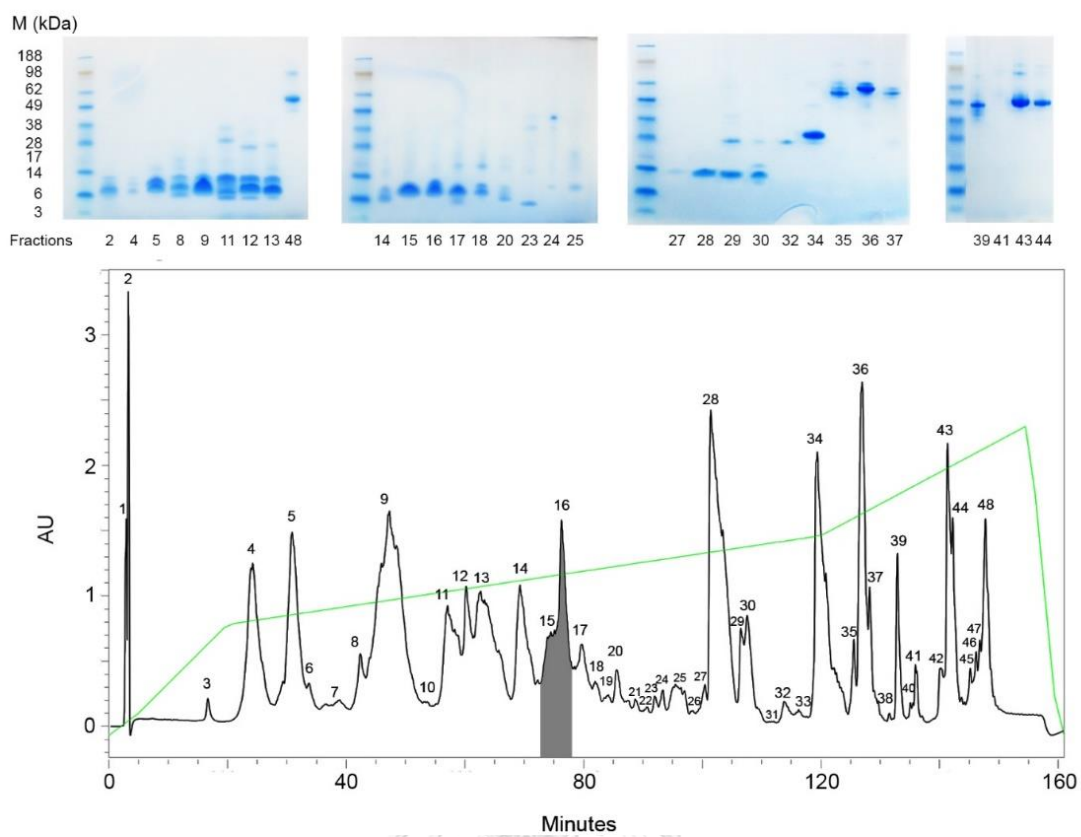


Figure S 2. Extended SDS-PAGE regarding the reverse phase HPLC. Notably, grey shaded represents β -CTX containing fractions. M = Molecular weight marker (SeeBlue[®] Plus stain).

Table S 1. N-terminal sequencing of the first 14 residues of each fraction regarding the SDS-PAGE from figure S1. Proteins were identified using the online protein blasting application.

RP-HPLC peak	Apparent mass (kDa)	Amino acid sequence (14 residues)	Identification	Accession No.
F2	7.89	LIPFNQETYYPPTT	Polypeptide DE-1	771760A
F4	7.73	LIPFNQETYYPPTT	WNTX-33	Q2VBN3.1
F5	7.75	LIPFNQETYYPPTT	WNTX-33	Q2VBN3.1
F8	7.75	GKVYNHESTTPRPT	Haditoxin	A8N286.1
	7.85	GIPFNQETYYPPTT	WNTX-33	Q2VBN3.1
	10.56	GIPYKTELIIKTT	PLA ₂	P80966.2
F11	10.59	GKPYKTGERISET	LNTX Oh55	P01387.1
F12	6.82	VFVVKVNVTFGETP	Thioredoxin	Q98TX1.3
	11.01	GKRYKTGERISET	LNTX Oh55	P01387.1
F13	10.95	GKPTKTGEEFMSTT	LNTX Oh55	P01387.1
F15	7.78	GKPLNTPLPLIYTT	β -CTX	AAR10440.1
F16	8.02	GKPLNTPLPLIYTT	β -CTX	AAR10440.1
F17	8.76	GIPLKQEPFOIIT	WTX DE-1	P01412.2
F34	26.52	GVDFNSEMTRRDKK	CRiSP (Opharin)	Q7ZT98.1
cIEx Peak	Apparent mass (kDa)	Amino acid sequence (14 residues)	Identification	Accession No.
F3	7.56	RKLLNTPLPLIYTT	β -CTX	AAR10440.1
F4	7.58	GKLLNTPLPLIYTT	β -CTX	AAR10440.1

Appendix B

In vitro cellular viability assay

B1. Cellular viability of different mammalian cell lines treated with β -CTX

1.1. Cell lines and Chemicals

1. Mouse myoblast cell line; C2C12 (ATCC[®], CRL[™]-1772)
2. Rat smooth muscle cell line; A7r5 (Sigma[®], Cat No. 86050803)
3. Rat cardiac myoblast cell line; H9c2 (ATCC[®], CRL[™]-1446)
4. Cultured medium
 - Dulbeccos' minimum essential medium; DMEM (ATCC[®], 30-2002)
 - Fetal bovine serum; FBS (Thermo Fisher, 10100139)
 - Penicillin-Streptomycin solution (ATCC[®], 30-2300)
5. 0.025% Trypsin-EDTA
 - 2.5 mL of 1X Trypsin-EDTA (ATCC[®], 30-2300)
 - 97.5 mL of cultured medium
6. Methylthiazolyldiphenyl-tetrazolium bromide; MTT (Sigma[®], M5655)
7. Dimethyl sulfoxide; DMSO (ATCC[®], 4-X-1197)
8. Phosphate buffer saline (Sigma[®], 806552)

1.2. Procedures

1. Culture cell lines in the cultured medium. Change the media every 2-3 days.
2. Harvest the cell from the flask using 0.025% trypsin EDTA for 1 mL. Incubate for 10 min.
3. Add 10 mL of the fresh media and gently flush to detach cells from the flask. Use the same serological pipette to transfer the cells into 15 mL centrifuge tube
4. Centrifuge for 1,000 rpm 10 minutes
5. Meanwhile, take 25 μ L of cell solution and load into the automated cell counter (Cellometer[™] T4, Nexcelom Bioscience). The value gathered (in the number of cells/mL) should be multiplied by 11 to get total cell counts.

6. Calculate the number of cells loaded into each well
 - C2C12: 1.5×10^5 cells/well
 - A7r5: 5×10^4 cells/well
 - H9c2: 1.5×10^4 cells/well
7. After finishing centrifuge, discard the supernatant and adding the fresh media using the volume calculated from 6.
8. Load the cell solution into each well for 100 μ L. Incubate at 37°C, 5% CO₂ overnight.
9. Add 20 μ L of various concentration of β -CTX in PBS as following:

	1	2	3	4	5	6	7	8	9	10	11	12
	Beta-CTX 2 (mg/mL)			Beta-CTX 2 (mg/mL)			Beta-CTX 2 (mg/mL)			Control		
A	0.80000			0.80000			0.80000			No cell + PBS 20 μ L		
B	0.40000			0.40000			0.40000			Cells + PBS 20 μ L		
C	0.20000			0.20000			0.20000					
D	0.10000			0.10000			0.10000			No cell + PBS 20 μ L		
E	0.05000			0.05000			0.05000			Cells + PBS 20 μ L		
F	0.02500			0.02500			0.02500					
G	0.01250			0.01250			0.01250			No cell + PBS 20 μ L		
H	0.00625			0.00625			0.00625			Cells + PBS 20 μ L		

10. Incubated at 37°C for 24 hours. Capture the cellular morphology at 0 and 24 hours.
11. Add 12 μ L of MTT (5 mg/mL) into each well, incubated at 37°C for 4 hours.
12. Take off supernatants.
13. Add 100 μ L of DMSO to lyse the cell and incubate at 37°C for 20 minutes. Formazan color is detected at 570 nm using a microplate reader (Beckman Coulter™ AD340).

B2. Cellular viability of different mammalian cell lines treated with crude king cobra venom

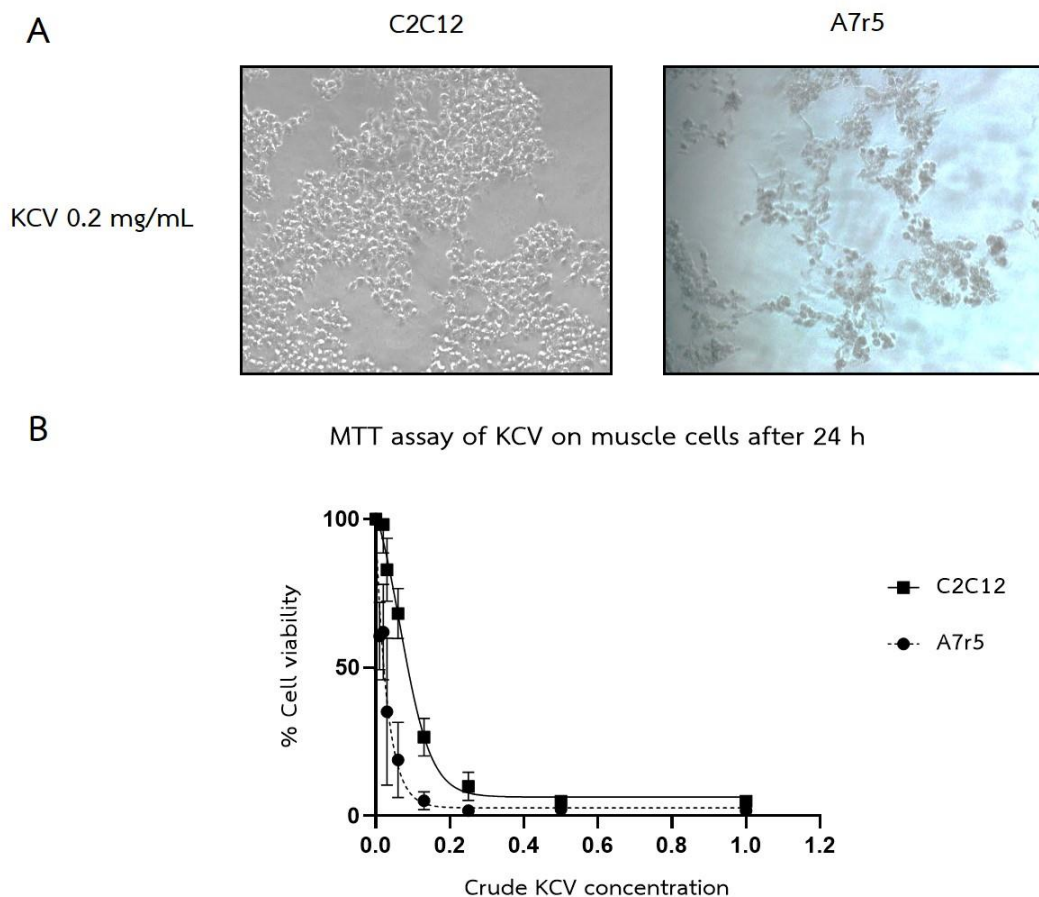


Figure S 3. (A) Representative microscopic of C2C12 and A7r5 treated with 0.2 mg/mL of crude king cobra venom (KCV). Cytotoxicity is indicated by the morphological changes of the cells and the density in both cell lines. (B). MTT assay demonstrates the live cells upon the KCV concentration. Reduced cell viability was observed in both cell lines represented by the CC_{50} of 0.07 ± 0.02 mg/mL and 0.02 ± 0.01 mg/mL, respectively.

Appendix C

Impact of β -CTX on isolated ventricular myocyte functions

C1. Isolation of adult rat cardiomyocyte

1.1. Chemicals and Solutions

1. Control solution (10X)

Ingredient	mM	MW	g/500 mL	g/250 mL
NaCl	1335	58.44	39.009	19.5045
KCl	40	74.55	1.491	0.7455
NaH ₂ PO ₄	12	120.00	0.720	0.3600
HEPES	100	238.30	11.915	5.9575
MgSO ₄	12	120.40	0.722	0.3610

2. Calcium stock solution (100 mM)

- 1 mL of 1 M CaCl₂ solution (Lot No. 21115, Sigma[®]) in 9 mL of MQ H₂O

3. Drugs

- Heparin (10,000 U/mL)
- Pentobarbital (Fatal Plus[®], 50-65 mg/mL)
- Collagenase type II (Worthington[®], Lot No. 4177)
- Protease XIV (Sigma[®], Lot No. P5147)
- Bovine serum albumin; BSA (Sigma[®], Lot No. A3600)

1.2. Procedure

1. Making 1X of control solution

- 100 mL of 10X control solution into 1 L beaker + MQ water for 800 mL
- Adding 2 g of Dextrose.
- Adjust pH to 7.4; then, bring the volume up to 1 L
- Separated into 2 beakers of 500 mL, one will be used for isolation, another will be used for cell measurement.

2. Making control-BSA solution

- Adding 500 mg of BSA into one 500 mL beaker
- Stir and filter

3. Making an enzyme solution
 - a. Take 100 mL of control-BSA into the new beaker.
 - b. Weigh 0.025 mg of Collagenase II and 0.003 mg of protease XIV into the boat, use the transfer pipette to draw control-BSA solution and rinse enzymes on the weigh boats until completely dissolved.
 - c. Add 20 μL of 100 mM Ca^{2+} stock into the solution, stir and filter.
4. Making Ca^{2+} -solutions
 - a. 50 μM : 25 mL control-BSA solution + 12.5 μL of 100 mM Ca^{2+} stock
 - b. 100 μM : 25 mL control-BSA solution + 25 μL of 100 mM Ca^{2+} stock
 - c. 200 μM : 25 mL control-BSA solution + 50 μL of 100 mM Ca^{2+} stock
 - d. 500 μM : 25 mL control-BSA solution + 125 μL of 100 mM Ca^{2+} stock
 - e. 1 mM μM : 25 mL control-BSA solution + 250 μL of 100 mM Ca^{2+} stock
5. Preparing perfusion system
 - a. Using new connectors, 50 mL syringes and wash the cannula every time.
 - b. Wash the system with MQ water twice. Put the bubblers, connected to 100% oxygen gas, into both 50 mL syringes.
 - c. Turn on the oxygen gas and adjust the rate and size of the bubble in the syringe.
 - d. Let the water run through the system at the rate 3 drops per second; meanwhile, measure the temperature (should be at 36.3-36.6 $^{\circ}\text{C}$) at the very tip of the cannula.
 - e. Pour control-BSA solution and enzyme solution into syringes.
 - f. Let the enzyme solution run through, get rid of all bubbles.
 - g. Let the control solution run through; likewise, eradicate the bubbles of the system.
 - h. Sutures, small scissors and small forceps are prepared nearby the perfusion system.
6. Preparing surgical area
 - a. Fill the bucket with ice
 - b. Put in 2 petri dishes and 2 disposable beakers, fill up with a control-BSA solution
 - c. One of the disposable beakers should be labeled and use for weighing the heart. Tear the weight with that beaker.
 - d. Scissors and forceps (and artery forceps if needed) are prepared.
7. Preparing animals
 - a. Weight the rats (the proper size should be around 180-250 g).
 - b. Heparinize and anesthetize the rat with heparin 5,000 U/kg and Pentobarbital sodium for 65 mg/kg, inject intraperitoneally. Wait 15 minutes before start.

8. Surgery and cannulation

- a. Incise the abdomen and access the thorax through the diaphragm. Cut the diaphragm and the intercostal muscles to widely open the chest.
- b. Clear all connective tissue to clearly see the aorta, hold it by your left hand and use the scissors to cut the above part of your hand.
- c. Put the heart and aorta into the first dish, trim all unwanted tissue.
- d. Move to the first small beaker, squeeze the blood out of the heart as much as possible.
- e. Move to another beaker that calibrated with the weight. Weigh the heart and set the timer as follows:

Heart weight (g)	Enzyme perfusion time (min)
0.6	10
0.7	12
0.8	13
0.9	15
1.0	16
1.1	18
1.2	20
1.3	21
1.4	23

- f. Cannulate the aorta with suture, then, run the control-BSA for 3 minutes.
- g. Switch to enzyme solution, perfuse using the time which has been set.
- h. After the heart is completely digested, cut the ventricles and put it into the 50 μL Ca^{2+} solution. Mince the ventricle into small pieces.
- i. Put the solution into the prepared 50 mL tube at 37°C for 10 minutes. Meanwhile, gently mixed the pieces of tissue with transfer pipettes for every 1-2 minutes.
- j. Filter the cells through the strainer. Transfer to the U-bottom tube and gravitate the cells for 7 minutes in 37°C.
- k. After that, remove the supernatant as much as possible. Add 100 μM Ca solution to the tube, triturate and let it gravitate for 7 minutes in 37°C. Redo this step in 200, 500 and 1,000 μM Ca^{2+} solutions.

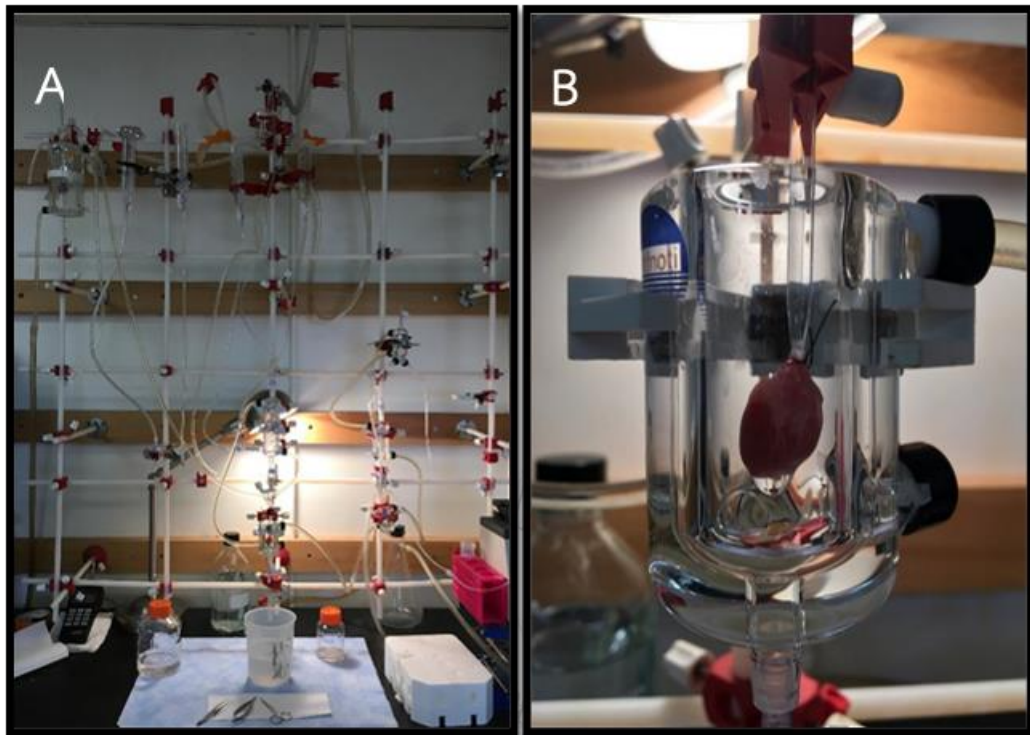


Figure S 4. (A) Setting up of Langendorff apparatus with the heart being perfused.
(B). Magnification of the perfused cannulated heart.

C2. Spontaneous measurement of cardiac contraction and calcium profiles

2.1. Equipment setting up

1. PTI imaging & fluorescence system (Photon Technology International; PTI[®] RatioMaster)
2. Light source:
 - DeltaRam X[™] High-speed random-access monochromator (Galvanometer-based) -> Fluorescence Illuminator with a Xenon lamp
 - Lamp power supply (including light source): LPS-220B -> 75-200 W
 - BryteBOX: Data acquisition system to PC (with FeliX32 software)
3. Inverted fluorescence microscope
 - Nikon Eclipse (TE-300) -> 40X0.60 with oil, rotate to "C" aperture for measuring (A is 100% on binocular and C is 100% on camera) and Fura-2 filter set at block "3"
 - Microscope light source (included with the microscope): TE-DH100W
 - Lamp power supply: TE-PS100
4. Photomultiplier tube: Model 814 PMT housing
 - PMT: R1527 (Model 814[™])
 - Photometer: D104C (Dual channel photometer)
5. CCD camera
 - Camera: Hamamatsu[®] XC-77
 - CCD control: Hamamatsu[®] Photonic C2400
 - Oscilloscope: HAMEG[®] HM205-3
 - Video edge detector: Crescent electronics[®] VED-105
 - Data acquisition system: Digidata[®] 1440a
6. Stimulator: Grass Medical Instruments[®] SD-5
 - Frequency: 0.5 Hz
 - Delay: 0 ms
 - Duration: 5 ms
 - Volts: 40-80 V
 - Stimulus: Regular
7. Infusion pump Bio-Rad[®] EP-1: Set flow rate at 0.5 mL/min
8. Software setup (FeliX32[™] 1.42B): Fura-2 and contraction (excitation at 340 and 380 nm, emission at 505 nm), for 20 secs.

2.2. Procedure

1. After cells isolation, used the cells as soon as possible
2. Turn on all equipment in the sequence as follow:
 - a. Light source: Lamp power supply -> DeltaRam X -> BryteBox
 - b. Microscope: Nikon eclipse (TE-300)
 - c. Acquisition system
 - d. Computer
 - e. Turn on Vacuum
3. Use the cotton swab with 70% ethyl alcohol to firstly clean the chamber and the underneath coverslip. Use transfer pipets with MQ water to wash after that.
4. Measure the background of the system (fluorescence) by loading 950 μL of control 1X solution w/ calcium 1.0 mM + 50 μL of cells solution (without any Fura-2 AM) into the tube. Load into the chamber.
5. Put the stimulator into the chamber. Adjust the position of the stimulator to the bottom of the chamber. Turn on the stimulator.
6. Searching for the “isolated cells” which contracting, adjust the position of the cells by rotating the CCD camera to make the cells align with the edge detection line. Move the stage of the microscope to set the cell aligned with the detection line. Adjust the edge detection line to both ends of the cells. Raster line is for the vertical and the position is for the horizontal adjustment. You can also adjust the length of the edge detection line and threshold to show up the edge detector (white dot). Rotate the diaphragm aperture on the PMT tube to limit the field of fluorescence detection. Use the black cloth to cover the monitor to obscure the noise. Monitor the contraction from the oscilloscope.
7. After everything is set, turn off the room light, TV and computer screen to generate a very dark room. Then, turn on the PMT tube switch. Start measuring the background.
8. Measure the “BACKGROUND” for at least 2 cells.
9. Wash out the chamber by manually moving the sucker tube down to the bottom of the chamber. Clean the chamber with 70% ethanol and wash with MQ water.
10. Fura-2 AM (F1221, Invitrogen[®]) is made by reconstituted in 50 μL DMSO to make 1 μM .
11. For cells measurement, 950 μL of control 1X solution w/ calcium 1.0 mM + 50 μL of cells solution + 3 μL of Fura-2 AM is needed to be incubated and de-esterified. Load the mixture of solution into chambers and let it incubate for 10 minutes and de-esterification for 20 minutes by perfusing with a control solution containing calcium 1.8 mM.

12. Put the stimulator into a chamber and load the prepared cells after. Find an isolated cell and adjust the edge detecting system as previously described.
13. Measure the baseline, the cells contraction and calcium profile in the normal control solution.
14. Start perfusing with the first concentration of the drug, 8-10 minutes for each concentration (flow rate is 0.5 mL/min) is enough to make a stable effect. Stop perfusing before recording. Redone this with other concentrations of the drugs.
15. After finishing the last concentration, flushing out the perfusing tube with either MQ water or control solution by pressing on the “purge” on the infusion pump. This should be done for at least 5 minutes, to make sure that there is no longer drug stuck in those tubing.



2.3. Calculation

1. The data will be recorded as 5 rows
 - a. A1 340:100 and A1 380:100 -> these are the mechanical contraction information.
 - b. D1: 340:505 -> This is the Fura-calcium profile
 - c. D1: 380:505 -> This is the Fura-free profile
 - d. Ratio – 340/380 -> This is the calcium profile
 - e. Unused data
2. After measuring, make an average of the D1 340:505 and D1 380:505 of the backgrounds. Go to math -> combine constant, then, the D1 340:505 and D1 380:505 of each measurement will be subtracted by the mean average than we have calculated.
3. After that, go to math -> combine, and make a ratio between the normalized D1 340:505 and D1 380:505 (this will be the exact $F_{340/380}$).
4. Export each measurement as a .txt file. Transfer those data to Microsoft excel and make 4 columns, contraction, time, calculated contraction, and calcium ($F_{340/380}$) profile as follow. In this study, the equation of calculated contraction from the preliminary was equaled $34.32 \times (\text{measured contraction} + 3.65)$.
5. Copy the time, calculated contraction and $F_{340/380}$ columns back to .txt. This new file will be used for calculating in LabChart™ 7 program. Do this to all files.
6. Open LabChart program, insert the .txt file that we have made. The first two rows will automatically show the contraction and calcium profile simultaneously. At the Chart view, we can right-click on the right-handed side feature and click on “smoothing” to remove noises.
7. At “Peak analysis” settings, go to calculation and set as follows:

Peak Analysis Settings [X]

Setup
 Analysis type: **General - Unstimulated** Source: **Channel 1 (Smoothing)** Selection Channel

Detector Calculations Table Options

TStart
 Start is % of the height away from the baseline

Area
 Use region from ms to ms after peak start

TRise, TFall, SlopeRise, SlopeFall
 Rise and fall between % and % of the peak height

Slope
 Average slope from ms to ms after the start of the peak

Tau
 In "A exp(-t/Tau) + B", use fitted B B set to baseline B set to kV
 Use data from % to % of peak height

[?] [OK] [Cancel]

8. At "Peak analysis" settings, go to detector -> customize and change the triggers to "minimum".
9. Go to table view and copy the auto-calculation data from the program onto Microsoft excel.

LabChart

File Edit Setup Commands Macro Blood Pressure Cardiac Output Dose Response ECG Analysis HRV Peak Analysis PV Loop Video Capture Window Help

File Commands Data Pad Comments Window Layout Blood Pressure Dose Response ECG Analysis HRV Sampling

Peak Analysis PV Loop Video Capture

Cell 4 ISO 300 nM: Chart View

Channel: 1 Comment

Cell 4 ISO 300 nM: Peak Analysis Table View

	Baseline (kV)	TStart (s)	TEnd (s)	Width (ms)	Height (kV)	TimeToPeak (ms)	APeak (kV)	PeakArea (kV.s)	MaxSlope (kV/s)	MinSlope (kV/s)	TMaxSlope (ms)	TMinSlope (ms)	AV
1	120.6	0.7788	3.683	943.8	-11.63	198.0	109.0	-3.830	56.67	-138.1	349.8	39.60	113
2	120.5	2.739	3.683	943.8	-11.35	198.0	109.1	-4.029	59.84	-134.9	349.8	33.00	113
3	120.6	4.693	5.960	1267	-11.49	171.6	109.1	-4.150	63.17	-135.4	343.2	33.00	113
4	120.7	6.653	8.158	1505	-11.55	211.2	109.1	-4.123	59.21	-137.5	363.0	26.40	114
5	120.6	8.613	10.03	1412	-11.56	191.4	109.1	-3.890	59.36	-138.7	356.4	26.40	114
6	120.5	10.57	11.53	963.6	-11.37	198.0	109.1	-3.946	60.16	-138.6	349.8	26.40	113
7	120.6	12.52	13.62	1096	-11.33	158.4	109.2	-3.892	68.57	-132.5	376.2	33.00	113
8	120.5	14.47	15.58	1109	-11.32	217.8	109.2	-4.050	64.44	-144.3	349.8	33.00	113
9	120.7	16.43	17.83	1406	-11.40	191.4	109.3	60.00	-143.8	376.2	33.00	115	
10	120.8	18.39			-11.58	231.0	109.2						
	Baseline (kV)	TStart (s)	TEnd (s)	Width (ms)	Height (kV)	TimeToPeak (ms)	APeak (kV)	PeakArea (kV.s)	MaxSlope (kV/s)	MinSlope (kV/s)	TMaxSlope (ms)	TMinSlope (ms)	AV
Avg	120.6	9.585	10.80	1213	-11.46	196.7	109.1	-3.989	60.87	-138.3	351.8	31.02	113
Min	120.5	0.7788	3.683	943.8	-11.63	158.4	109.0	-4.150	56.67	-144.3	336.6	26.40	113
Max	120.8	18.39	17.83	1505	-11.32	231.0	109.3	-3.830	58.57	-132.5	376.2	33.00	115
Count	10	10	8	8	10	10	10	8	10	10	10	10	10

Export... Settings... Add to Data Pad

Cell 4 ISO 300 nM 74.57 GB

10. Move to channel 2, this will be your calcium profiles, setup the same thing, but do not change to “minimum” as we are measuring the peak calcium transient.
11. Complete every single file and transfer it to Microsoft excel. Selected parameters are used as the following:

a. Inotropic Parameters

- i. Peak cell shortening: $=\text{Baseline(kV)} - \text{APeak(kV)} / \text{Baseline(kV)} * 100$
- ii. Time-to-peak shortening: $=\text{TimeToPeak(ms)}$
- iii. Shortening velocity (+dL/dt): $=\text{SlopeRise(kV/s)}$

b. Lusitropic Parameters

- i. Time-to-90% relengthening (TR_{90}): $=\text{TFall(ms)}$
- ii. Relaxation constant: $=\text{Tau(s)}$
- iii. Re-lengthening velocity (-dL/dt): $=\text{SlopeFall(kV/s)}$

c. Calcium homeostasis (Use the calcium profiles)

- i. Peak calcium transient: $=\text{Apeak(kV)} - \text{Baseline(kV)} * 100$
- ii. Time-to-peak Calcium transient: $=\text{TimeToPeak(ms)}$
- iii. Calcium decaying constant: $=\text{Tau(ms)}$

C3. Hysteresis loop comparing between the propranolol and β -CTX

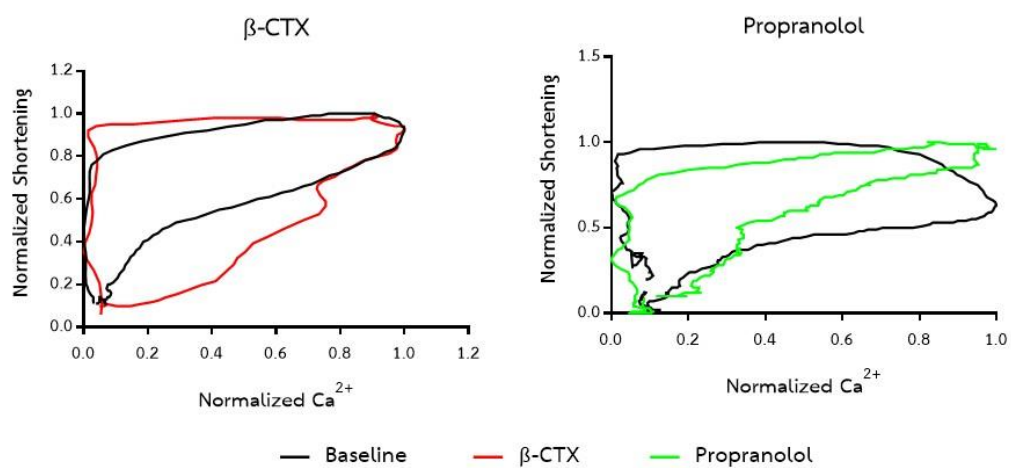


Figure S 5. Comparison of the hysteresis loop between β -CTX (A) and propranolol (B). Of note, the novel protein seems to enhance the area of the loop indicating the reduction in Ca^{2+} sensitivity; whereas, propranolol acts oppositely.

C4. Comparison effects between pre-treated β -CTX or propranolol on cardiomyocyte functions with the presence of isoproterenol (ISO).

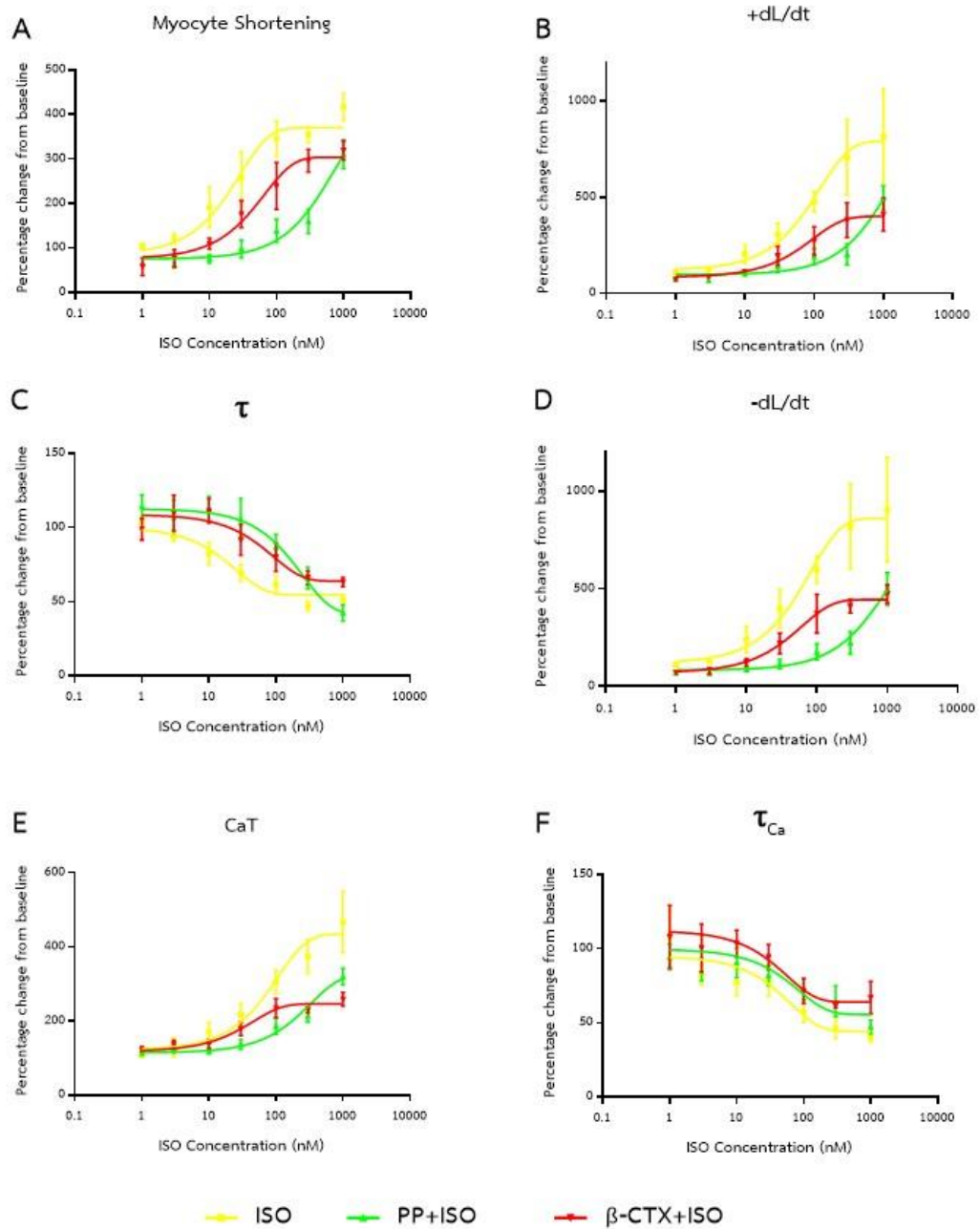


Figure S 6. Comparison of the cardiomyocyte functions between cells treated with isoproterenol (ISO), propranolol and ISO (PP+ISO) and β -CTX+ISO. Dose-response curve representing percentage changes from baseline of (A) cell length shortening, (B) +dL/dt, (C) τ , (D) -dL/dt, (E) CaT and (F) τ_{Ca} . Data are represented as mean \pm S.E.M.

Table S 2. Comparison effects of EC₅₀ (IC₅₀) and the estimated maximal (minimal) value of isolated cardiomyocyte parameters among groups. Data are shown in mean ± S.E.M. and comparing between groups using one-way ANOVA following by Tukey's method.

	ISO	PP+ISO	β-CTX ISO
Myocyte shortening			
EC ₅₀ (nM)	19.93 ± 3.88	451.40 ± 108.77 [†]	45.90 ± 8.82 [†]
Max (%)	370.10 ± 28.06	371.20 ± 87.47	304 ± 26.51 [§]
+dL/dt			
EC ₅₀ (nM)	84.28 ± 15.58	884.9 ± 275.89 [†]	67.05 ± 14.18 [†]
Max (%)	792.5 ± 36.84	824.9 ± 254.41	400.3 ± 21.35 [§]
τ			
IC ₅₀ (nM)	17.80 ± 3.11	173.50 ± 37.62 [†]	63.56 ± 15.11 [§]
Min (%)	54.63 ± 1.65	41.81 ± 5.68	63.90 ± 3.78 ^{†,§}
-dL/dt			
EC ₅₀ (nM)	57.01 ± 10.94	638.30 ± 173.20 [†]	42.38 ± 8.52 [§]
Max (%)	862.60 ± 40.50	705.40 ± 127.64	445.40 ± 20.68 [†]
CaT			
EC ₅₀ (nM)	74.59 ± 12.76	230.80 ± 39.78 [†]	32.05 ± 6.08 [§]
Max (%)	434.10 ± 14.73	324.90 ± 11.70 [†]	246 ± 5.96 ^{†,§}
τ_{Ca}			
IC ₅₀ (nM)	44.81 ± 9.99	58.92 ± 14.79	39.1 ± 9.26
Min (%)	44.21 ± 7.72	55.61 ± 9.21	64.03 ± 7.99
	† p-value < 0.05 vs ISO, § p-value < 0.05 vs PP+ISO		

C5. Comparison effects between pre-treated β -CTX or propranolol on cardiomyocyte functions with the presence of forskolin (FSK)

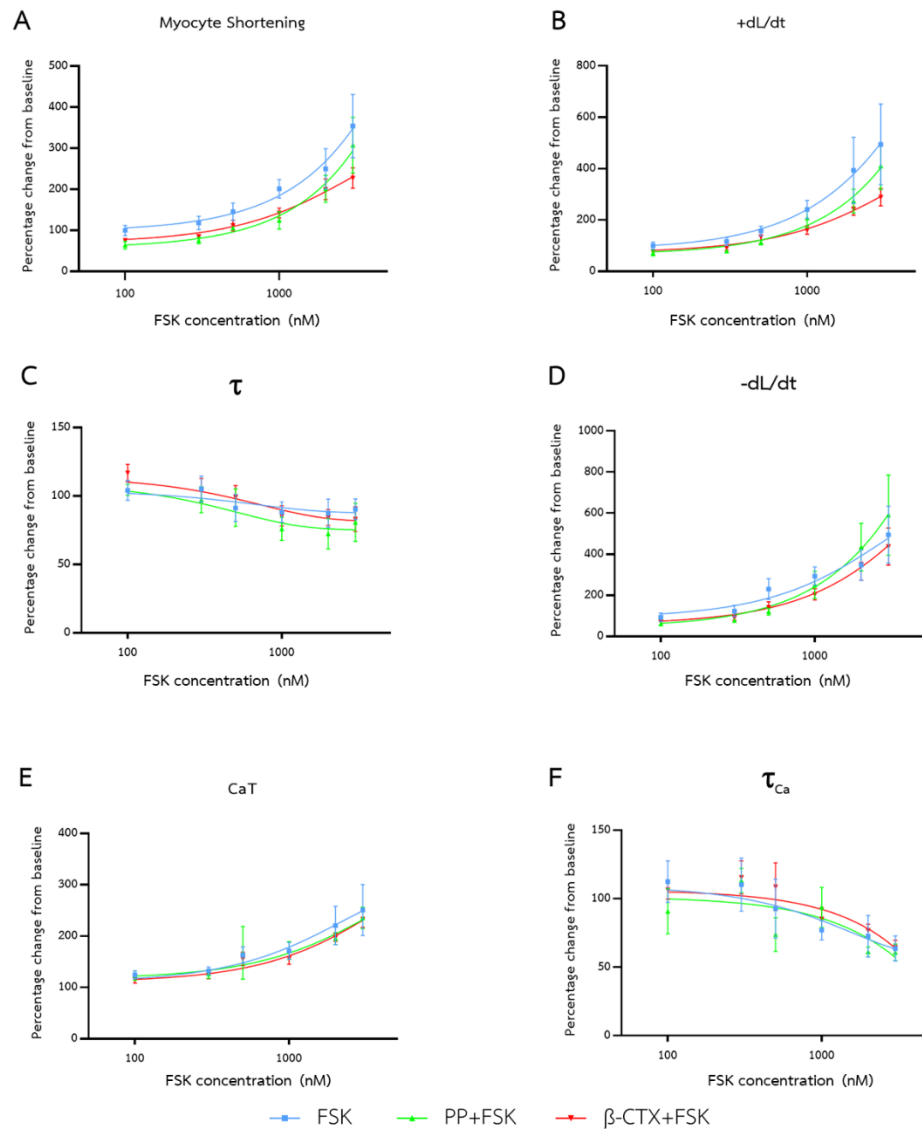


Figure S 7. Comparison of the cardiomyocyte functions represented by dose-response curve between cells treated with forskolin (FSK), propranolol and ISO (PP+FSK) and β -CTX+FSK. Dose-response curve representing percentage changes from baseline of (A) cell length shortening, (B) +dL/dt, (C) τ , (D) -dL/dt, (E) CaT and (F) τ_{Ca} . Data are represented as mean \pm S.E.M.

Appendix D

ProQ[®] phosphor-staining and western blot

D1. Myofibril preparation from isolated cardiomyocytes

1.1. Materials and solutions

1. Control solution (with 1 mM CaCl₂)
2. SRB (0.5 L)

Ingredients	Concentration (mM)	Amount to add (g)
KCl	75	2.796
Imidazole	10	0.340
MgCl ₂	2	0.203
EGTA	2	0.380
NaN ₃	1	0.033

3. SRB-TX100
 - SRB 49.5 mL + 0.5 mL Triton X-100 Stock
 - Protease inhibitors & phosphatase inhibitors cocktail (Halt[™], Thermo Scientific[™], Cat No. 78440) for 1:100 dilution.
 - Calyculin A (Sigma[®], C2552) for 500 nM (1:2000 dilution).
4. Duall homogenizing pestle
5. Industrial sample buffer; ISB (100 mL)

Ingredients	Concentration	Amount to add
Urea	8 M	48 g
Thiourea	2 M	15.2 g
Mixed bed resin (BioRad [®] AG 501-X8)	-	10 g
Tris Base	0.05 M	0.605 g
DTT	75 mM	1.155 g
SDS	0.3%	3 g
Bromophenol blue	0.005%	5 mg

6. Protein assay kit (Pierce[™] 660nm, Cat No. 22660)
7. Ionic detergent compatibility reagent; IDCR (Pierce[™], Cat No. 22662)

1.2. Procedure

1. Perform ventricular myocyte isolation
2. At the last calcium reintroducing concentration (1 mM), mix all the cells into 1 tube, let it settle down for 10-15 minutes. Transferred the cells into pre-weighed microfuge tubes.
3. Incubate the cells 16 minutes with different treatments as described in the main text.
4. Spin at 200 xg 4°C for 3 minutes.
5. Remove supernatant and add 0.5 mL of SRB-TX100 to each tube.
6. Homogenize with Duall plastic pestle in 1.5 mL tube, vortex and incubate for 5 minutes.
7. Spin the solution at max speed (~16,000 xg) 4°C for 1 minute. Repeat steps 5 & 6 twice; for the third time, homogenizing is not needed, just do the only vortex.
8. Spin the solution at max speed for another 1 minute, remove the supernatant as much as possible. Weigh the tube to obtain the weight of the myofibers.
9. Add ISB buffer at a 1:15 ratio (1 mg of protein and 15 μ L of ISB). Mix it up by trituration with pipet and vortex.
10. Freeze the solution in -80°C until used.
11. On the day of gel loading, thaw the solution at room temperature and heat at 100°C for 3 minutes.
12. Determine the protein concentration using the protein assay kit (Pierce™ 660nm).
 - a. 150 μ L of agent / 10 μ L of sample
 - b. Since samples have SDS; IDCR is added to the solution (1 g / 20 mL).
 - c. Make ISB 1:1 buffer (with H₂O) -> to dilute with samples and standard
 - d. Make a two-fold dilution of standard (Bovine serum albumin stock, 3 mg/mL) dilute the first with 100% ISB; use 1:1 ISB for others. Make six solutions; the last one would be ISB only.
 - e. Make a 10-fold dilution of the sample by adding 9 μ L of ISB 1:1 buffer and 1 μ L of the sample in each well. For standard, add 10 μ L of each into well.
13. Add 150 μ L of Pierce reagent (mixed with IDCR) to each well, shake for 1 minute, incubate for 5 minutes and read at 655 nm.

D2. SDS-PAGE protocols

2.1. Materials and solutions

1. 30% Acrylamide 0.5% bis-acrylamide (500 mL)
 - 373.1 mL of 40% Acrylamide solution (BioRad[®], Cat No. 1610140)
 - 0.75 g Bis-acrylamide solution (Sigma[®], Cat No. 146072)
 - Add water up to 500 mL
2. 1.5 M Tris-base pH 8.8 (200 mL)
 - 36.342 g of Tris base in water
 - Titrate with HCl to make pH 8.8 -> bring up to 200 mL
3. 50% glycerol (200 mL)
 - Equal amount of water & 100% glycerol
4. 10% SDS
 - 10 g of SDS in 100 mL of ddH₂O
5. 10% Acrylamide 15% DATD (100 mL)
 - 21.25 mL of 40% Acrylamide solution (BioRad[®], Cat No. 1610140)
 - 1.5 g of DATD crosslinker (Sigma[®], Cat No. 156868)
6. 0.5 M Tris-base pH 6.8 (200 mL)
 - 6.057 g of Tris base in water
 - Titrate with HCl -> bring up to 100 mL
7. Stacking dye (50 mL)
 - 0.125 M Tris-HCl, 0.1% bromophenol blue, pH 6.8
 - 0.985 g of Tris-HCl + 50 mg of bromophenol blue
 - Titrate with HCl -> bring up to 50 mL
8. Running buffer (1 L)
 - 3.03 g of Tris-base (0.025 M)
 - 14.41 g of glycine (0.192 M)
 - Add water bring up to 1 L
9. 10% Ammonium persulfate (APS)
 - 100 mg of APS in 1 mL
10. Tetramethyl ethylenediamine (TEMED); (Sigma[®], T9281)
11. Criterion[™] precast gels (BioRad[®])

Procedures

1. Prepare the resolving gel using the following table (add volumes in mL)

Resolving gels	15%	12%	10%	8%
30% Acrylamide 0.5% C	6.250	5.000	4.166	3.333
1.5 M Tris-base pH 8.8	3.125	3.125	3.125	3.125
50% glycerol	2.500	2.500	2.500	2.500
Water	0.412	1.662	2.495	3.329
10% SDS	0.125	0.125	0.125	0.125
10% APS	0.080	0.080	0.080	0.080
TEMED	0.008	0.008	0.008	0.008

2. After adding APS and TEMED the gel is starting to polymerize -> load the gel into Criterion™ gel preparation cassette as soon as possible using a serological pipette. Fill up nearly to the well box in the uppermost part of the cassette. Leave a gap and fill up with water to level the gel and clear the bubbles. Wait for 45 minutes.
3. Preparing 500 mL of 1X Tris-glycine-0.1% SDS running buffer: Add 50 mL of 10X running buffer + 5 mL of 10% SDS -> bring up to 500 mL.
4. After 45 minutes, pour out the water. Prepare the stacking gel using the following table

Stacking gels	2.95% T 15% C
10% Acrylamide 1.5% DATD	1.475
0.5 M Tris-base pH 6.8	1.250
Water	1.140
50% glycerol	1.000
10% SDS	0.050
10% APS	0.030
Stacking dye	0.030
TEMED	0.025

5. Likewise, after adding APS and TEMED, the gel is formed; load the solution into the upper part of the cassette up to the top; then, put the comb (26 wells) onto it. Let the polymerization works for 45 minutes.
6. After stacking is ready, removed the comb gently and slowly, load the sample to the gel.
7. Run for constant 200 V at 1 hr 15 minutes.

D3. Staining protocol for phosphor-protein and total protein

3.1. Solutions

1. Electrophoresed gels
2. ProQ[®] Diamond phosphoprotein gel stain kit (Molecular probes[®]; Invitrogen[™])
 - Phosphoprotein gel staining solution (Invitrogen[™], 33330)
 - Phosphoprotein gel de-staining solution (Invitrogen[™], 33310)
3. Gel fixation: 50% methanol and 10% acetic acid
 - 100% methanol 500 mL
 - MQ H₂O 400 mL
 - Glacial acetic acid 100 mL
4. Biosafe[™] Coomassie G-250 stain
5. Imaging system (ChemiDoc[™] MP, BioRad[®])

3.2. Procedure

1. After finish SDS-PAGE, wash the gel with ultrapure water, fix the gel with a gel fixation solution 100 mL for 3 hours.
2. Discard the solution and refill the gel fixation 100 mL overnight.
3. The day after, discard the fixation solution and wash the gel using ultrapure water 3 times; 10 minutes interval.
4. After the last wash, put 80 mL of ProQ[®] staining solution into the box. Let it stains for 60-90 minutes. Protect the gel from the light.
5. After finished, discard the staining solution and pour 100 mL destaining solution. Destains for 30 minutes. Protect the gel from the light.
6. Redo step 5 twice (total 3 times).
7. Wash with ultrapure water twice, 5 minutes interval.
8. Image the gel: protein assay tab -> ProQ diamond staining and black tray.
9. After finishing ProQ staining, wash gel with MQ water 3X for 200 mL, 5 minutes interval.
10. Stain the gel with Coomassie stain for 1 h.
11. De-stain the gel with MQ water 3X, 30 minutes interval, or until the background is clear.
12. Image the gel: protein assay tab -> select Coomassie white tray.

D4. Western blot protocol

4.1. Solutions and Equipment

1. Transfer buffer (20X)
 - 0.2 M CAPS (BioRad®) pH 11.0 titrated with NaOH; store at room temperature.
2. 0.2 µM PVDF membrane (Immobilon™)
3. Fiber pads (four per one membrane) and sponge (2 per membrane)
4. 10X TBS (1 L)
 - 60.57 g of Tris-base (0.5 M)
 - 117 g of NaCl (2 M)
 - Titrate with HCl to make pH 7.5 -> bring up to 1 L
5. TBS-T solution (1 L)
 - 50 mM Tris-Base, 200 mM NaCl, 0.1% (v/v) Tween®-20, pH 7.5.
 - Add 100 ml of 10X TBS and 1 ml of stock Tween®-20 (Merck®, CAS 9005-64-5)
 - Bring up to 1 L with MQ water.
6. 5% Non-fat dry milk (20 mL/Criterion™ gel)
 - 5 g of Dry milk powder (RPI®, C791K18) in 100 mL TBS-T
7. Primary antibodies (10 mL/Criterion™ gel) in TBS-T
 - a. Cardiac myosin binding protein-C; cMyBP-C
 - p-S273 (1:500 polyclonal rabbit Ab; courtesy to Saddayapan Sakthivel)
 - p-S282 (1:25,000 polyclonal rabbit Ab; courtesy to Saddayapan Sakthivel)
 - p-S302 (1:10,000 polyclonal rabbit Ab; courtesy to Saddayapan Sakthivel)
 - Total cMyBP-C (1:50,000 polyclonal rabbit Ab; courtesy to Rick Moss)
 - b. Cardiac troponin I; cTnI
 - p-S23/24 (1:1000 monoclonal rabbit Ab; Cell Signaling Technology®, Cat No. 4004B)
 - Total cTnI (1:5000 monoclonal mouse Ab; Fitzgerald®, Cat No. 10R-T123k)
 - c. Phospholamban; PLN, and Sarcoplasmic reticulum Ca pump; SERCa
 - p-S16 (1:1,000 polyclonal rabbit Ab; Millipore™, 07052)
 - p-T17 (1:2,500 polyclonal rabbit Ab; Badrilla™, A010-13AP)
 - Total PLN (1:5,000 monoclonal mouse Ab; Badrilla™, A010-14)
 - SERCa2a (1:1,000 monoclonal polyclonal rabbit Ab; Badrilla™, A010-23)
8. Secondary antibodies (20 mL/Criterion™ gel)
 - Goat anti-rabbit Ab (1:20,000; Cell Signaling Technology®, 7074)

- Horse anti-mouse Ab (1:25,000; Cell Signaling Technology[®], 7076)
- 9. Housekeeping control protein
 - Beta-actin (1:1,000 monoclonal mouse Ab; Protein tech[™], 60008-1)
- 10. Swift[™] membrane stain-Destaining Solutions (G-Biosciences[®])
- 11. Peroxidase substrate for enhanced chemiluminescence; ECL (Clarity[™], BioRad[®])
- 12. Stripping solution (10-20 mL/criterion gel)
 - a. Guanidine HCl: 6 M
 - b. Nonidet P-40 (Sigma[®]): 0.3% v/v
 - c. Tris-(2-carboxyethyl)-phosphine; TCEP Sigma[®]: 5 mM
 Or Restore[™] PLUS Western Stripping buffer (Thermo Fisher[®], Cat No. 46430).

4.2. Procedure

1. Transferring process
 - a. While SDS PAGE is running, soak PVDF membrane in 100% MeOH for 1 min, wash out with MQ water, then, equilibrate in 1X transfer buffer for 30 minutes.
 - b. After SDS-PAGE was done, prepare the transferring equipment. Put the sandwich cassette in the tray. Soak up with 1X CAPS, put the sponge at the bottom layer. Use the roller to get rid of bubbles as much as possible. Then, 2 fiber pads followed by the gel and membrane and another two fiber pads and sponge are covered on top in a sequence. Then the cassette is closed. Put the cassette into the transferring box that already filled up with transferring buffer and ice pack. Fill the buffer up to cover the cassette and close the box.
 - c. To transfer, use constant 20 V (or 30 V for cMyBP-C or larger proteins) for 90 minutes.
2. Swift[™] staining
 - a. After the transfer is finished, soak the membrane with MeOH for 30 seconds wash with water and stain with Swift[™] stain. Manually shake until bands are presented.
 - b. Put the stained membrane on the sheet protector and image using Protein -> Colorimetric assay.
 - c. Destain the membrane using the de-staining solution form the kit. Manually shake until the bands are disappeared.
3. Developing blots of the phosphorylation proteins
 - a. Prepare the 5% non-fat dry milk to block the membrane.
 - b. Rinse the gel with MQ water 3X and TBS-T 3X. Put the non-fat dry milk into the membrane. Shake for 1 hour.

- c. Remove the 5% milk solution, wash with water quickly and add the primary antibodies of the specific phosphorylation sites of proteins into the membrane, shake it overnight at 4°C.
 - d. On the day after, pour the antibodies back into tubes. Rinse the gel quickly with water 3X and TBS-T 3X.
 - e. Pour the secondary antibodies onto membrane. Incubate and shake for 90 minutes.
 - f. Rinse with water for 3X and add TBS-T with 5 minutes incubation for 3 times.
 - g. Add ECL-2 substrate onto the membrane. Manually shake for 5 minutes.
 - h. Put membrane into a sheet protector and image using Protein -> Colorimetric assay and Protein -> Chemiluminescence assay.
4. Membrane stripping process
- a. To strip off the antibodies, wash the membrane quickly with ultrapure water, then add the stripping buffer and shake for 10 minutes. After that, wash the membrane quickly with water at least two times. Redo this step twice. After finish, wash the membrane with TBS-T 2X.
 - b. Some primary antibodies may need additional use of the commercial stripping buffer (Restore™ PLUS). By using this, use 15 mL of the solution for each blot. Incubate at 37°C for 10 minutes and shake at room temperature for 20 minutes. Repeat this 4X, wash with MQ water 3X, and put into TBS-T buffer.
 - c. Check the completion of stripping, add 5% non-fat dry milk, shake and incubate for 1 hour. Wash the membrane with water 3X quickly and add secondary antibodies. Incubate for 90 minutes.
 - d. After finished, wash the membrane quickly with MQ water 3X and TBS-T 3X. Add ECL substrate and manually shake for 5 minutes. Image the membrane using Protein -> Chemiluminescence assay. Use manual exposure for 5 minutes, if the bands are not presented, the stripping process is completed.
5. Developing blots of the total proteins
- a. Add 5% non-fat dry milk, shake and incubate for 1 hour. Wash the membrane with water 3X.
 - b. Put the Primary antibodies of total protein (of that phosphorylated one) onto each membrane. Let it shake and incubate overnight at 4°C.
 - c. Wash the membrane quickly with MQ water 3X, then TBS-T 3X. Put secondary antibodies into the blot and let it incubate for 90 minutes at room temperature.

- d. After finish, quickly rinse the blot with MQ water 3X and TBS-T 3X.
 - e. Put the ECL substrates into a blot, manually shake for 5 minutes and put it into a sheet protector and take imaging again.
6. Developing blots of the housekeeping protein
- a. Prepare primary antibodies of beta-actin in 5% non-fat dry milk.
 - b. Rinse the membrane quickly with MQ water 3X and TBS-T 3X. Pour primary antibodies onto the membrane. Incubate overnight at 4°C.
 - c. Add secondary antibodies and incubate at room temperature for 90 minutes.
 - d. Quickly rinse the blot with MQ water 3X and TBS-T 3X with 5 minutes interval.
 - e. Put the ECL substrates into a blot, manually shake for 5 minutes, put into a sheet protector and take imaging.



D5. Additional results from Phosphor-staining of other myofilament proteins

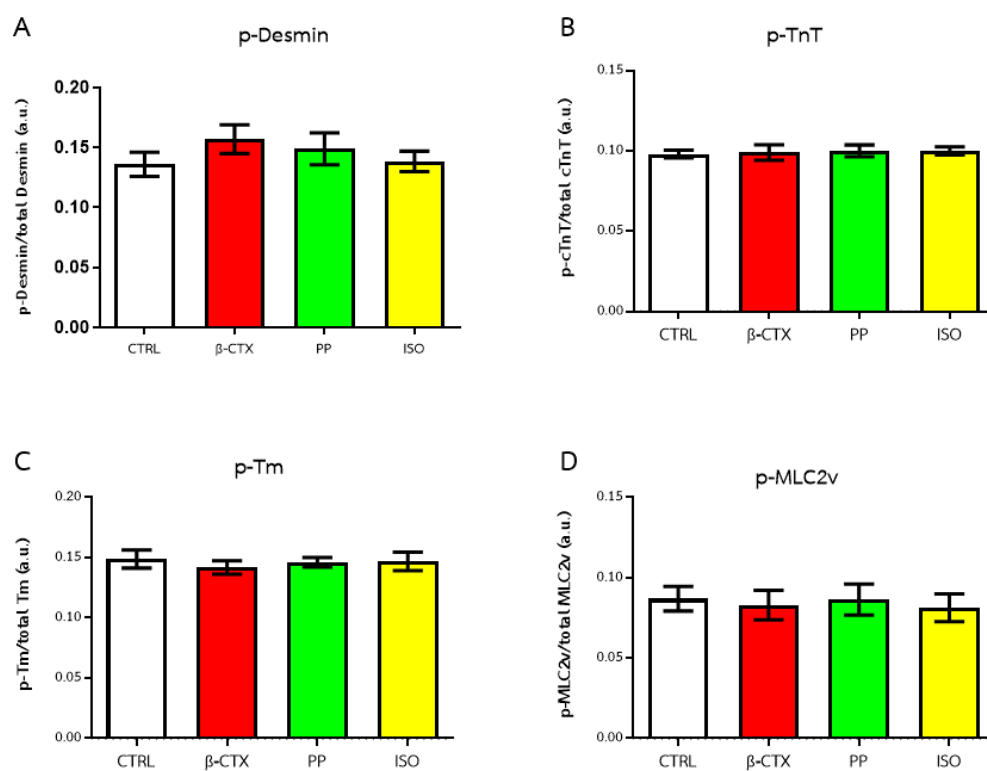


Figure 5 9 Bar graphs demonstrate the analysis of band intensities acquired from the ProQ[®] phosphor-staining gel (Figure 14). Comparison is made between four treatments; 1) control, 2) β -CTX, 3) propranolol (PP) and 4) isoproterenol (ISO) on the total phosphorylation levels of (A) desmin, (B) cardiac troponin T (TnT), (C) tropomyosin (Tm) and (D) myosin light chain (MLC2v). Data are shown in mean \pm S.E.M.

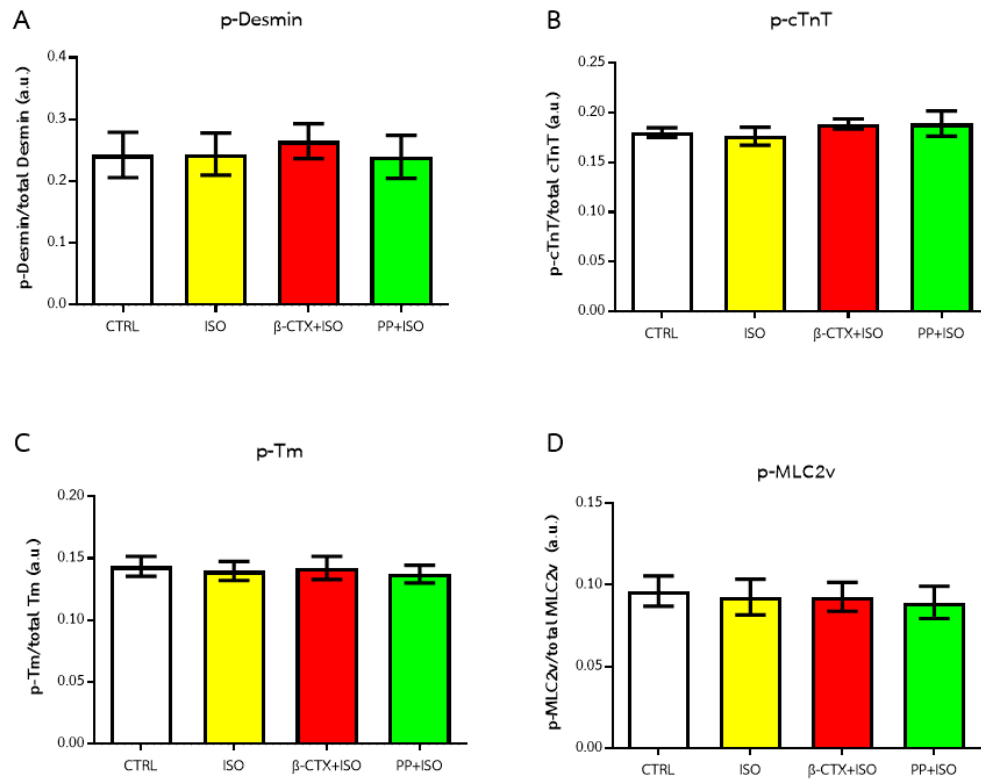


Figure S 10. Bar graphs demonstrate the analysis of band intensities acquired from the ProQ[®] phosphor-staining gel (Figure 15). Comparison is made between four treatments; 1) control, 2) ISO, 3) β -CTX and 4) PP+ISO on the total phosphorylation levels of (A) desmin, (B) cardiac troponin T (TnT), (C) tropomyosin (Tm) and (D) myosin light chain (MLC2v). Data are shown in mean \pm S.E.M.

D6. Additional results from western blot analysis

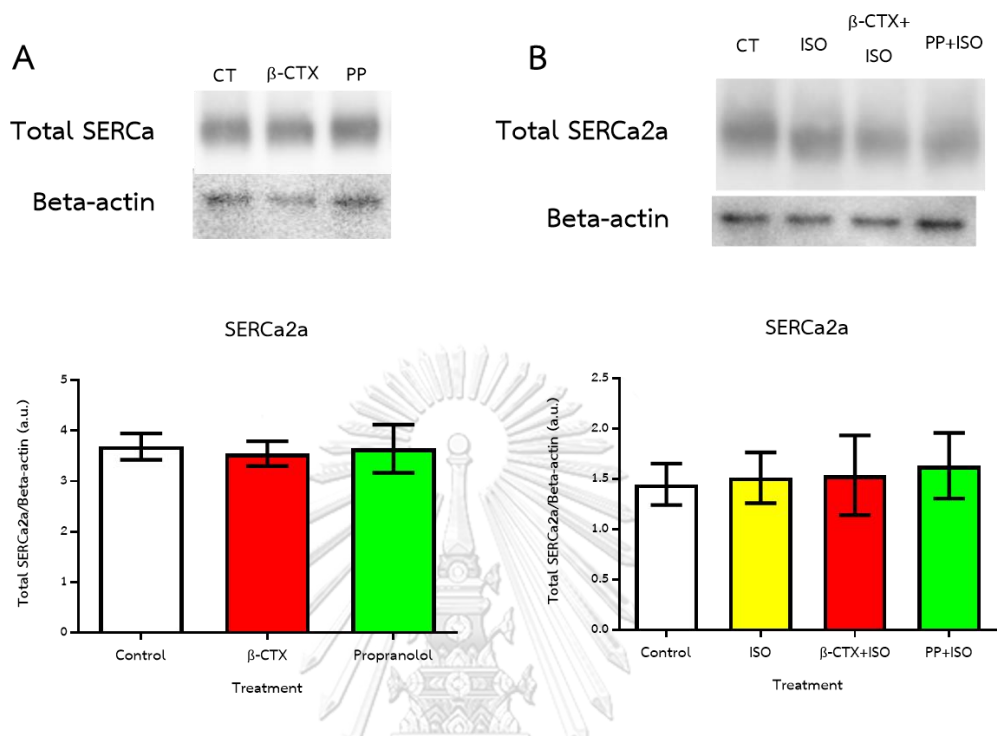


Figure S 11. Western blot analysis of SERCa2a expression. (A) At the basal condition, comparison is performed between control, 0.3 μ M of β -CTX and 0.3 μ M of propranolol. (B) During the ISO stimulation, the analysis is compared between control, ISO-treated cells (ISO), cells receiving β -CTX and ISO (β -CTX+ISO) and cells pre-treated with propranolol prior to ISO (PP+ISO). Data are shown in mean \pm S.E.M.

Appendix E

Detergent extracted (skinned) fibers and Force-pCa measurement

E1. Isolation of skinned fiber bundles

1.1. Materials and solutions

1. 0.1 M stock EGTA (ethylene glycol-bis (β -aminoethyl ether)-N,N,N',N'-tetraacetic acid)
 - 38.035 g of EGTA (Sigma[®], Cat No. E4378)
 - Titrate using 6M KOH to pH at 7.0 -> bring up to 1 L
2. 0.5 M stock BES (**N,N-Bis(2-hydroxyethyl)taurine**)
 - 106.625 g of BES (Sigma[®], Cat No. B9879) -> add water up to 1 L
3. 1 M of MgCl₂ (Sigma[®], Cat No. M1028)
4. 1 M of CaCl₂ (Fluka[®], Cat No. 21114)
5. Phosphocreatine; Cr-PO₄ (Sigma[®], P7936)
 - Add the amount in the specified table below
6. 1 U/ μ L Creatine phosphokinase; CPK
 - Dissolve CPK (Sigma[®], Cat No. C-3755) for 1 mL in 1 L water
7. Na-ATP (Sigma[®], Cat No. A3377)
 - Correct the H₂O content (MW = 551.1 g/mol)
 - (Anhydrous MW) * (% H₂O content/100) = X + 551.
 - Add the amount in the specified table below
8. 6 M of stock KOH
 - 336.66 g of KOH (Fisher[®], Cat No. P250)
9. 1 M of Potassium propionate; K-prop
 - 300 mL of Propionic Acid (Sigma[®], Cat No. P1386)
 - 74.08 g Potassium Hydroxide (Fischer[®], Cat No. P250-1)
 - 56.11 g of KOH -> Bring up to 1 L with MQ water

10. High relaxing buffer (HRB; pCa 10.0) and Activating solution (pCa 4.5) pH 7.0:

Stock Conc. (M)		HR pCa 10.0 (1L)		Activating pCa 4.5 (0.5 L)	
		Final Conc. (mM)	mL/g to Add	Final Conc. (mM)	mL/g to Add
EGTA	0.1	10.00	100.00 mL	10.00	50.00 mL
CaCl ₂	1.0	0.00	0.00 mL	9.98	4.99 mL
KCl	1.0	41.89	41.89 mL	22.16	11.08 mL
MgCl ₂	1.0	6.57	6.57 mL	6.20	3.10 mL
BES	0.5	100.00	200.00 mL	100.00	100.00 mL
ATP	589.68*	6.22	3.67 g*	6.29	1.85 g*
CrP	255.10	10.00	2.55 g	10.00	1.28 g
Na Azide	1.0	5.00	5.00 mL	5.0	2.50 mL

- On the day of experiment, add protease and phosphatase inhibitors to each solution

Compound	For 40 mL solution	For 35 mL solution
Pepstatin (1mg/ml in EtOH)	100 µL	87.5 µL
Leupeptin(5mg/ml in MQ water))	8 µL	7 µL
PMSF (100 mM in EtOH)	20 µL	17.5 µL

11. HR + 1% Triton X-100

- 2 mL of HR
- 200 µL 10% Triton-X stock

1.2. Procedure

1. Isolation of the heart and aorta

- Heparinize and anesthetize the mouse using Heparin (5000 U/kg) and pentobarbital sodium (Fatal plus[®], 65 mg/kg). Inject intraperitoneally. Wait until the rat becomes fully unconscious, without any reflexes.
- Open the chest by cutting through the abdominal wall just below the diaphragm, with forceps grab the xiphoid process and cut through the diaphragm muscle and down the left and right sides of the rib cage.
- Remove the heart, being cautious to preserve the aorta.
- Quickly transfer the heart to the small cup filled with HRB that is on ice. Trim away any excess tissue and gently push out any remaining blood from the heart.

- e. Transfer the heart to the petri dish with silicone under the stereoscope. Make sure the heart is covered with an HRB solution.

2. Isolating the Papillary Muscles

- a. With two forceps, use the stereoscope to maneuver the heart so the ventral aspect of the heart (front of the heart) is facing up towards you.
- b. Also, ensure that the apex of the heart is pointing towards the top of the field of view in the scope and that the base is pointing to the bottom.
- c. Take the thinnest of the dissection pins and put it through the apex of the heart to pin it to the silicon surface.
- d. Identify the right atria (they should look like small, deflated pink bags hanging over the very large body of the heart - the ventricles).
- e. Grab the right atrium with a pair of forceps and pull it away from the ventricles. Cut into the stalk of the atrium with the larger of the two micro-dissection scissors.
- f. Once you remove the right atrium, there should be a hole where it connected to the ventricle. Grab part of the heart near that hole with forceps and stick your scissors into it. Cut down laterally until you reach the apex.
- g. With your forceps maneuver the flaps of the right ventricle that you just cut so they can each be pinned down to the silicon. The dorsal flap can be pinned in place. The ventral flap will have to be pulled back over the rest of the heart and pinned down. This should expose the septum, which separates the right and left ventricles.
- h. With your forceps, you now need to locate the aorta. Maneuver it so you can stick one of the blades of your scissors into the lumen of the aorta.
- i. Cut down the aorta and continue down through the septal wall.
- j. Take the pins originally used to hold down the flaps of the right ventricle and reposition them so that they now pin down both flaps of the left ventricle.
- k. Cutaway any connective tissue (, the left atrium, and perhaps, the valvular tissue) that may keep you from opening up the left ventricle completely.
- l. At this point, you should see a bunch of tubular muscles along the walls of the chamber. The majority of these tubular structures are the trabeculae carneae.
- m. The papillary muscles will be the two largest and most superficial of all the tubular structures. They will also run in angles that are different than the trabeculae and connect to the valvular tissue (whitish tissue). Look for the muscles that run at a diagonal to the trabeculae and meet at the apex to form what might look like a V.
- n. You will begin cutting at the end of the muscle that is opposite the apex. Use your forceps to grab the white valve tissue which is holding the papillary muscle in place.

- o. Grab the valve tissue attached to the desired papillary muscle and cut it away from the wall of the chamber.
 - p. Using the smaller of the two insect dissection scissors, make shallow cuts along the papillary muscle to gently free it from the chamber wall.
 - q. When you reach the apex, keep cutting to take away a chunk of the left ventricular wall as well. When you reach the limit of the apex, cut the muscle completely free and immediately transfer it to the petri dish lid which contains the chilled HRB.
 - r. Repeat this for the remaining papillary muscle as well.
3. Isolating myofibers from papillary muscles and skinning
- a. In this final step, it is very important to remember to not grip the papillary muscle or the individual fibers with the forceps. All maneuvers must be performed by grabbing the very ends of the muscle/fiber.
 - b. Flip the cold plate so that the black side is up. Move the petri dish lid with the dissected papillary muscles on to the black plate move the dissecting lights near the sides of the petri dish so that the light is illuminating the papillary fibers.
 - c. Give the lid a gentle shake. If you see that the muscles are floating around too freely, then it usually indicates that you have them in too much HR. Use a disposable pipette to suction out excess HRB, so that the muscles will not float too freely, but be sure to leave enough so that they remain submerged in the solution.
 - d. Using a scalpel fitted with a 10-blade, begin cutting out the visible fibers, trying not to move the blade backward (this may risk severing the freed fiber)
 - e. Use a ruler placed under the petri dish to measure and gauge the size of your fiber. It should be 4-5mm in length and should be no thicker than a line on the ruler (this will be approximately 200-250 μm in width).
 - f. Once you have isolated a fiber that is appropriately sized, carefully transfer the fiber to the dish with HR + 1% Triton.
 - g. Allow the Triton to permeabilize the fibers for 30 minutes at room temperature.

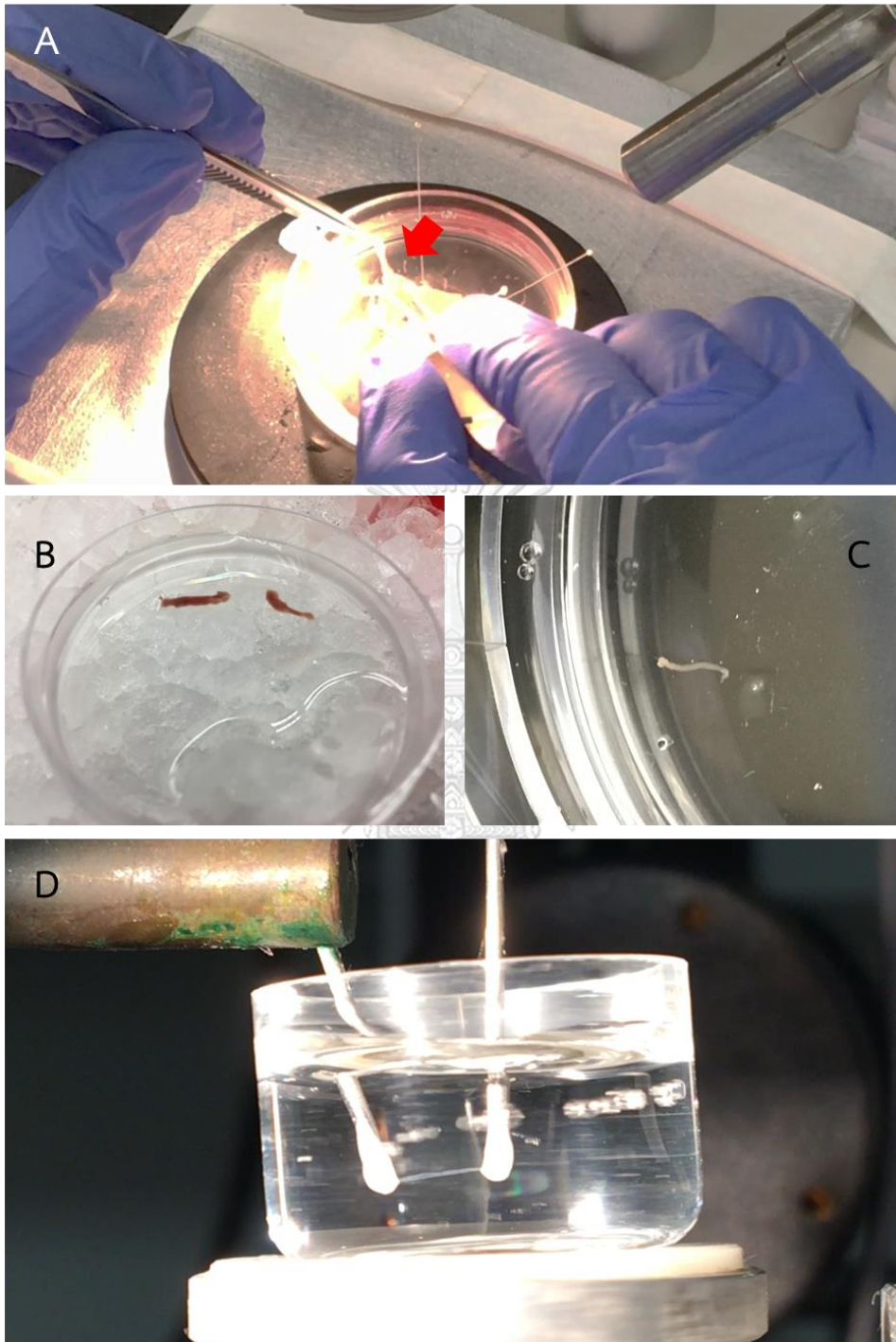


Figure S 15. (A) Left ventricular papillary muscle (red arrow) is being dissected. (B). The dissected muscles are incubated in high relaxing buffer containing Triton-X to remove cell membrane. (C) Dissected skinned fiber with the size of 4 mm in length and 200-250 μm in width. (D). The fiber is mounted onto the force transducer to measure the force generation.

E2. Measurement of the force-pCa relationship

2.1. Solutions

1. Calcium (pCa) solutions

pCa	[Ca ²⁺]	For 8.5 mL		For 4.5 mL	
		HRB	4.5	HRB	4.5
8.00	0.26	8.279	0.211	4.383	0.117
7.00	2.08	6.730	1.770	3.563	0.937
6.50	4.54	4.638	3.862	2.455	2.045
6.25	5.96	3.429	5.071	1.815	2.685
6.00	7.24	2.339	6.161	1.238	3.262
5.85	7.88	1.794	6.706	0.950	3.550
5.75	8.24	1.489	7.011	0.788	3.712
5.61	8.60	1.182	7.318	0.626	3.874
5.50	8.94	0.894	7.606	0.473	4.027
5.25	9.38	0.519	7.982	0.275	4.226

- Add 2 mL of each solution with 10 μ L of CPK stock
- Make two sets of the pCa solutions, with and without β -CTX.

2. Acetonic glue (homemade)

2.2. Procedure

1. Mount the fibers onto the force transducer using acetonic glue
2. Setting the sarcomere length
 - a. Fill the sawed-off cuvette with HRB solution and stop the plate rotor.
 - b. Remove the dish with HRB and replace it with the cuvette (ensure that the smooth surfaces of the cuvette are lined up with the projected path of the laser).
 - c. When the fiber is submerged in the cuvette, place the wooden board exactly 10 cm away from the fiber (there is a right-edged ruler to measure this) in an orientation such that the fiber is between the laser and the board.
 - d. Calculation equation: Sarcomere length (SL) = $n\lambda/(\sin(\tan^{-1}(xn/h)))$
 - λ = laser beam wavelength
 - h = distance

- x_n = measurement of the distance between the 0th order to the nth diffraction order
 - <http://muscle.ucsd.edu/musintro/diffraction>: for more information
- e. Turn on the power source for the laser and open the shutter to allow the laser to hit the center of the fiber.
 - f. Adjust the length of the fiber, using the top-most knob on the mounting post apparatus, so that the 1st diffraction line is overlaid with the measured line on the board for the sarcomere length you desire.
 - g. Once this is set, shutter the laser and turn off the power. Once the sarcomere length is set, no adjustments to the fiber mounting system should be made.
3. Measuring the cross-sectional area (CSA)
- a. Fill the chamber containing the 45° mirror with HRB. Remove cuvette and submerge the fiber in the HRB-filled mirror chamber.
 - b. Turn on and aim the light source directly at the fiber, and move the scope mounted on wheels in front of the fiber.
 - c. Find the fiber using the scope at the lowest magnification, and then zoom in to the maximum magnification indicated by position 5, on the knob.
 - d. Measure and record the height of the fiber, by number of marks (count tick marks on the ruler in microscope eyepiece – fibers are typically 15-30 marks), in 3 locations of the fiber – typically the left and right side as well as the middle. The “x” values will come from looking through the scope at the actual fiber.
 - e. Move the microscope downward until you see the fiber reflection in the mirror. Make an additional 3 measurements (left, right center) and record these as the “y” values.
 - f. Average the values and multiply them by the calibration factor indicated on the side of the microscope (i.e. if the calibration says: 8.06 μm per mark than 20 marks \times 8.06 $\mu\text{m}/1$ mark = 161.2 μm or 0.1612 mm)
 - g. Since $A = \pi r^2$; $CSA = \pi xy$ (in mm^2)
 - a. When finished, turn off the light source, remove the mirrored box and replace it with the dish containing HRB. Set the dish to spin.
4. Measurement of force generated by fibers
- a. Remove the HRB dish and replace it with pCa 4.5 for maximal activation. As the fiber begins to produce force the chart recorder needle will move. Allow the needle to plateau/stabilize making sure that the force registered is within the recording range. Adjust the sensitivity and speed of the physiograph if needed

- b. Replace the 4.5 dish with HRB. Allow the needle to return to the baseline and stabilize.
- c. Once more replace the HRB dish with 4.5 to obtain the initial maximal activating force measurement.
- d. Replace the 4.5 dish with HRB and allow for a stabilized return to baseline again.
- e. Measure the force in different pCa solutions (pCa 7.0, 6.5, 6.0, 5.85, 5.75, 5.5, 4.5).
- f. Once you have reached the highest stable point of the curve, remove the pCa 4.5 dish, and replace it with the HRB dish, allowing the fiber to return to baseline.
- g. Repeat force measurements with pCa 4.5 to obtain the final maximal force measurement.



Appendix F

Measurement of myofibrillar ATPase activity

F1. Isolation of myofibrils

1.1. Solutions and tools

1. Standard Relax Buffer (SRB)

Ingredients	Conc (mM)	MW	Volume (L)	Weight (g)
KCl	75	74.55	0.5	2.796
Imidazole	10	68.08	0.5	0.340
MgCl ₂	2	203.31	0.5	0.203
EGTA	2	380.35	0.5	0.380
NaN ₃	1	65.01	0.5	0.033

- Add all items together, pH to 7.2
- Bring volume up to 500 mL with MQ water.

2. Standard Relax Buffer w/ TX-100 (SRB-X100)

- 100 mL of SRB
- 1 mL of stock Triton X-100 to give a final (1% v/v).

3. A-70 solution

Ingredients	Conc (mM)	MW (g/mol)	Volume (L)	Weight (g)
NaCl	70	58.44	0.5	2.045
MgCl ₂	10	203.31	0.5	1.017
MOPS	40	209.3	0.5	4.186

- Add all items together, pH to 7.0. Bring volume up to 500 ml with MQ water.

4. Collagenase II (Worthington®) 245 g/IU

5. Dounce homogenizer (A and B pestle with homogenizing tube)

6. Protein assay kit (DC assay, BioRad®)

1.2. Procedure

1. Anesthetize and heparinize rat using heparin (5000 U/kg) and pentobarbital sodium (Fetal Plus[®], 65 mg/kg). Inject intraperitoneally.
2. Dissect the heart and aorta, put into the cold SRB to wash and remove blood.
3. Cut the ventricular tissue for 35-50 mg.
4. Add 1 mg/mL collagenase type II in 1 mL SRB solution into the ventricular tissue.
5. Transfer into the homogenizing tube. Homogenize the tissue using a 2 ml Dounce homogenizer (about 10 times using a loose-fitting pestle A). Allow to incubate, on ice, for 5 minutes, then homogenize another 10 strokes.
6. Transfer into a pre-weighed microfuge tube.
7. Spin in cold (4° C) microfuge for 1 min at max speed (~16000 xg).
8. Decant the supernatant.
9. Add 1 mL of cold SRB-X100 to pellet, resuspend, transfer to homogenizer used previously, and homogenize with tight-fitting pestle B.
10. Remove supernatant and transfer myofibrils back to the same homogenizer used previously. Repeat steps 6-7 twice. (Total of 3 times SRB-X100 washing and homogenizing)
11. Remove supernatant and add 1 mL of SRB to the pellet, vortex 30 sec. to resuspend, and spin again 1 min at 5000 xg in a microfuge.
12. Remove supernatant and add 1 mL of A-70 buffer to each tube, vortex to resuspend, and spin at 3000 xg speed for 5 minutes. Remove the supernatant, repeat A-70 wash. (Total of 2 washed with A-70).
13. Remove supernatant, weigh the tube with the pellet, and resuspend in cold A-70 buffer based on a 1:20 (w/v) ratio (ie. 1 mg = 1 μ L so if you have 20 mg of MF then add 400 μ L of buffer). Take 10 μ L of this solution and mix with 10 μ L of 10% SDS and 80 μ L of A-35 (A-70 diluted 1:1 with H₂O).
14. Make a tube of A-35 (50% A-70 in water) and SDS/A35 (20 μ L f 10% SDS, 100 μ L A-70 and 80 μ L water). Then, make a standard protein solution (from BSA 3 mg/mL), starting from 1.5 mg/mL and make 2-fold dilution with SDS/A35 solutions for 6 concentrations.
15. Determine the concentration of the samples via the BioRad[®] DC assay. Briefly, take 5 μ L of each solution (6 of standard solutions and the samples) and mix with 25 μ L of the solution A' (1 mL solution A and 20 μ L solution S of Protein DC assay) and 200 μ L solution B. Stir and leave in room temperature for 15 minutes and read with a microplate reader at 750 nm.

F2. *In vitro* S1 actomyosin ATPase malachite green assay

2.1. Solutions

1. Stop Solution (0.2 M Perchloric Acid (PCA))
 - 21.74 mL of 60% PCA
 - 978.26 of water
2. Calcium solutions (pCa)

20 mM EGTA ^a	20 mM Ca ²⁺ -EGTA ^b	Free Ca*	pCa**
9.5 mL	0.5 mL	1.98E ⁻⁰⁸	7.704
9.0 mL	1.0 mL	4.18E ⁻⁰⁸	7.379
6.0 mL	4.0 mL	2.51E ⁻⁰⁷	6.600
4.0 mL	6.0 mL	5.67E ⁻⁰⁷	6.247
3.0 mL	7.0 mL	8.82E ⁻⁰⁷	6.055
2.0 mL	8.0 mL	1.50E ⁻⁰⁶	5.824
1.0 mL	9.0 mL	3.30E ⁻⁰⁶	5.481
0.6 mL	9.4 mL	5.60E ⁻⁰⁶	5.252
0.4 mL	9.6 mL	8.10E ⁻⁰⁶	5.092
0.2 mL	9.8 mL	1.35E ⁻⁰⁵	4.870
0.0 mL	10.0 mL	2.65E ⁻⁰⁵	4.577
		9.34E ⁻⁰⁵	4.030***

^a 20 mM EGTA: 10 mL of 0.2 M EGTA + 90 mL H₂O

^b 20 mM Ca²⁺-EGTA: 25 mL of 0.2 M EGTA + 50 mL of 0.1 M CaCl₂ + 175 mL H₂O)

* Calculated using online website: WEBMAXC STANDARD; under the condition of 35 mM NaCl, 5 mM MgCl₂, 2 mM EGTA, 0.67 mM ATP, 20 mM MOPS/NaOH, pH 7.0, 25°C

** pCa was calculated from $-\log [\text{Free Ca}^{2+}]$

*** A 10 µL of 0.1 mM CaCl₂ was added directly instead of EGTA/Ca²⁺-EGTA solution

3. A-70 solution
4. Free phosphate standard
 - Stock: 0.5 mM NaH_2PO_4 solution: 3.45 g/50 mL in H_2O .
 - Dilute stock to 0.1 mM NaH_2PO_4 : 20 μL stock + 99.98 mL A-70.
 - Make 0, 0.2, 0.4, 0.6, 0.8, 1 nM Pi standard following the table below

Standard Pi (nM)	μL 0.1 mM NaH_2PO_4 (mL)	μL Buffer A-70 (mL)
0	0	2
0.2	0.4	1.6
0.4	0.8	1.2
0.6	1.2	0.8
0.8	1.6	0.4
1.0	2	0

5. 0.1 mM ATP:
 - Dilute 10 μL of 100 mM ATP in 590 μL H_2O (Prepare freshly before start the reaction)
6. Malachite Green (MGS) solution:
 - 700 mL of 1 M HCl
 - 2.0 g of ammonium molybdate
 - 0.3 g malachite green oxalate
 - 0.5 mL of Triton X-100
 - Bring up to 1 L with MQ water; stir overnight

2.2. Procedure

1. From the stock myofibril solution (determined from DC assay), make a 550 μL stock with A-70 buffer at 0.3 $\mu\text{g}/\mu\text{L}$. Keep all tubes containing myofibrils on ice.
2. Place a 96-well plate with a flat well bottom on plate warmer/cooler at 10°C or on ice.
3. Add 90 μL PCA (Stop solution) to all wells to be used.
4. Add 10 μL of the prepared standard solutions into the last two rows. Quadruplicate the reaction.
5. Each sample will contain 40 μL of myofibrils. Incubate myofibrils for 5 min at 25°C and then, add 10 μL of pCa solutions, and 10 μL of either A-70 (control) or 1 μM β -CTX in A-70 into the reaction tubes. Vortex and incubate for 15 minutes. (In this study, 12 reaction tubes were used according to 12 different pCa solutions).

6. To begin ATPase reaction, add 40 μL of pre-warmed 1.67 mM ATP. Vortex to resuspend and mix. start the timer. Add ATP into 12 reaction tubes with 15 seconds interval per tube.
7. After being done, remove 10 μL of the appropriate sample and inject it into the well containing PCA. Redo this until the plate is full.
8. After samples have all been taken, add 100 μL of a malachite green solution to each well, shake for 1 min, then incubate for 30 min at 27°C.
9. Read at 655 nm on a microplate reader.



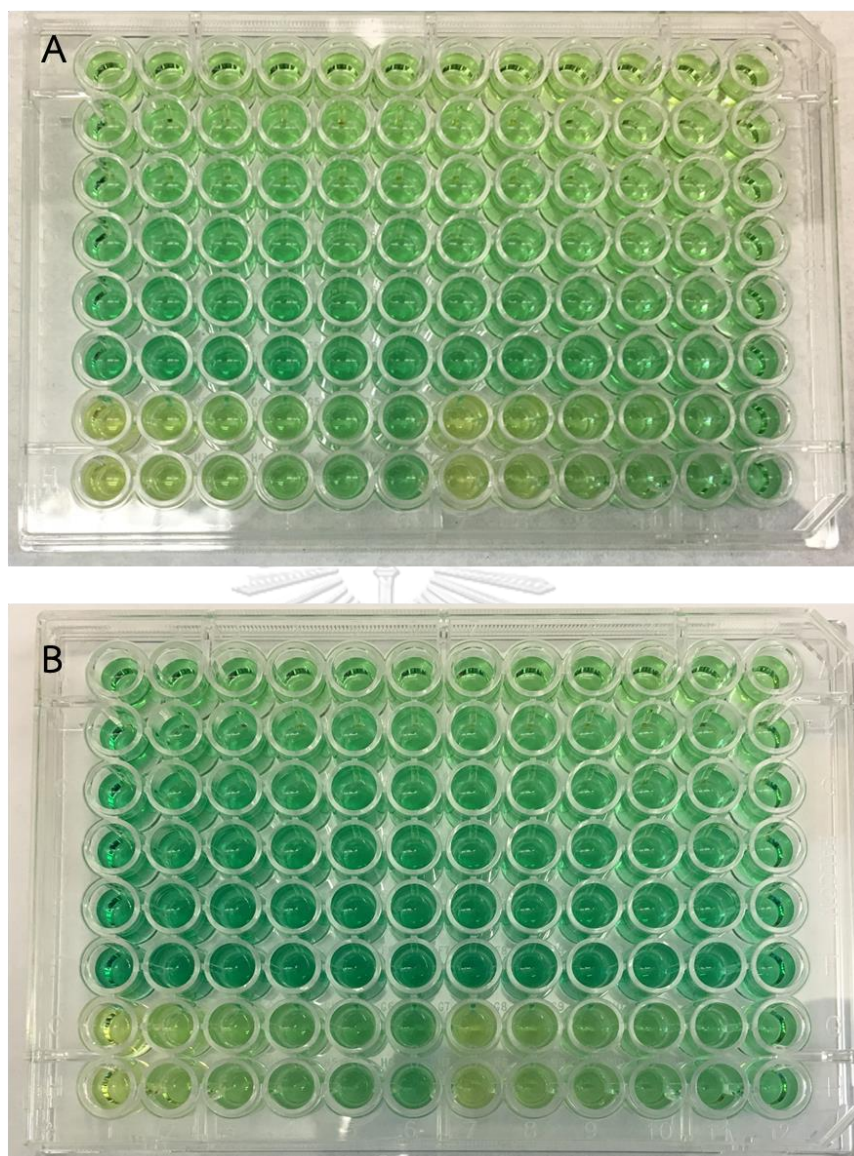


Figure S 16. Malachite green assay results from the myofibrils treated with (A) A-70 solution or (B) β -CTX. Each column representing different pCa and each row represent time for 3 minutes interval. Of note, the last two rows are the standard phosphate solutions.

Appendix G

Synthesis of recombinant β -CTX protein (r β -CTX)

G1. Construction and transformation of cleavable His₆-tag β -CTX in vector

Plasmids containing DNA fragments of β -CTX with a His₆-tag and tobacco etch virus (TEV) protease cleavage site (ENLYFQ/X, where X is the desired first amino acid of the native protein) at the N-terminal site was commercially produced (300 bp, Integrated DNA Technology Inc; IDT[®], USA). The plasmid was cut using two restriction enzymes, NdeI and HindIII-HF (NEB[®], USA) and electrophoresed (Owl[™] Easy-cast[™] B2 Mini gel electrophoresis system) in 1.5% agarose gel (SeaKem[®] LE) to separate the plasmid and the DNA sequence (Figure S1B). The gel was stained with GelRed[™] pre-stained loading dye (Biotium[®], USA) to determine the presence of the cut sequence. The gel with the interesting band was cut and extracted from the gel using a commercial kit (NucleoSpin[®]). The extracted solution was then ligated to the pET28a vector (Novagen[®], USA), containing a His₆-tag and a T7 promoter coding sequence, using commercial DNA ligation kit (NEB[®], USA) and restriction enzymes, NdeI and HindIII-HF (Figure S1A). Confirmation of the His-tag β -CTX gene in the pET28a vector was performed using 1.5% agarose gel electrophoresis (Figure S1C). Meanwhile, the solution was sent for analysis to confirm the sequence of the DNA fragments. Vector was then transformed into BL21 (DE3) competent *E.coli*

(NEB[®], USA) in Luria agar containing 40 µg/mL kanamycin and cultured at 37°C, overnight. To express the transcription of our protein, one colony per construct was selected and grown in a 4-mL Luria broth, containing kanamycin, at 37°C overnight. Colonies were split into two aliquots; one was induced (I) by 1 mM of isopropyl-β-D-1-thiogalactopyranoside (IPTG) and another was kept uninduced (U). To check the expression of the rβ-CTX, SDS-PAGE was run on pre-casted 4-20% polyacrylamide gel (BioRad[®]) after three hours of IPTG induction (Figure S2). Constructs were centrifuged at 16,000 xg for 5 minutes. The supernatant was discarded, and the pellets were then re-suspended with LSB standard protein mix. Ten micrograms of all isolates were loaded and electrophoresed on 15% polyacrylamide gel. After finished performing SDS-PAGE, the gel was fixed with Coomassie blue staining for 30 minutes. Then, the gel was de-stained using a 10% acetic acid and 10% methanol solution. The photo of bands was taken under the BioRad[®] ChemiDoc[™] MP imaging system.

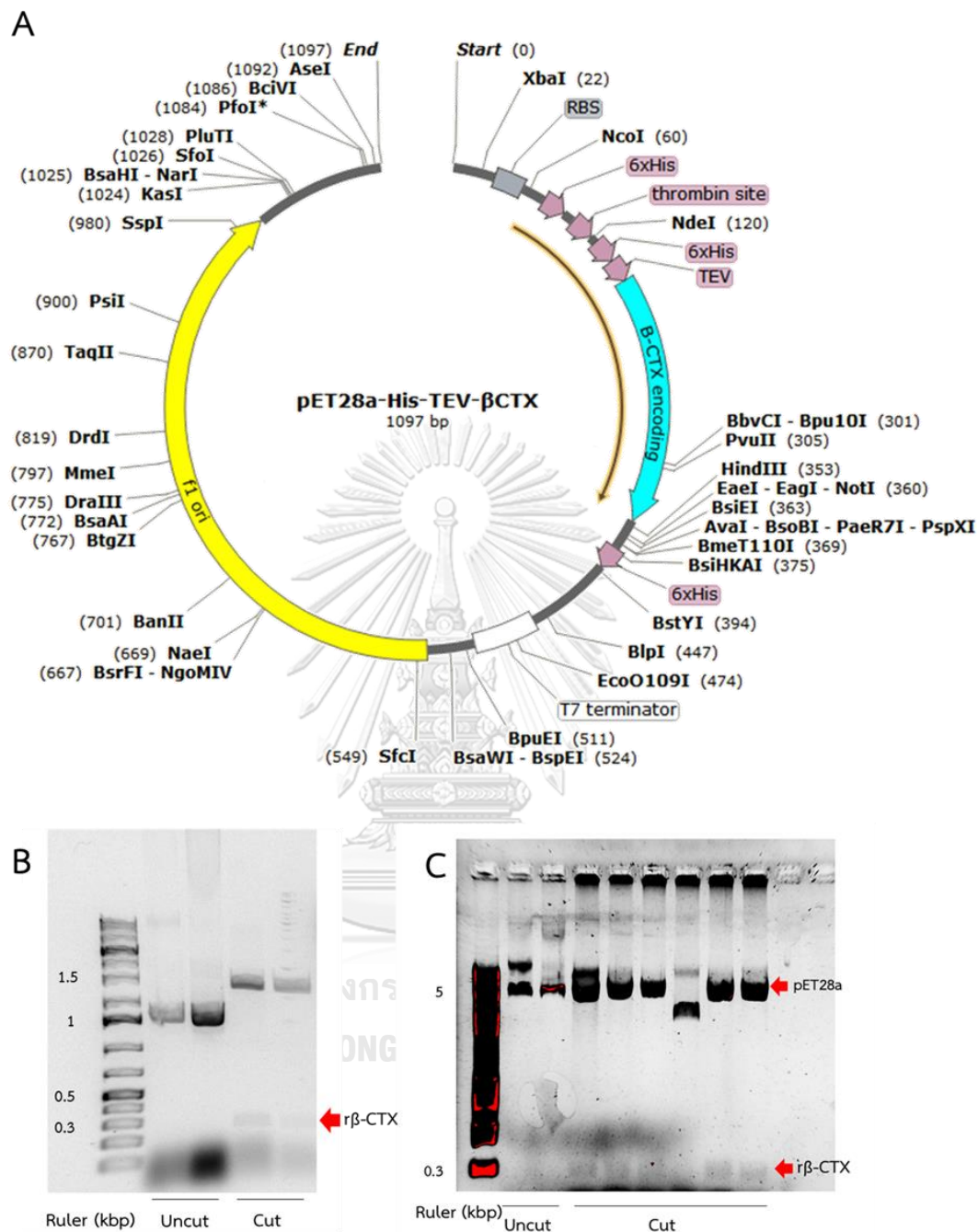


Figure S 17. (A) Design of vector- β -CTX encoding gene, the sites of restriction enzymes (NdeI and HindIII), and the TEV cleavage site. Electrophoresis conducted to confirm the presence of recombinant β -CTX (r β -CTX) gene after incubated with restriction enzyme (B) and ligated with pET28a vector (C). Molecular ruler: 100bp PCR (BioRad®)

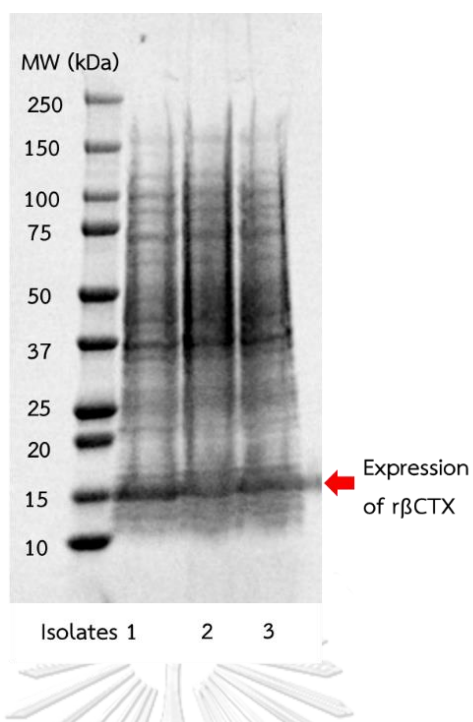


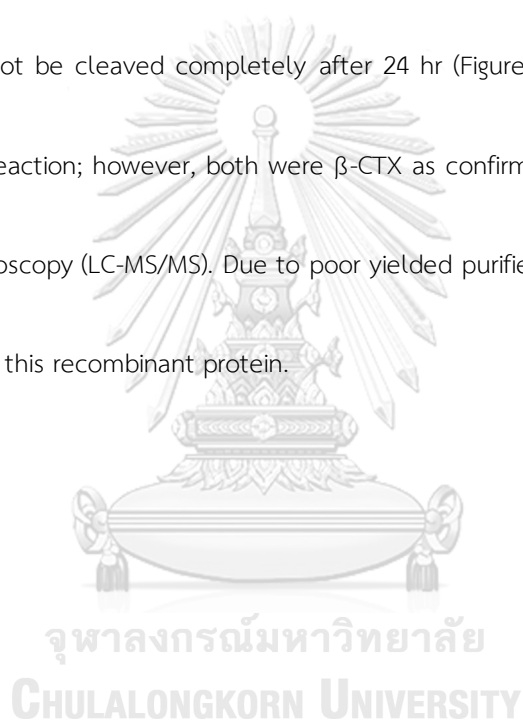
Figure S 18. SDS-PAGE of lysates after three hours of IPTG-induction. Off note, the enhancement of the band intensity presence at 15 kDa, which is the estimated recombinant protein size. Lane 1: BioRad® Dual protein standard; Lane 2-4: Isolates 1-3, respectively.

G2. Large scale production and purification

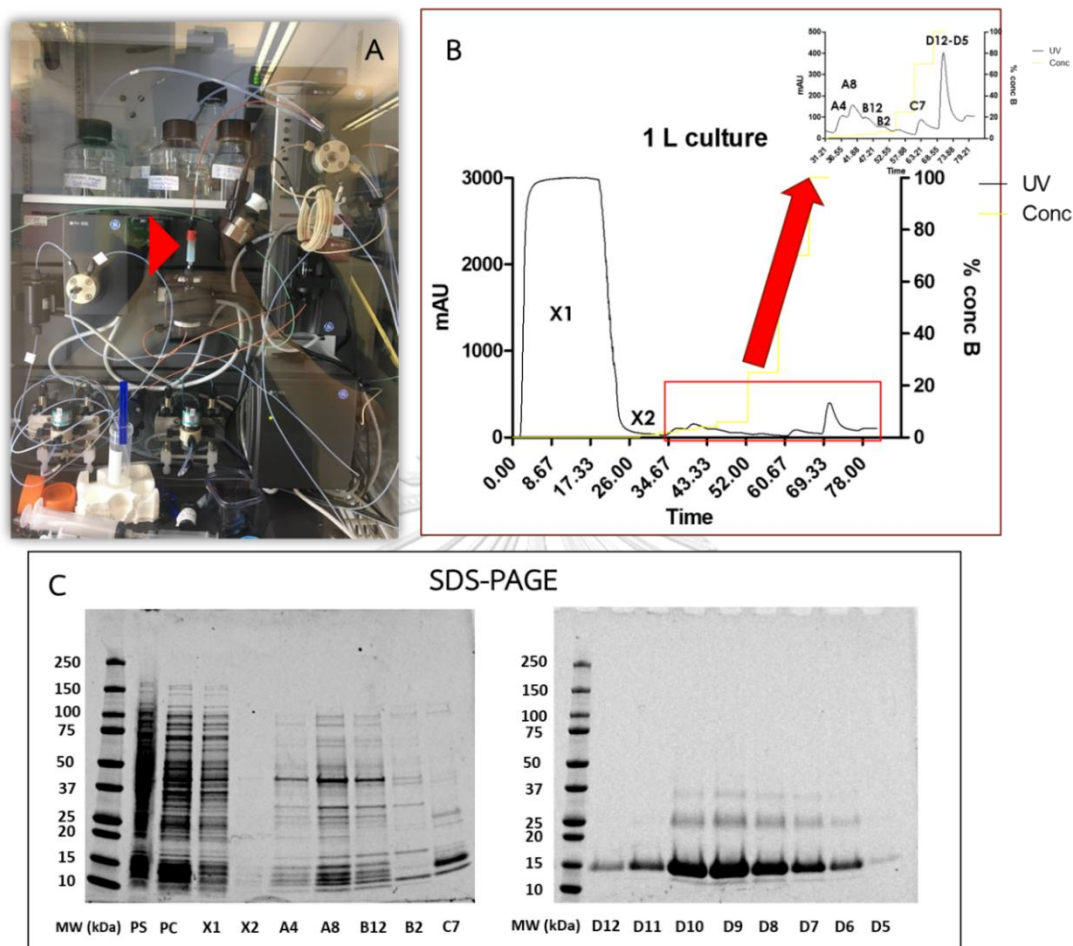
A colony of bacteria/construct was picked up and cultured in 10 mL of Luria broth containing Kanamycin. After an overnight of 37°C incubation, isolates were transferred into 1 L of Luria broth. Bacteria were grown until OD₆₀₀ reached 0.6-0.8. After that, 1 mM of IPTG was added and incubated at 30°C for overnight. On the day after, Bacteria were pelleted by centrifuging at 30,000 xg for 10 minutes. The supernatant was discarded, and pellets were stored at -80°C until used.

On the purification day, bacterial pellet was resuspended and homogenized in equilibration buffer (6M urea, 50 mM NaH₂PO₄ and 300 mM NaCl; pH 7.5) containing reducing agent (5% Dithiothreitol; DTT). The solution was then sonicated seven times (20-second on and 3-minute off) on ice. The lysate was centrifuged at 30,000xg for 10 minutes. The supernatant was collected for further purifying. Purification steps consisted of two phases, *Phase 1* was loading the clarified solution into automated fast protein liquid chromatography (fPLC) system (AKTÄ, GE Healthcare®) using HisTrap nickel affinity column (GE healthcare®) equilibrated with equilibration buffer (Figure S3A). Eluting solution (6M urea, 50 mM NaH₂PO₄ and 300 mM NaCl, 500 mM imidazole; pH 7.5) was then washing the column as following steps: 5 minutes of 1%, 2%, 3% 4% and 6% of eluting solution, respectively. Then a linear gradient of 25-70% of eluting solution was set at 40 minutes and ended up at a linear gradient from 70-100% for 5 minutes (Figure S3B). The

flow rate was set at 1 mL/min and the collecting SDS-PAGE was run on BioRad[®] pre-casted 4-20% polyacrylamide gel to confirm the presence of the clarified protein (Figure S3C). The solution was then dialyzed using the specific buffer (50 mM HEPES and 0.5 mM EDTA; pH 7.0). In *phase II*, the his-tag and TEV region were then cleaved using the TEV protease (ProMega[®]) at 10-20 units/mg target protein under either DTT or glutathione reductase. Although optimization was performed, the enzyme could not be cleaved completely after 24 hr (Figure S5). Moreover, two products appeared after the reaction; however, both were β -CTX as confirmed by liquid chromatography-tandem mass spectroscopy (LC-MS/MS). Due to poor yielded purified r β -CTX, we decided to stop our attempt to make this recombinant protein.



fPLC



จุฬาลงกรณ์มหาวิทยาลัย

Figure S 19. (A) fPLC machine and the HisTrap nickel affinity column (GE healthcare®; arrowhead). (B) Chromatographic profiles in accordance with fPLC. Inlet represents fractions A1 to D12 obtained from fPLC (C) SDS-PAGE of collected fractions from fPLC. Proteins are electrophoresed in pre-casted 4-12% polyacrylamide gel. Off note, fractions D11 and D12 show pure protein approximately 15 kDa which is r β -CTX suspected. Lane 1: BioRad® Dual Protein Marker; PS = Post-sonicated isolates; PC = Pre-column lysates; X1-2 = Waste fractions; A4-D12 = automatically collected fractions.

REFERENCES

Adukauskiene D, Varanauskiene E and Adukauskaite A 2011. Venomous snakebites.

Medicina (Kaunas). 47(8): 461-467.

Aird SD, Villar Briones A, Roy MC and Mikheyev AS 2016. Polyamines as snake toxins

and their probable pharmacological functions in envenomation. Toxins (Basel).

8(10).

Al-Khatib SM, Stevenson WG, Ackerman MJ, Bryant WJ, Callans DJ, Curtis AB, Deal BJ,

Dickfeld T, Field ME, Fonarow GC, Gillis AM, Granger CB, Hammill SC, Hlatky MA,

Joglar JA, Kay GN, Matlock DD, Myerburg RJ and Page RL 2018. 2017

AHA/ACC/HRS guideline for management of patients with ventricular

arrhythmias and the prevention of sudden cardiac death: Executive summary.

Circulation. 138(13): e210-e271.

Alvarenga LM, Zahid M, di Tommaso A, Juste MO, Aubrey N, Billiald P and Muzard J

2014. Engineering venom's toxin-neutralizing antibody fragments and its

therapeutic potential. *Toxins (Basel)*. 6(8): 2541-2567.

Araki M, Hasegawa K, Iwai-Kanai E, Fujita M, Sawamura T, Kakita T, Wada H, Morimoto T

and Sasayama S 2000. Endothelin-1 as a protective factor against beta-

adrenergic agonist-induced apoptosis in cardiac myocytes. *J Am Coll Cardiol*.

36(4): 1411-1418.

Averin AS, Astashev ME, Andreeva TV, Tsetlin VI and Utkin YN 2019. Cardiotoxins from

cobra *Naja oxiana* change the force of contraction and the character of

rhythmoinotropic phenomena in the rat myocardium. *Dokl Biochem Biophys*.

487(1): 282-286.

Bardswell SC, Cuello F, Kentish JC and Avkiran M 2012. cMyBP-C as a promiscuous

substrate: phosphorylation by non-PKA kinases and its potential significance. *J*

Muscle Res Cell Motil. 33(1): 53-60.

Barki-Harrington L, Luttrell LM and Rockman HA 2003. Dual inhibition of beta-adrenergic

and angiotensin II receptors by a single antagonist: A functional role for

receptor-receptor interaction *in vivo*. *Circulation*. 108(13): 1611-1618.

Bassani RA and Bassani JW 2003. Inhibition of the sarcoplasmic reticulum Ca^{2+} pump with thapsigargin to estimate the contribution of $\text{Na}^{+}\text{-Ca}^{2+}$ exchange to ventricular myocyte relaxation. *Braz J Med Biol Res*. 36(12): 1717-1723.

Biesiadecki BJ, Davis JP, Ziolo MT and Janssen PML 2014. Tri-modal regulation of cardiac muscle relaxation; intracellular calcium decline, thin filament deactivation, and cross-bridge cycling kinetics. *Biophys Rev*. 6(3-4): 273-289.

Bottinelli R, Canepari M, Reggiani C and Stienen GJ 1994. Myofibrillar ATPase activity during isometric contraction and isomyosin composition in rat single skinned muscle fibres. *J Physiol*. 481 (Pt 3): 663-675.

Bredt DS 2003. Nitric oxide signaling specificity - the heart of the problem. *J Cell Sci*. 116(Pt 1): 9-15.

Brixius K, Bundkirchen A, Bolck B, Mehlhorn U and Schwinger RH 2001. Nebivolol, bucindolol, metoprolol and carvedilol are devoid of intrinsic sympathomimetic

activity in human myocardium. *Br J Pharmacol.* 133(8): 1330-1338.

Brixius K, Lu R, Boelck B, Grafweg S, Hoyer F, Pott C, Mehlhorn U, Bloch W and

Schwinger RH 2007. Chronic treatment with carvedilol improves Ca^{2+} -dependent

ATP consumption in triton X-skinned fiber preparations of human myocardium. *J*

Pharmacol Exp Ther. 322(1): 222-227.

Brunet S, Emrick MA, Sadilek M, Scheuer T and Catterall WA 2015. Phosphorylation sites

in the Hook domain of CaV beta subunits differentially modulate CaV1.2

channel function. *J Mol Cell Cardiol.* 87: 248-256.

Bundkirchen A, Brixius K, Bolck B, Mehlhorn U, Bloch W and Schwinger RH 2001.

Nebivolol, carvedilol and metoprolol do not influence cardiac Ca^{2+} sensitivity.

Eur J Pharmacol. 422(1-3): 175-180.

Butler L, Cros C, Oldman KL, Harmer AR, Pointon A, Pollard CE and Abi-Gerges N 2015.

Enhanced characterization of contractility in cardiomyocytes during early drug

safety assessment. *Toxicol Sci.* 145(2): 396-406.

Cappelli V, Bottinelli R, Poggesi C, Moggio R and Reggiani C 1989. Shortening velocity and myosin and myofibrillar ATPase activity related to myosin isoenzyme composition during postnatal development in rat myocardium. *Circ Res.* 65(2): 446-457.

Cawley SM, Kolodziej S, Ichinose F, Brouckaert P, Buys ES and Bloch KD 2011. sGC α 1 mediates the negative inotropic effects of NO in cardiac myocytes independent of changes in calcium handling. *Am J Physiol Heart Circ Physiol.* 301(1): H157-163.

Chan HC, Filipek S and Yuan S 2016a. The Principles of Ligand Specificity on beta-2-adrenergic receptor. *Sci Rep.* 6: 34736.

Chan YS, Cheung RC, Xia L, Wong JH, Ng TB and Chan WY 2016b. Snake venom toxins: toxicity and medicinal applications. *Appl Microbiol Biotechnol.* 100(14): 6165-6181.

Chang HC, Tsai TS and Tsai IH 2013. Functional proteomic approach to discover

geographic variations of king cobra venoms from Southeast Asia and China. J Proteomics. 89: 141-153.

Chang LS, Chen KC, Lin SR and Huang HB 2006. Purification and characterization of *Ophiophagus hannah* cytotoxin-like proteins. Toxicon. 48(4): 429-436.

Chang LS, Liou JC, Lin SR and Huang HB 2002. Purification and characterization of a neurotoxin from the venom of *Ophiophagus hannah* (king cobra). Biochem Biophys Res Commun. 294(3): 574-578.

Chen KC, Kao PH, Lin SR and Chang LS 2007. The mechanism of cytotoxicity by *Naja naja atra* cardiotoxin 3 is physically distant from its membrane-damaging effect. Toxicon. 50(6): 816-824.

Chippaux JP, Williams V and White J 1991. Snake venom variability: methods of study, results and interpretation. Toxicon. 29(11): 1279-1303.

Chu G and Kranias EG 2002. Functional interplay between dual site phospholamban phosphorylation: insights from genetically altered mouse models. Basic Res

Cardiol. 97(1): 143-148.

Chung CS, Mechas C and Campbell KS 2015. Myocyte contractility can be maintained by storing cells with the myosin ATPase inhibitor 2,3 butanedione monoxime.

Physiol Rep. 3(6).

CIBIS-II 1999. The cardiac insufficiency bisoprolol study II (CIBIS-II): A randomised trial.

Lancet. 353(9146): 9-13.

Collins DR, Tompson AC, Onakpoya IJ, Roberts N, Ward AM and Heneghan CJ 2017.

Global cardiovascular risk assessment in the primary prevention of cardiovascular disease in adults: Systematic review of systematic reviews. BMJ

Open. 7(3): e013650.



Colson BA, Bekyarova T, Locher MR, Fitzsimons DP, Irving TC and Moss RL 2008. Protein

kinase A-mediated phosphorylation of cMyBP-C increases proximity of myosin heads to actin in resting myocardium. Circ Res. 103(3): 244-251.

Colson BA, Locher MR, Bekyarova T, Patel JR, Fitzsimons DP, Irving TC and Moss RL

2010. Differential roles of regulatory light chain and myosin binding protein -C phosphorylations in the modulation of cardiac force development. *J Physiol.* 588(Pt 6): 981-993.

Danpaiboon W, Reamtong O, Sookrung N, Seesuyay W, Sakolvaree Y, Thanongsaksrikul J,

Dong-din-on F, Srimanote P, Thueng-in K and Chaicumpa W 2014. *Ophiophagus hannah* venom: proteome, components bound by *Naja kaouthia* antivenin and neutralization by *N. kaouthia* neurotoxin-specific human ScFv. *Toxins (Basel).* 6(5): 1526-1558.

Dargie H 1999. Recent clinical data regarding the use of beta blockers in heart failure: focus on CIBIS II. *Heart.* 82 Suppl 4: IV2-4.

de Lucia C, Eguchi A and Koch WJ 2018. New insights in cardiac beta-adrenergic signaling during heart failure and aging. *Front Pharmacol.* 9: 904.

de Weille JR, Schweitz H, Maes P, Tartar A and Lazdunski M 1991. Calciseptine, a peptide isolated from black mamba venom, is a specific blocker of the L-type

calcium channel. Proc Natl Acad Sci U S A. 88(6): 2437-2440.

Doughty RN, Whalley GA, Walsh HA, Gamble GD, Lopez-Sendon J, Sharpe N and Investigators CES 2004. Effects of carvedilol on left ventricular remodeling after acute myocardial infarction: The CAPRICORN echo substudy. Circulation. 109(2): 201-206.

Edes I and Kranias EG 1990. Phospholamban and troponin I are substrates for protein kinase C *in vitro* but not in intact beating guinea pig hearts. Circ Res. 67(2): 394-400.

Fairley NH 1934. Snake bite: its mechanism and modern treatment: (Section of tropical diseases and parasitology). Proc R Soc Med. 27(8): 1083-1094.

Ferreira SH 1965. A bradykinin-potentiating factor (BPF) present in the venom of *Bothrops Jararaca*. Br J Pharmacol Chemother. 24: 163-169.

Finch A, Burtet-Sarramegna V and Graham R 2006. Ligand binding, activation, and agonist trafficking. In: The Receptors: The Adrenergic Receptors: In the 21st

Century. D. Perez (ed). Totowa, NJ: Humana Press Inc. 25-85.

Flashman E, Redwood C, Moolman-Smook J and Watkins H 2004. Cardiac myosin binding protein C: Its role in physiology and disease. *Circ Res.* 94(10): 1279-1289.

G.B.D. collaborators MaCoD 2015. Global, regional, and national age-sex specific all-cause and cause-specific mortality for 240 causes of death, 1990-2013: a systematic analysis for the Global Burden of Disease Study 2013. *Lancet.* 385(9963): 117-171.

Galaz-Montoya M, Wright SJ, Rodriguez GJ, Lichtarge O and Wensel TG 2017. β_2 -Adrenergic receptor activation mobilizes intracellular calcium via a non-canonical cAMP-independent signaling pathway. *J Biol Chem.* 292(24): 9967-9974.

Gao B, Qu Y, Sutherland W, Chui RW, Hoagland K and Vargas HM 2018. Decreased contractility and altered responses to inotropic agents in myocytes from tachypacing-induced heart failure canines. *J Pharmacol Toxicol Methods.* 93: 98-

107.

Gautel M, Zuffardi O, Freiburg A and Labeit S 1995. Phosphorylation switches specific for the cardiac isoform of myosin binding protein-C: a modulator of cardiac contraction? EMBO J. 14(9): 1952-1960.

Geeves MA and Ranatunga KW 2012. Tuning the calcium sensitivity of cardiac muscle. Biophys J. 103(5): 849-850.

Gheorghiade M and Lukas MA 2004. Role of carvedilol in atrial fibrillation: insights from clinical trials. Am J Cardiol. 93(9A): 53B-57B.

Goldstein S and Hjalmarson A 1999. The mortality effect of metoprolol CR/XL in patients with heart failure: results of the MERIT-HF Trial. Clin Cardiol. 22 Suppl 5: V30-35.

Gresham KS and Stelzer JE 2016. The contributions of cardiac myosin binding protein C and troponin I phosphorylation to β -adrenergic enhancement of *in vivo* cardiac function. J Physiol. 594(3): 669-686.

Gupta MK and Robbins J 2014. Post-translational control of cardiac hemodynamics through myosin binding protein C. *Pflugers Arch.* 466(2): 231-236.

Gutierrez JM, Calvete JJ, Habib AG, Harrison RA, Williams DJ and Warrell DA 2017. Snakebite envenoming. *Nat Rev Dis Primers.* 3: 17079.

Hamilton S, Polina I, Terentyeva R, Bronk P, Kim TY, Roder K, Clements RT, Koren G, Choi BR and Terentyev D 2019. PKA phosphorylation underlies functional recruitment of sarcolemmal SK2 channels in ventricular myocytes from hypertrophic hearts. *J Physiol.* doi: 10.1113/JP277618.

Hartmann M and Schrader J 1992. Protein kinase C phosphorylates a 15 kDa protein but not phospholamban in intact rat cardiac myocytes. *Eur J Pharmacol.* 226(3): 225-231.

Harvey AL, Marshall RJ and Karlsson E 1982. Effects of purified cardiotoxins from the Thailand cobra (*Naja naja siamensis*) on isolated skeletal and cardiac muscle preparations. *Toxicon.* 20(2): 379-396.

Harvey RD 2012. Muscarinic receptor agonists and antagonists: Effects on cardiovascular function. *Handb Exp Pharmacol.* (208): 299-316.

Hermesmeyer K, Mason R, Griffen SH and Becker P 1982. Rat cardiac muscle single cell automaticity responses to α - and β -adrenergic agonists and antagonists. *Circ Res.* 51(4): 532-537.

Hohl CM and Li QA 1991. Compartmentation of cAMP in adult canine ventricular myocytes. Relation to single-cell free Ca^{2+} transients. *Circ Res.* 69(5): 1369-1379.

Housmans PR, Kudsioglu ST and Bingham J 1995. Mechanism of the negative inotropic effect of thiopental in isolated ferret ventricular myocardium. *Anesthesiology.* 82(2): 436-450.



Ishizaka T, Yoshimatsu Y, Maeda Y, Chiba K and Mori K 2019. Negative lusitropic property of nifekalant identified using ventricular pressure-volume loop analyses in anesthetized monkeys. *Exp Anim.* 68(1): 91-102.

Isogaya M, Sugimoto Y, Tanimura R, Tanaka R, Kikkawa H, Nagao T and Kurose H 1999.

Binding pockets of the β_1 - and β_2 -adrenergic receptors for subtype-selective agonists. *Mol Pharmacol.* 56(5): 875-885.

Jia W, Shaffer JF, Harris SP and Leary JA 2010. Identification of novel protein kinase A phosphorylation sites in the M-domain of human and murine cardiac myosin binding protein-C using mass spectrometry analysis. *J Proteome Res.* 9(4): 1843-1853.

Joubert FJ 1973. Snake venom toxins the amino acid sequences of two toxins from *Ophiophagus hannah* (king cobra) venom. *Biochim Biophys Acta.* 317(1): 85-98.

Joubert FJ 1977. Snake venoms. The amino-acid sequence of polypeptide DE-1 from *Ophiophagus hannah* (king cobra) venom. *Hoppe Seylers Z Physiol Chem.* 358(5): 565-574.

Karczewski P, Bartel S, Haase H and Krause EG 1987. Isoproterenol induces both cAMP- and calcium-dependent phosphorylation of phospholamban in canine heart *in vivo*. *Biomed Biochim Acta.* 46(8-9): S433-439.

Kasturiratne A, Wickremasinghe AR, de Silva N, Gunawardena NK, Pathmeswaran A,

Premaratna R, Savioli L, Lalloo DG and de Silva HJ 2008. The global burden of snakebite: a literature analysis and modelling based on regional estimates of envenoming and deaths. *PLoS Med.* 5(11): e218.

Katritch V, Reynolds KA, Cherezov V, Hanson MA, Roth CB, Yeager M and Abagyan R

2009. Analysis of full and partial agonists binding to β_2 -adrenergic receptor suggests a role of transmembrane helix V in agonist-specific conformational changes. *J Mol Recognit.* 22(4): 307-318.

Kini RM 2003. Excitement ahead: structure, function and mechanism of snake venom phospholipase A₂ enzymes. *Toxicon.* 42(8): 827-840.

Kini RM, Caldwell RA, Wu QY, Baumgarten CM, Feher JJ and Evans HJ 1998. Flanking

proline residues identify the L-type Ca²⁺ channel binding site of calciseptine and FS2. *Biochemistry.* 37(25): 9058-9063.

Kini RM and Doley R 2010. Structure, function and evolution of three-finger toxins: mini

proteins with multiple targets. *Toxicon*. 56(6): 855-867.

Kobayashi S, Susa T, Ishiguchi H, Myoren T, Murakami W, Kato T, Fukuda M, Hino A,

Suetomi T, Ono M, Uchinoumi H, Tateishi H, Mochizuki M, Oda T, Okuda S, Doi

M, Yamamoto T and Yano M 2015. A low-dose beta1-blocker in combination

with milrinone improves intracellular Ca^{2+} handling in failing cardiomyocytes by

inhibition of milrinone-induced diastolic Ca^{2+} leakage from the sarcoplasmic

reticulum. *PLoS One*. 10(1): e0114314.

Kocic I, Dworakowska D and Dworakowski R 1999. 4-Aminopyridine induces positive

lusitropic effects and prevents the negative inotropic action of phenylephrine in

the rat cardiac tissue subjected to ischaemia. *J Physiol Pharmacol*. 50(3): 381 -

389.

Koh CY and Kini RM 2012. From snake venom toxins to therapeutics - cardiovascular

examples. *Toxicon*. 59(4): 497-506.

Konrad D, Oldner A, Wanecek M, Rudehill A, Weitzberg E, Biber B, Johansson G,

Haggmark S and Haney M 2005. Positive inotropic and negative lusitropic effects of endothelin receptor agonism *in vivo*. *Am J Physiol Heart Circ Physiol*. 289(4): H1702-1709.

Kumar TK, Jayaraman G, Lee CS, Arunkumar AI, Sivaraman T, Samuel D and Yu C 1997. Snake venom cardiotoxins-structure, dynamics, function and folding. *J Biomol Struct Dyn*. 15(3): 431-463.

Kurmani S and Squire I 2017. Acute heart failure: Definition, classification and epidemiology. *Curr Heart Fail Rep*. 14(5): 385-392.

Layland J, Solaro RJ and Shah AM 2005. Regulation of cardiac contractile function by troponin I phosphorylation. *Cardiovasc Res*. 66(1): 12-21.

Lee CY, Tsai MC, Tsaur ML, Lin WW, Carlsson FH and Joubert FJ 1985. Pharmacological study on angusticeps-type toxins from mamba snake venoms. *J Pharmacol Exp Ther*. 233(2): 491-498.

Lei M, Xu J, Gao Q, Minobe E, Kameyama M and Hao L 2018. PKA phosphorylation of

Cav1.2 channel modulates the interaction of calmodulin with the C terminal tail of the channel. *J Pharmacol Sci.* 137(2): 187-194.

Li Lee M, Chung I, Yee Fung S, Kanthimathi MS and Hong Tan N 2014. Antiproliferative activity of king cobra (*Ophiophagus hannah*) venom L-amino acid oxidase. *Basic Clin Pharmacol Toxicol.* 114(4): 336-343.

Lin Shiau SY, Huang MC and Lee CY 1976. Mechanism of action of cobra cardiotoxin in the skeletal muscle. *J Pharmacol Exp Ther.* 196(3): 758-770.

Liu X, Wu G, Shi D, Zhu R, Zeng H, Cao B, Huang M and Liao H 2015. Effects of nitric oxide on notexin-induced muscle inflammatory responses. *Int J Biol Sci.* 11(2): 156-167.



Louis WJ, Louis SN and Krum H 1994. Beta-blockers. *Med J Aust.* 161(9): 555-557.

Lu QW, Hinken AC, Patrick SE, Solaro RJ and Kobayashi T 2010. Phosphorylation of cardiac troponin I at protein kinase C site threonine 144 depresses cooperative activation of thin filaments. *J Biol Chem.* 285(16): 11810-11817.

Mahjoub Y, Malaquin S, Mourier G, Lorne E, Abou Arab O, Massy ZA, Dupont H and

Ducancel F 2015. Short- versus long-Sarafotoxins: Two structurally related snake toxins with very different *in vivo* haemodynamic effects. PLoS One. 10(7): e0132864.

Maiga A, Mourier G, Quinton L, Rouget C, Gales C, Denis C, Lluel P, Senard JM, Palea S,

Servent D and Gilles N 2012. G protein-coupled receptors, an unexploited animal toxin targets: Exploration of green mamba venom for novel drug candidates active against adrenoceptors. Toxicon. 59(4): 487-496.

Maisel AS, Duran JM and Wettersten N 2018. Natriuretic peptides in heart failure: atrial

and B-type natriuretic peptides. Heart Fail Clin. 14(1): 13-25.

Maron BA and Rocco TP 2015. Pharmacotherapy of Congestive Heart Failure. In:

Goodman & Gilman's: The Pharmacological Basis of Therapeutics, 12e.

Laurence L. Brunton, Bruce A. Chabner, and Björn C. Knollmann (eds). New York,

NY: McGraw-Hill Education.

Martin-Garrido A, Biesiadecki BJ, Salhi HE, Shaifta Y, Dos Remedios CG, Ayaz-Guner S, Cai

W, Ge Y, Avkiran M and Kentish JC 2018. Monophosphorylation of cardiac

troponin-I at Ser-23/24 is sufficient to regulate cardiac myofibrillar Ca^{2+}

sensitivity and calpain-induced proteolysis. *J Biol Chem.* 293(22): 8588-8599.

Matsuda Y, Akita H, Terashima M, Shiga N, Kanazawa K and Yokoyama M 2000.

Carvedilol improves endothelium-dependent dilatation in patients with

coronary artery disease. *Am Heart J.* 140(5): 753-759.

Mazurek JA and Jessup M 2017. Understanding Heart Failure. *Heart Fail Clin.* 13(1): 1-19.

Meier S, Andressen KW, Aronsen JM, Sjaastad I, Hougen K, Skomedal T, Osnes JB,

Qvigstad E, Levy FO and Moltzau LR 2017. PDE3 inhibition by C-type natriuretic

peptide-induced cGMP enhances cAMP-mediated signaling in both non-failing

and failing hearts. *Eur J Pharmacol.* 812: 174-183.

Menges L, Krawutschke C, Fuchtbauer EM, Fuchtbauer A, Sandner P, Koesling D and

Russwurm M 2019. Mind the gap (junction): cGMP induced by nitric oxide in

cardiac myocytes originates from cardiac fibroblasts. *Br J Pharmacol.* 176(24): 4696-4707.

MERIT-HF 1999. Effect of metoprolol CR/XL in chronic heart failure: Metoprolol CR/XL randomised intervention trial in congestive heart failure (MERIT-HF). *Lancet.* 353(9169): 2001-2007.

Metra M, Nodari S and Dei Cas L 2001. Beta-blockade in heart failure: selective versus nonselective agents. *Am J Cardiovasc Drugs.* 1(1): 3-14.

Mochizuki M, Yano M, Oda T, Tateishi H, Kobayashi S, Yamamoto T, Ikeda Y, Ohkusa T, Ikemoto N and Matsuzaki M 2007. Scavenging free radicals by low-dose carvedilol prevents redox-dependent Ca²⁺ leak via stabilization of ryanodine receptor in heart failure. *J Am Coll Cardiol.* 49(16): 1722-1732.

Mohamed Abd El-Aziz T, Garcia Soares A and Stockand JD 2019. Snake venoms in drug discovery: valuable therapeutic tools for life saving. *Toxins (Basel).* 11(10).

Moodie DS 2016. The global burden of cardiovascular disease. *Congenit Heart Dis.* 11(3):

213.

Mourier G, Hajj M, Cordier F, Zorba A, Gao X, Coskun T, Herbet A, Marcon E, Beau F,

Delepierre M, Ducancel F and Servent D 2012. Pharmacological and structural characterization of long-sarafotoxins, a new family of endothelin-like peptides: Role of the C-terminus extension. *Biochimie*. 94(2): 461-470.

Role of the C-terminus extension. *Biochimie*. 94(2): 461-470.

Nixon BR, Walton SD, Zhang B, Brundage EA, Little SC, Ziolo MT, Davis JP and

Biesiadecki BJ 2014. Combined troponin I Ser-150 and Ser-23/24 phosphorylation sustains thin filament Ca^{2+} sensitivity and accelerates deactivation in an acidic environment. *J Mol Cell Cardiol*. 72: 177-185.

O'Brien J, Lee SH, Gutierrez JM and Shea KJ 2018. Engineered nanoparticles bind elapid

snake venom toxins and inhibit venom-induced dermonecrosis. *PLoS Negl Trop Dis*. 12(10): e0006736.

Olsson MC, Patel JR, Fitzsimons DP, Walker JW and Moss RL 2004. Basal myosin light

chain phosphorylation is a determinant of Ca^{2+} sensitivity of force and activation

dependence of the kinetics of myocardial force development. *Am J Physiol*

Heart Circ Physiol. 287(6): H2712-2718.

Ou YJ, Leung YM, Huang SJ and Kwan CY 1997. Dual effects of extracellular Ca^{2+} on cardiotoxin-induced cytotoxicity and cytosolic Ca^{2+} changes in cultured single cells of rabbit aortic endothelium. *Biochim Biophys Acta.* 1330(1): 29-38.

Park SA, Kim TG, Han MK, Ha KC, Kim SZ and Kwak YG 2012. Dendroaspis natriuretic peptide regulates the cardiac L-type Ca^{2+} channel activity by the phosphorylation of $\alpha_1\text{c}$ proteins. *Exp Mol Med.* 44(6): 363-368.

Petras D, Heiss P, Sussmuth RD and Calvete JJ 2015. Venom proteomics of Indonesian king cobra, *Ophiophagus hannah*: Integrating top-down and bottom-up approaches. *J Proteome Res.* 14(6): 2539-2556.

Piacentino V, 3rd, Weber CR, Chen X, Weisser-Thomas J, Margulies KB, Bers DM and Houser SR 2003. Cellular basis of abnormal calcium transients of failing human ventricular myocytes. *Circ Res.* 92(6): 651-658.

Ponicke K, Heinroth-Hoffmann I and Brodde OE 2003. Demonstration of functional M3-muscarinic receptors in ventricular cardiomyocytes of adult rats. *Br J Pharmacol.* 138(1): 156-160.

Ponnam S, Sevrieva I, Sun YB, Irving M and Kampourakis T 2019. Site-specific phosphorylation of myosin binding protein-C coordinates thin and thick filament activation in cardiac muscle. *Proc Natl Acad Sci U S A.* 116(31): 15485-15494.

Pons F, Lupon J, Urrutia A, Gonzalez B, Crespo E, Diez C, Cano L, Cabanes R, Altimir S, Coll R, Pascual T and Valle V 2010. Mortality and cause of death in patients with heart failure: findings at a specialist multidisciplinary heart failure unit. *Rev Esp Cardiol.* 63(3): 303-314.

Poole-Wilson PA, Swedberg K, Cleland JG, Di Lenarda A, Hanrath P, Komajda M, Lubsen J, Lutiger B, Metra M, Remme WJ, Torp-Pedersen C, Scherhag A, Skene A and Carvedilol Or Metoprolol European Trial I 2003. Comparison of carvedilol and metoprolol on clinical outcomes in patients with chronic heart failure in the

Carvedilol Or Metoprolol European Trial (COMET): randomised controlled trial.

Lancet. 362(9377): 7-13.

Pratje E and Heilmeyer LM 1972. Phosphorylation of rabbit muscle troponin and actin

by a 3', 5'-c-AMP-dependent protein kinase. FEBS Lett. 27(1): 89-93.

Pu XC, Wong PT and Gopalakrishnakone P 1995. A novel analgesic toxin (hannalgesin)

from the venom of king cobra (*Ophiophagus hannah*). Toxicon. 33(11): 1425-

1431.

Pucelik P 2007. Pharmacological blockade of sarcoplasmic reticulum induces a negative

lusitropic effect. Gen Physiol Biophys. 26(3): 214-220.

Raifman TK, Kumar P, Haase H, Klusmann E, Dascal N and Weiss S 2017. Protein kinase

C enhances plasma membrane expression of cardiac L-type calcium channel,

CaV1.2. Channels (Austin). 11(6): 604-615.

Rajagopalan N, Pung YF, Zhu YZ, Wong PT, Kumar PP and Kini RM 2007. Beta-

cardiotoxin: a new three-finger toxin from *Ophiophagus hannah* (king cobra)

venom with beta-blocker activity. *FASEB J.* 21(13): 3685-3695.

Rao V, Cheng Y, Lindert S, Wang D, Oxenford L, McCulloch AD, McCammon JA and

Regnier M 2014. PKA phosphorylation of cardiac troponin I modulates activation and relaxation kinetics of ventricular myofibrils. *Biophys J.* 107(5): 1196-1204.

Rehsia NS and Dhalla NS 2010. Mechanisms of the beneficial effects of beta-

adrenoceptor antagonists in congestive heart failure. *Exp Clin Cardiol.* 15(4): e86-95.

Riegger GA, Liebau G and Kochsiek K 1982. Antidiuretic hormone in congestive heart failure. *Am J Med.* 72(1): 49-52.

Rosas PC, Liu Y, Abdalla MI, Thomas CM, Kidwell DT, Dusio GF, Mukhopadhyay D, Kumar

R, Baker KM, Mitchell BM, Powers PA, Fitzsimons DP, Patel BG, Warren CM,

Solaro RJ, Moss RL and Tong CW 2015. Phosphorylation of cardiac myosin-

binding protein-C is a critical mediator of diastolic function. *Circ Heart Fail.* 8(3): 582-594.

Roy A, Qingxiang S, Alex C, Rajagopalan N, Jobichen C, Sivaraman J and Kini RM 2019.

Identification of a alpha-helical molten globule intermediate and structural characterization of β -cardiotoxin, an all β -sheet protein isolated from the venom of *Ophiophagus hannah* (king cobra). *Protein Sci.*

Roy A, Zhou X, Chong MZ, D'Hoedt D, Foo CS, Rajagopalan N, Nirthanan S, Bertrand D,

Sivaraman J and Kini RM 2010. Structural and functional characterization of a novel homodimeric three-finger neurotoxin from the venom of *Ophiophagus hannah* (king cobra). *J Biol Chem.* 285(11): 8302-8315.

Russell F 2001. Toxic effects of terrestrial animal venoms and poisons. In: Casarett and

Doull's Toxicology: The basic science of poisons. 6th ed. Klassen CD (ed). New York: McGraw-Hill. 945-964.

Ryba DM, Li J, Cowan CL, Russell B, Wolska BM and Solaro RJ 2017. Long-term biased

beta-arrestin signaling improves cardiac structure and function in dilated cardiomyopathy. *Circulation.* 135(11): 1056-1070.

Sadayappan S, Gulick J, Osinska H, Barefield D, Cuello F, Avkiran M, Lasko VM, Lorenz

JN, Maillet M, Martin JL, Brown JH, Bers DM, Molkentin JD, James J and Robbins

J 2011. A critical function for Ser-282 in cardiac Myosin binding protein-C

phosphorylation and cardiac function. *Circ Res.* 109(2): 141-150.

Saha A, Gomes A, Giri B, Chakravarty AK, Biswas AK, Dasgupta SC and Gomes A 2006.

Occurrence of non-protein low molecular weight cardiotoxin in Indian King

Cobra (*Ophiophagus hannah*) Cantor 1836, venom. *Indian J Exp Biol.* 44(4): 279-

285.

Salas MA, Vila-Petroff MG, Palomeque J, Aiello EA and Mattiazzi A 2001. Positive

inotropic and negative lusitropic effect of angiotensin II: intracellular

mechanisms and second messengers. *J Mol Cell Cardiol.* 33(11): 1957-1971.

Salgado HC, Simoes GM, Santana Filho VJ, Dias da Silva VJ, Salgado MC and Fazan R, Jr.

2007. Negative inotropic and lusitropic effects of intravenous amiodarone in

conscious rats. *Clin Exp Pharmacol Physiol.* 34(9): 870-875.

Savarese G and Lund LH 2017. Global public health burden of heart failure. *Card Fail*

Rev. 3(1): 7-11.

Schleifer KJ 1997. Comparative molecular modelling study of the calcium channel

blockers nifedipine and black mamba toxin FS2. *J Comput Aided Mol Des.* 11(5):

491-501.

Seagren SC, Skelton CL and Pool PE 1971. Relation of cardiac myofibrillar ATPase

activity to increased contractile state. *Am J Physiol.* 220(4): 847-851.

Servent D, Blanchet G, Mourier G, Marquer C, Marcon E and Fruchart-Gaillard C 2011.

Muscarinic toxins. *Toxicon.* 58(6-7): 455-463.

Servent D and Fruchart-Gaillard C 2009. Muscarinic toxins: tools for the study of the

pharmacological and functional properties of muscarinic receptors. *J*

Neurochem. 109(5): 1193-1202.

Shin SY, Choo SM, Woo SH and Cho KH 2008. Cardiac systems biology and parameter

sensitivity analysis: intracellular Ca^{2+} regulatory mechanisms in mouse

ventricular myocytes. *Adv Biochem Eng Biotechnol.* 110: 25-45.

Smith DT, Farzaneh-Far R, Ali S, Na B, Whooley MA and Schiller NB 2010. Relation of beta-blocker use with frequency of hospitalization for heart failure in patients with left ventricular diastolic dysfunction (from the Heart and Soul Study). *Am J Cardiol.* 105(2): 223-228.

Solaro RJ and van der Velden J 2010. Why does troponin I have so many phosphorylation sites? Fact and fancy. *J Mol Cell Cardiol.* 48(5): 810-816.

Strader CD, Sigal IS, Candelore MR, Rands E, Hill WS and Dixon RA 1988. Conserved aspartic acid residues 79 and 113 of the beta-adrenergic receptor have different roles in receptor function. *J Biol Chem.* 263(21): 10267-10271.

Strang KT, Sweitzer NK, Greaser ML and Moss RL 1994. Beta-adrenergic receptor stimulation increases unloaded shortening velocity of skinned single ventricular myocytes from rats. *Circ Res.* 74(3): 542-549.

Stuart B, Wogan G, Grismer L, Auliya M, Inger RF, Lilley R, Chan-Ard T, Thy N, Nguyen

TQ, Srinivasulu C and Jelić D 2012. *Ophiophagus hannah*. The IUCN Red List of Threatened Species 2012: e.T177540A1491874., [Available online]: <http://dx.doi.org/10.2305/IUCN.UK.2012-1.RLTS.T177540A1491874.en>, 13 pp.

Stull JT, Brostrom CO and Krebs EG 1972. Phosphorylation of the inhibitor component of troponin by phosphorylase kinase. *J Biol Chem.* 247(16): 5272-5274.

Tan CH, Tan KY, Fung SY and Tan NH 2015. Venom-gland transcriptome and venom proteome of the Malaysian king cobra (*Ophiophagus hannah*). *BMC Genomics.* 16: 687.

Tan KY, Ng TS, Bourges A, Ismail AK, Maharani T, Khomvilai S, Sitprija V, Tan NH and Tan CH 2019. Geographical variations in king cobra (*Ophiophagus hannah*) venom from Thailand, Malaysia, Indonesia and China: On venom lethality, antivenom immunoreactivity and in vivo neutralization. *Acta Trop.* 203: 105311.

Tan NH and Hj MN 1989. Enzymatic and toxic properties of *Ophiophagus hannah* (king cobra) venom and venom fractions. *Toxicon.* 27(6): 689-695.

Tanai E and Frantz S 2015. Pathophysiology of heart failure. *Compr Physiol*. 6(1): 187-214.

Tasoulis T and Isbister GK 2017. A review and database of snake venom proteomes. *Toxins (Basel)*. 9(9).

ter Keurs HE, Bucx JJ, de Tombe PP, Backx P and Iwazumi T 1988. The effects of sarcomere length and Ca^{2+} on force and velocity of shortening in cardiac muscle. *Adv Exp Med Biol*. 226: 581-593.

Thomas H, Diamond J, Vieco A, Chaudhuri S, Shinnar E, Cromer S, Perel P, Mensah GA, Narula J, Johnson CO, Roth GA and Moran AE 2018. Global atlas of cardiovascular disease 2000-2016: The path to prevention and control. *Glob Heart*. 13(3): 143-163.

Thomas MR and Lip GY 2017. Novel risk markers and risk assessments for cardiovascular disease. *Circ Res*. 120(1): 133-149.

Tobin AB 1997. Phosphorylation of phospholipase C-coupled receptors. *Pharmacol*

Ther. 75(2): 135-151.

Tong CW, Gaffin RD, Zawieja DC and Muthuchamy M 2004. Roles of phosphorylation of myosin binding protein-C and troponin I in mouse cardiac muscle twitch dynamics. *J Physiol.* 558(Pt 3): 927-941.

Tong CW, Stelzer JE, Greaser ML, Powers PA and Moss RL 2008. Acceleration of crossbridge kinetics by protein kinase A phosphorylation of cardiac myosin binding protein C modulates cardiac function. *Circ Res.* 103(9): 974-982.

Tsai CH, Yang SH, Chien CM, Lu MC, Lo CS, Lin YH, Hu XW and Lin SR 2006. Mechanisms of cardiotoxin III-induced apoptosis in human colorectal cancer colo205 cells. *Clin Exp Pharmacol Physiol.* 33(3): 177-182.

Utkin YN 2013. Three-finger toxins, a deadly weapon of elapid venom - milestones of discovery. *Toxicon.* 62: 50-55.

Valenta J 2010. Zoological basis. In: *Venomous snakes - Envenoming, Therapy.* 2nd ed. Jiri Valenta (ed). New York: Nova Science Publishers, Inc. 1-16.

Vanni S, Neri M, Tavernelli I and Rothlisberger U 2011. Predicting novel binding modes of agonists to beta adrenergic receptors using all-atom molecular dynamics simulations. *PLoS Comput Biol.* 7(1): e1001053.

Vecchio EA, White PJ and May LT 2017. Targeting adenosine receptors for the treatment of cardiac fibrosis. *Front Pharmacol.* 8: 243.

Verduyn SC, Zaremba R, van der Velden J and Stienen GJ 2007. Effects of contractile protein phosphorylation on force development in permeabilized rat cardiac myocytes. *Basic Res Cardiol.* 102(6): 476-487.

Vila-Petroff M, Perez GN, Alvarez B, Cingolani HE and Mattiazzi A 1996. Mechanism of negative lusitropic effect of alpha 1-adrenoceptor stimulation in cat papillary muscles. *Am J Physiol.* 270(2 Pt 2): H701-709.

Vonk FJ, Casewell NR, Henkel CV, Heimberg AM, Jansen HJ, McCleary RJ, Kerkkamp HM, Vos RA, Guerreiro I, Calvete JJ, Wuster W, Woods AE, Logan JM, Harrison RA, Castoe TA, de Koning AP, Pollock DD, Yandell M, Calderon D, Renjifo C, Currier

RB, Salgado D, Pla D, Sanz L, Hyder AS, Ribeiro JM, Arntzen JW, van den Thillart GE, Boetzer M, Pirovano W, Dirks RP, Spaink HP, Duboule D, McGlenn E, Kini RM and Richardson MK 2013. The king cobra genome reveals dynamic gene evolution and adaptation in the snake venom system. *Proc Natl Acad Sci U S A*. 110(51): 20651-20656.

Waldo AL, Camm AJ, deRuyter H, Friedman PL, MacNeil DJ, Pauls JF, Pitt B, Pratt CM, Schwartz PJ and Veltri EP 1996. Effect of d-sotalol on mortality in patients with left ventricular dysfunction after recent and remote myocardial infarction. The SWORD investigators. Survival with oral d-sotalol. *Lancet*. 348(9019): 7-12.

Wang CH, Monette R, Lee SC, Morley P and Wu WG 2005. Cobra cardiotoxin-induced cell death in fetal rat cardiomyocytes and cortical neurons: different pathway but similar cell surface target. *Toxicol*. 46(4): 430-440.

Wang HX, Lau SY, Huang SJ, Kwan CY and Wong TM 1997. Cobra venom cardiotoxin induces perturbations of cytosolic calcium homeostasis and hypercontracture in adult rat ventricular myocytes. *J Mol Cell Cardiol*. 29(10): 2759-2770.

Watanabe H, Honda Y, Deguchi J, Yamada T and Bando K 2017. Usefulness of cardiotoxicity assessment using calcium transient in human induced pluripotent stem cell-derived cardiomyocytes. *J Toxicol Sci.* 42(4): 519-527.

Watanabe TX, Itahara Y, Kuroda H, Chen YN, Kimura T and Sakakibara S 1995. Smooth muscle relaxing and hypotensive activities of synthetic calciseptine and the homologous snake venom peptide FS2. *Jpn J Pharmacol.* 68(3): 305-313.

Wegener AD, Simmerman HK, Lindemann JP and Jones LR 1989. Phospholamban phosphorylation in intact ventricles. Phosphorylation of serine 16 and threonine 17 in response to beta-adrenergic stimulation. *J Biol Chem.* 264(19): 11468-11474.

จุฬาลงกรณ์มหาวิทยาลัย
CHULALONGKORN UNIVERSITY

Whitehurst VE, Vick JA, Alleva FR, Zhang J, Joseph X and Balazs T 1999. Reversal of propranolol blockade of adrenergic receptors and related toxicity with drugs that increase cyclic AMP. *Proc Soc Exp Biol Med.* 221(4): 382-385.

WHO 2010. Guidelines for the management of snake-bites. David A Warrell, ed. World

Health Organization, India, 162 pp.

WHO 2013. Global action plan for the prevention and control of non-communicable

diseases 2013-2020., [Available online]:

apps.who.int/iris/bitstream/handle/10665/94384/9789241506236_eng.pdf, 55

pp.

Williams DJ, Faiz MA, Abela-Ridder B, Ainsworth S, Bulfone TC, Nickerson AD, Habib AG,

Junghanss T, Fan HW, Turner M, Harrison RA and Warrell DA 2019. Strategy for a

globally coordinated response to a priority neglected tropical disease: Snakebite

envenoming. *PLoS Negl Trop Dis.* 13(2): e0007059.

Witcher DR, Kovacs RJ, Schulman H, Cefali DC and Jones LR 1991. Unique

phosphorylation site on the cardiac ryanodine receptor regulates calcium

channel activity. *J Biol Chem.* 266(17): 11144-11152.

Witte K, Schnecko A, Hauth D, Wirzius S and Lemmer B 1998. Effects of chronic

application of propranolol on beta-adrenergic signal transduction in heart

ventricles from myopathic BIO TO2 and control hamsters. *Br J Pharmacol.*

125(5): 1033-1041.

Wolska BM and Solaro RJ 1996. Method for isolation of adult mouse cardiac myocytes

for studies of contraction and microfluorimetry. *Am J Physiol.* 271(3 Pt 2):

H1250-1255.

Yancy CW, Jessup M, Bozkurt B, Butler J, Casey DE, Jr., Drazner MH, Fonarow GC, Geraci

SA, Horwich T, Januzzi JL, Johnson MR, Kasper EK, Levy WC, Masoudi FA,

McBride PE, McMurray JJ, Mitchell JE, Peterson PN, Riegel B, Sam F, Stevenson

LW, Tang WH, Tsai EJ and Wilkoff BL 2013. 2013 ACCF/AHA guideline for the

management of heart failure: executive summary: a report of the American

College of Cardiology Foundation/American Heart Association Task Force on

practice guidelines. *Circulation.* 128(16): 1810-1852.

Zhang B, Li F, Chen Z, Shrivastava IH, Gasanoff ES and Dagda RK 2019. *Naja*

mossambica mossambica cobra Cardiotoxin targets mitochondria to disrupt

mitochondrial membrane structure and function. *Toxins (Basel).* 11(3).

Zhang J, Zhou Q, Smith CD, Chen H, Tan Z, Chen B, Nani A, Wu G, Song LS, Fill M, Back

TG and Chen SR 2015. Non-beta-blocking R-carvedilol enantiomer suppresses

Ca²⁺ waves and stress-induced ventricular tachyarrhythmia without lowering

heart rate or blood pressure. *Biochem J.* 470(2): 233-242.

Zhang SJ, Liu ZH, Zou C and Wang L 2012. Effect of metoprolol on sarcoplasmic

reticulum Ca²⁺ leak in a rabbit model of heart failure. *Chin Med J (Engl).* 125(5):

815-822.

Zhang SY, Cai ZX, Li P, Cai CY, Qu CL and Guo HS 2010. Effect of dendroaspis natriuretic

peptide (DNP) on L-type calcium channel current and its pathway. *Regul Pept.*

164(2-3): 120-125.

Zhao D, Liu J, Xie W and Qi Y 2015. Cardiovascular risk assessment: a global

perspective. *Nat Rev Cardiol.* 12(5): 301-311.

Ziaeian B and Fonarow GC 2016. Epidemiology and aetiology of heart failure. *Nat Rev*

Cardiol. 13(6): 368-378.



จุฬาลงกรณ์มหาวิทยาลัย
CHULALONGKORN UNIVERSITY



จุฬาลงกรณ์มหาวิทยาลัย
CHULALONGKORN UNIVERSITY

VITA

NAME Tuchakorn Lertwanakarn

DATE OF BIRTH 03 May 1990

PLACE OF BIRTH Bangkok

INSTITUTIONS ATTENDED Chulalongkorn University

HOME ADDRESS 457/206 Charoenkrung107th rd Bangkhlo Bangkoklaem BKK
10120

PUBLICATION Effects of coenzyme Q10 supplementation on cardiac troponin I level, heart rate variability, and echocardiographic profiles in canine with myxomatous degenerative mitral valve disease: a pilot study. 2018. Thai J Vet Med. 48(3): 443-452.

AWARD RECEIVED 2nd Runner up, Javelina 9th annual undergraduate and graduate research symposium, Texas A&M University-Kingsville, Texas, USA, 2017

"Cytotoxicity of a Beta-cardiotoxin isolated from king cobra venom (*Ophiophagus hannah*) on three different mammalian cell types"

